TÉCNICO LISBOA

Pumped Hydropower Storage and Integration of Renewables in Hybrid Energy Solutions

Multi-Objective Optimization with GRG Nonlinear and NSGA-II Algorithm

João Soares Tavares Coelho

Thesis to obtain the Master of Science Degree in

Energy Engineering and Management

Supervisor: Prof. Helena M. Ramos

Examination Committee

Chairperson: Prof. Jorge de Saldanha Gonçalves Matos
Supervisor: Prof. Helena M. Ramos
Members of the Committee: Prof. João Filipe Pereira Fernandes
Dr. Alban Kuriqi

December 2024

Declaration

I declare that this document is an original work of my own authorship and that it fulfills all the requirements of the Code of Conduct and Good Practices of the Universidade de Lisboa.

Acknowledgments

I want to thank my family for their encouragement, caring and fueling my curiosity over all these years. I thank my friends and colleagues who accompanied me throughout this long and tough journey. Without your support, it would have not been possible and I immensely appreciate all the memories made during these academic years. More important, thank you for helping me grow, as an engineer, but more importantly, as a person.

I would also like to acknowledge my dissertation supervisor Prof. Helena Ramos for her excellent insight, support and dedication to improving my skills and knowledge that contributed to the broadening of my experience in various engineering fields. I want to recognize the help and partnership developed with other professors, colleagues and students during the development of this master's thesis, especially from the HY4RES project, CERIS laboratory, Instituto Superior Técnico (IST), Universidad de Córdoba and Universitat Politècnica de València (UPV).

To each and every one of you – Thank you.

Research Grant:

Master's Thesis developed under the research grant by the project HY4RES (Hybrid for Renewable Energy Systems) EAPA_0001/2022 from INTERREG ATLANTIC AREA PROGRAMME, as well Foundation for Science and Technology's support to UIDB/04625/2020, the research unit CERIS.

Publications in International Journals:

- J. Coelho, M. van de Loo, J. Díaz, O. Coronado-Hernández, M. Perez-Sanchez and H. M. Ramos, "Multi-objective and multi-variable optimization models of hybrid renewable energy solutions for water-energy nexus", Water, vol.16, 17, 2024. https://doi.org/10.3390/w16172360
- J. Coelho, A. Alves, J. Morillo, O. Coronado-Hernández, M. Perez-Sanchez and H. M. Ramos, "Hybrid energy solution to improve irrigation systems: Hy4res vs. homer optimization models", Energies, vol. 17, 16, 2024. https://doi.org/10.3390/en17164037
- J. Coelho, M. Perez-Sanchez, O. E. Coronado-Hernández, M. Besharat, R. L. Feng, E. Tasca, L. Zhou and H. M. Ramos, "Hydropneumatic Storage Methodology Towards a New Era of Hybrid Energy System's Efficiency and Flexibility", Results in Engineering, vol.24, 2024. https://doi.org/10.1016/j.rineng.2024.103117
- J. Coelho, M. Perez-Sanchez, O. E. Coronado-Hernández, F. Sánchez-Romero, A. McNabola and H. M. Ramos, "Hybrid Renewable Systems for Small Energy Communities: What Is the Best Solution?", Applied Sciences, vol.14, 21, 2024. https://doi.org/10.3390/app142110052

International Conferences:

Participation in the 8th International Electronic Conference on Water Sciences (ID:sciforum-102599) as oral speaker: J. Coelho, H. Ramos, Multi-criteria optimization modeling of hybrid energy solutions for the water-energy nexus, 14-16 October 2024.

Abstract

This thesis explores pumped hydropower storage (PHS) and its integration in hybrid energy solutions (HES). It presents experimental and simulation results concerning the performance of the pumped-storage process. A new algorithmic model, HY4RES, was designed to simulate and optimize hybrid energy solutions by integrating PHS, on Excel-Solver or Python within water-energy nexus applications. The optimization methods explored are single and multi-objective with flexible decision variables to assess solutions for the HES systems. The model was deployed for large and small-scale case studies. The first, an irrigation system, analyzes different optimization methods for three scenarios, that combine renewable sources and storage systems. The scale of the water needs for irrigation highly dictated the flexibility of the system's results and its reliability throughout the season. The comparison with a parallel analysis in the HOMER commercial software evidences the importance of designing models assessing energy and water demands. The second case study, based on a small energy community, explores the model's performance for a floating load demand, in both stand-alone and grid-connected scenarios. Since the load profile is greater in winter months, where solar is minimal, the grid-connected scenario with wind energy is the most economically attractive with just 8.3% grid dependency, whereas the stand-alone scenario of solar, wind and PHS stands as a reliable and sustainable off-grid solution. The HY4RES model proved its capacity for technical and economic analysis of hybrid solutions within the water-energy nexus.

Keywords

Pumped Hydropower Storage (PHS); Renewable Energy Systems; Hybrid Energy Solutions; Water-Energy Nexus; NSGA-II Algorithm; GRG Nonlinear

Resumo

A presente tese explora o armazenamento de energia hidroelétrica por bombagem (PHS) e sua integração em soluções híbridas de energias (HES). O processo de armazenamento foi analisado laboratorialmente e por simulação no WaterGEMS. Um novo modelo algorítmico, HY4RES, foi desenvolvido para simulação e otimização de soluções híbridas com integração de PHS, com MS-Solver ou Python, no âmbito do *water-energy nexus*. Os métodos de otimização incorporam uma ou duas funções objetivo com variáveis flexíveis para avaliar diferentes soluções. O modelo foi implementado em casos de estudo de grande e pequena escala. O primeiro, um sistema de irrigação, analisa diferentes métodos de otimização para três cenários. A dimensão do consumo de água para irrigação ditou fortemente a flexibilidade do sistema e a sua fiabilidade ao longo da época. A importância de conceber modelos que avaliem tanto as necessidades de energia como de água é evidenciada pela comparação com a análise realizada no software HOMER. O segundo caso de estudo, baseado numa pequena comunidade energética, explora o desempenho do modelo para um perfil flutuante de consumo energético. Sendo este maior nos meses de inverno, em que a energia solar é também mínima, o cenário com energia eólica, ligado à rede, é o mais atrativo economicamente, com apenas 8.3% de dependência da rede, enquanto o cenário autónomo de energia solar, eólica e PHS se apresenta como uma solução independente da rede elétrica e sustentável. Em última análise, o modelo HY4RES mostrou excelência na análise técnica e económica de sistema híbridos.

Palavras Chave

Armazenamento de energia hidroelétrica por bombagem (PHS); Sistemas de energia renovável; Soluções híbridas de energia; Nexos de Água-Energia; NSGA-II Algoritmo; GRG Não Linear

Contents

List of Figures

List of Tables

List of Symbols

A^i	Water consumption	m^3
A^{LR}	Lower reservoir total area	m^2
A_R	Reservoir area	m^2
A^i_m	Monthly water allocation	m^3
A	bottom area of the hydropneumatic tank	m^2
B^i	Battery capacity	kWh
B^{i-1}	Previous battery capacity	kWh
B^i_c	Battery charge	kWh
B^i_d	Battery discharge	kWh
B^i_e	Battery discharge for energy needs	kWh
B^i_p	Battery discharge for pump station	kWh
B_{max}	Maximum battery capacity	kWh
C^i	Grid costs	€
E^a	compressed air energy	kWh
E^i_+	Energy surplus	kWh
E^i_-	Energy deficit	kWh
E^i_c	Energy consumption	kWh
E^w_p	water potential energy	kWh
H^i	Feasible hydropower/Hydropower generated	kWh
H^H_i	initial head in the hydropneumatic tank	m
H^H	Hydropneumatic head	m
H_p	Average pump head	m
H_t	Average turbine head	m
H^i_{need}	Required hydropower	kWh
P^i	Total pump energy	kWh
P^H_f	final pressure in the hydropneumatic tank	bar
P^H_i	initial pressure in the hydropneumatic tank	bar
P_N	Pump station nominal power	kWh
P^i_S	Available renewable energy for pump	kWh
$P^i_{A/B}$	Possible alternative energy for pump	kWh
$P^i_{F-A/B}$	Feasible alternative energy for pump	kWh
P^i_{F-S}	Feasible renewable energy for pump	kWh
P	air pressure inside the hydropneumatic tank	Pa
R^i	Grid revenue	€
S^i	Solar energy	kWh
S^i_S	Solar surplus	kWh
S^i_{S+W}	Renewable surplus	kWh
T^i_b	Grid purchase tariffs	€$/kWh$
T^i_s	Grid sell tariffs	€$/kWh$

V^{air}	air volume inside the hydropneumatic tank	m^3
V^{water}	water volume inside the hydropneumatic tank	m^3
V_R^0	Initial reservoir volume	m^3
V_R^i	Reservoir volume	m^3
V_R^{i-1}	Previous reservoir volume	m^3
V_p^i	Pumped volume	m^3
V_t^i	Turbine volume	m^3
W^i	Wind energy	kWh
Z_i^H	initial water elevation in the hydropneumatic tank	m
Z_f^{LR}	final water elevation in the lower reservoir	m
Z_i^{LR}	initial water elevation in the lower reservoir	m
α	Hydropower factor	$[0, 1]$
β	Renewable factor	$[0, 1]$
η_p	Average pump+motor efficiency	%
η_t	Average turbine+generator efficiency	%
γ^{air}	heat capacity ratio	1.4
γ	Alternative factor	$[0, 1]$
ρ	water density	$998kg/m^3$
g	acceleration of gravity	$9.8m^2/s$
h_R^i	Reservoir level	m
i	Timestep	$seconds, hours, days, months$
u^i	Hourly wind speed	m/s
u_r	Rated wind speed	m/s
u_{ci}	Cut-in wind speed	m/s
u_{co}	Cut-out wind speed	m/s

Acronyms

BEP	Best Efficiency Point
BESS	battery energy storage system
CAES	Compressed Air Energy Storage
CERIS	Civil Engineering Research and Innovation for Sustainability
DE	Differential Evolution
ESS	Energy Storage System
FCV	Flow Control Valve
FSD	Fixed Speed Drive
GA	Genetic Algorithm
GC	Grid-connected
GD	Gradient Descent
GRG	Generalized Reduced Gradient
HES	Hybrid Energy Solution
HGL	hydraulic grade line
HRES	Hybrid Renewable Energy Solution
LCOE	levelized cost of energy
MG	Microgrid
ML	Machine Learning
NPV	net present value
NSGA-II	Non-dominated Sorting Genetic Algorithm II
NSWOA	Non-dominated Sorting Whale Optimization Algorithm
PHES	Pumped Hydropower Energy Storage

PHS Pumped Hydropower Storage

PSAT Power System Analysis Toolbox

PSH Pumped Storage Hydropower

PSO Particle Swarm Optimization

PV Photovoltaic

RE Renewable Energy

SA Stand-alone

TCV Throttle Control Valve

VSD Variable Speed Drive

VFD Variable Frequency Drive

Chapter 1

Introduction

1.1 Motivation

This Master's thesis examines the transition from traditional energy systems, highly dependent on fossil fuels, to Hybrid Renewable Energy Solutions (HRESs), to contribute to net carbon zero achievement and ensure a sustainable energy network. With rising renewable energy production and consumption, reliable energy storage solutions, such as Pumped Hydropower Storage (PHS), are essential to ensure the stability and flexibility of HRESs. Hybrid energy systems were modeled and studied to assess the impact of energy storage on the performance of intermittent renewable energy sources. With the development of this thesis, it has been possible to interact with real projects, contributing to the ongoing mission of sustainable energy solutions in today's research field, toward the energy transition in the near future.

1.2 Objectives and Contributions

The objective of this thesis is to study the performance and characteristics of pumped hydropower storage (PHS) and to develop a simulation and optimization model, capable of combining it with different energy sources, such as solar and wind, allowing the study of flexible and reliable energy solutions with storage capacity. PHS stands as an important solution for a stable and cost-effective storage mechanism, through the potential energy principle, induced by gravity and elevation. The developed model explores the feasibility of specific scenarios, based on an energy and water consumption analysis. It focuses on the simulation of the water-energy nexus balance, with the possibility of defining optimization algorithms to improve the sustainability of the system. The developed model makes three key contributions to the research field of hybrid renewable solutions: (I) development of a simulation model, HY4RES, that encompasses PHS, considering the water-energy nexus; (II) single and multi-objective optimization analysis; (III) model application to large and small-scale applications, demonstrating its flexibility and real-world applicability, assessing the economic and environmental advantages of HES.

1.3 Structure of the Thesis

The Literature Review, as Chapter 2, follows the present Introduction. It is divided into four sections, starting by stating the importance of enhancing energy storage systems. Then it presents the state of the art and the theory on PHS systems. Subsequently, Hybrid Energy Solutions (HESs), with pumped hydropower storage, are explored in terms of configuration, advantages, characteristics and status of recent research and projects. Finally, the literature review presents the existing algorithms for simulation and optimization methods to model and analyze hybrid energy systems. This thesis studies two optimization methods: Generalized Reduced Gradient (GRG) and multi-objective Non-dominated Sorting Genetic Algorithm II (NSGA-II).

In Chapter 3, Methodology, a detailed description of the developed work is presented. The first section relates to the analysis of the pumped hydropower storage, through laboratory and software environments. In this section, the pumped-storage element of PHS is characterized, regarding its hydraulic circuit specifications in the laboratory, to later be recreated in the software. The following section defines the HY4RES model, which is the main subject of this thesis. Its design and algorithm are explained, as well as the chosen optimization methods. Next, the last two sections of the methodology chapter present the two case studies, a large and a small energy system, defining their scenarios, optimization configurations, and economic and environmental parameters. Both case studies explore different scenarios and energy sources to assess their performance according to the defined consumption patterns.

Chapter 4, Laboratory and Simulation Results of PHS Systems, explores the storage performance of PHS systems, through experimental and software analysis. Both studies provide results for different initial configurations, assessing their similarity and characterizing the pumped-storage capability and efficiency.

In Chapter 5, Irrigation System - large-scale case study, the first case study analysis is presented. It details the input data to configure the designed model with the system characteristics for each energy source and consumption pattern. The model is optimized for different optimization configurations to explore the technical, economic and environmental aspects of the system.

In Chapter 6, Energy Community - small-scale case study, the input data and optimized results are presented. It assesses the economic viability of different system configurations, primarily classified by stand-alone or grid-connected, depending if the external grid is integrated or not. This case study is crucial for understanding the scalability and flexibility of hybrid energy systems with PHS in community-level energy management.

Finally, the last and Chapter 7, Conclusions and Recommendations, presents the main conclusions drawn from the obtained results and states recommendations for future work. Through this structured approach, the thesis aims to explore the integration of intermittent renewables with PHS, offering both experimental insights and software modeling applications to study the enhancement of the sustainability and efficiency of these solutions, under different applications of the water-energy nexus.

Chapter 2

Literature Review

In recent years, the imperative to reduce emissions and mitigate environmental impact has propelled advancements in the research, development, and implementation of various renewable energy systems. To face the environmental consequences provoked by fossil fuels and shift into a sustainable future, it is mandatory to adopt renewable energy sources [1–3]. As renewable energy production increases, a new challenge emerges: intermittency and reliability. The fundamental renewable energy sources, such as wind and solar, are characterized by their intermittency. The availability of solar energy is restricted to daylight hours, whereas wind energy exhibits considerable fluctuation throughout the day. This phenomenon presents a challenge to the integration and stable connection of these sources with the national electric grid [4].

To address the issue of intermittency, it is essential to develop resilient energy storage systems, that can work in conjunction with renewable energy sources. This hybridization ensures the optimal fulfillment of the service needs. Energy storage combined with renewables can provide stable energy output and be appropriate to feed the electric grid [5]. There are various types of energy storage, and pumped hydropower storage (PHS) presents as one of the suitable solutions for the problem of renewables intermittency [4].

2.1 Pumped hydropower energy storage

Pumped Hydropower Energy Storage (PHES) is an energy storage method that possesses two modes of operation: water/energy storage and energy production. The pumped-storage element of PHS systems is responsible for pumping water to a higher elevation, where it can be stored in a reservoir, hydropneumatic vessel, or pond. When water is pumped uphill, the height gain results in an accumulation of gravitational potential energy. This energy stored can later be discharged downhill and generate energy through a water turbine (hydropower). Figure 2.1 shows a large-scale pumped hydro storage facility, that uses a river as a water source and an elevated man-made reservoir [6]. In addition to open reservoirs, hydropneumatic vessels can also be utilized for water storage, employing compressed air, designated as Compressed Air Energy Storage (CAES). Despite their reduced volume capacity in contrast to common open reservoirs, they are capable of producing high hydraulic heads, by air compression, suitable for hydropower generation. This attribute is particularly advantageous for applications where energy consumption is the primary concern over water needs while saving in storage area and costs.

Figure 2.1: La Muela II Pumped Hydropower Storage Plant, Spain

Unlike batteries or other thermochemical and electrochemical storage techniques, pumped hydro storage systems do not require rare and expensive materials. Pumped hydro storage systems enable a versatility of operation strategies, for example maximizing profit, by pumping water for storage during low-cost hours of the day and producing energy when it is more expensive to save on grid imports [7]. Additionally, this flexibility of operation allows the integration with renewable energy sources, enabling the storage of excess green energy, hydropower production in periods of renewable scarcity and selling energy to the electric grid [4]. The reservoirs can be rivers, basins, tanks or dam reservoirs. The primary requisition imposed by PHS systems is the geographic location, which demands a suitable elevation variation to allow this type of technology integration. In 2024, there are approximately 200 GW of installed Pumped Storage Hydropower (PSH) capacity, worldwide. It accounts for 93% of the existent energy storage capacity, spreading across almost 50 countries [8]. However, due to the fast growth of renewable energy, PHS plants must overcome their location requirements and keep up with the growth of green energy. Therefore, research in recent decades focused on exploring the possibility of implementing PHS systems in old mines, caverns, un-powered dams and conventional hydroelectric plants [3] [9].

Apart from batteries, whose usage is rising for mobility, small and large-scale storage, pumped hydropower storage systems allow the usage for bi-consumption applications more efficiently. While batteries are restricted to energy management, PHS plants can store potential energy and water, managing two consumption needs in one storage unit. This versatility and capacity enhance the potential of PHS applications, in many different areas, such as industry, drinking systems, agriculture, communities (small or large), among others. The maturity, flexibility, energy cost and lifetime of PHS plants are crucial advantages compared to other methods of energy storage [10]. Additionally, battery lifetime may compromise hybrid energy systems, e.g. photovoltaic plants, whereas pumped hydro storage is more robust and easier to monitor and maintain in remote areas [11].

2.2 Hybrid renewable energy systems with PHS

Pumped hydro storage (PHS) capabilities as a solid energy storage solution are clearly stated. However, its full potential is not achieved by singularly implementing it. Combining with other renewable energy sources maximizes the potential of PHS systems and other energy sources, towards a sustainable energy solution. A hybrid renewable energy solution (HRES) can contribute to reducing greenhouse gas emissions and stand independent from traditional energy sources, like fossil fuels that still occupy a significant share of the electric grid energy. Several research studies have analyzed the implementation of pumped hydro storage (PHS) with other renewable sources, either exclusively wind, solar, or both.

Many renewable and conventional generation and energy storage sources are available, enabling the improvement of water-energy needs to accommodate diverse load requirements. It is regarded as the most suitable method for combining technologies into a single reliable operational platform, thereby enhancing the potential of each implemented energy source [12–16]. The emergence of autonomous Microgrid (MG) technology has a profound impact on the assessment of the advantages and drawbacks of renewable energy sources application in different sectors, especially with pumped hydro storage as an Energy Storage System (ESS) [10, 17, 18]. In order to achieve a cost-effective and sustainable solution at an optimal size in terms of water and energy needs, power installed from intermittent sources like wind and solar, pumped hydropower storage, reservoir volume, grid connection, or stand-alone solutions are required. Nevertheless, this is a challenging undertaking due to the numerous variables and constraints, which depend on the complexity of each system. Available power supply components, local resources data, technical and economic indicators information, cost specifications, and load profiles must be provided. Undersizing may result in unsuccessful operations and a demand that remains largely unmet. However, the level of reliability remains high through oversizing, although this may result in significant system costs contrary to the objective of this research [19–21].

The majority of studies examining hybrid energy systems with PHS are centered on its integration with photovoltaic energy, with the possibility of electric grid or battery assistance. Proposed solutions combining solar and PHS have a significantly reduced environmental and social impact, with minimal waste and water resources exploitation, while reducing greenhouse gas emissions. Moreover, hybrid systems comprising the two mentioned sources are adaptable to diverse climates, hydrological conditions, and geographic and geological settings [22–25]. Further research assesses the resilience of PV-PHS systems across varying climates, indicating that the integration of pumped hydro storage enhances the reliability of the photovoltaic farm, thereby ensuring demand satisfaction [26]. Renewable energy sources, such as wind and solar, highly benefit from pumped hydro storage, as the complete hybrid system is flexible to consumer load demand and reduces the cost of power generation [27].

Stand-alone hybrid renewable energy solutions are gaining interest, with research studies examining systems that integrate photovoltaic, pumped hydro storage (PHS), wind and battery technology to be ap-

plied in remote or off-grid locations. The integration of PHS plants in off-grid solutions offers a significant advantage over batteries, as they are capable of managing both energy and water consumption in certain applications, such as those serving small communities. The capacity inherent to PHS systems allows for optimal implementation in stand-alone systems with multi-consumption variables, including energy, water consumption and irrigation [11, 28]. The integration of pumped hydro storage has proved to increase the reliability of intermittent renewable sources, providing a stable power supply in remote areas, through sustainable hybrid solutions [29, 30]. However, batteries can supply consistent peak power during periods of high demand, which may present a challenge for PHS systems. In terms of their contribution to greenhouse gas emissions, primary energy industries, such as fuel refineries, are among the most significant sources. Recent research has invested in the analysis of integrating hybrid renewable energy systems in the industry sector to reduce the emissions footprint while ensuring power supply stability and resilience through energy storage [31]. Large-scale primary energy industries are a significant source of pollution and exert a considerable impact on the resource stock balance. For instance, the coal processing industry plays a substantial role in the energy and metallurgical sectors, accounting for 40% and 70% usage, respectively. A recent study, [32], investigates the potential of implementing wind, solar and hydro energy with coal-process units to reduce carbon emissions during the transformation of coal to chemicals. The integration of hybrid energy sources into the process industry can mitigate the impact of the combustion of fossil fuels. According to [32], renewable sources can boost the clean production of hydrogen from coal to the syngas production process and enable less environmental impact on the generation of refined chemicals, i.e. ammonia and methanol.

In Portugal, a large-scale hybrid energy system located in Alqueva has been upgraded over the years to improve its sustainability and energy production and storage capacity. Starting with a 520 MW hydroelectric power plant with an artificial reservoir, it has been transformed into a pumped hydropower storage system using Francis turbines that are capable of operating in reverse mode, i.e. pumping water. In addition, it has various mini-hydroelectric power stations [33]. Recently, a 4 MW floating photovoltaic farm was installed on the upper reservoir. Floating photovoltaic panels have many advantages, such as saving land area, reducing evaporation and increasing the efficiency of the modules [34].

In the global breakdown of emissions, the agricultural sector represents the fourth largest source. The main source of CO_2, is around 13%. Moreover, over 70% of the world's freshwater is withdrawn for agriculture, to enable the cultivation of crops such as fruits, vegetables, and grains in the water-energy-food nexus [35, 36]. To increase water-energy efficiency, a variety of strategies have been investigated. The division of district pressure areas into water networks based on their needs for water flow and pressure has been proposed as a means of reducing energy consumption in several studies. For example, in Andalusia (Spain), irrigation district sectoring was also implemented for olive production, resulting in a reduction of roughly 30% in energy consumption. In light of the necessity to advance more sustainable

water-energy networks concerning natural resources and enhanced social well-being, managers and stakeholders are allocating resources towards the development of renewable energy systems. Several renewable energy technologies have recently been incorporated into pressurized water systems to lower energy needs and associated greenhouse gas emissions. Specifically, the authors in [37–39] developed a real-time model (Smart Photovoltaic System Manager) to match the energy requirements of an irrigation system in Southern Portugal and Spain with the availability of Photovoltaic (PV) power. Hybrid energy solutions (HESs) are well suited for rural agricultural areas, process industry productions, and drinking and wastewater systems, due to their ability to combine multiple conventional and renewable energy sources into a dependable and economical electricity supply. The integration of diverse energy sources into HES represents a powerful approach to establishing a sustainable energy supply paradigm, flexible and optimized. HES effectiveness is contingent on careful planning and consideration of several variables, including the desired rate of water needs, operation schedule, and weather conditions [40–42].

In addition to heavy greenhouse emissions contributors, like industry and agriculture, the impact on communities also requires the attention of new hybrid energy solutions to improve efficiency, sustainability and grid independence. [43] examines the potential of hybrid renewable energy solutions (HES) to support coastal communities, with a particular focus on microgrids as a solution for remote locations. Solar and wind energy sources were integrated with hydropower and pumped storage to serve as the means of energy storage and a buffer for renewable intermittency. The proposed system is designed to meet the community's energy and water needs while providing affordable and clean energy. The expansion of water-energy consumption, industry, and food demand, coupled with improvements in the global supply chain presents a multitude of opportunities and incentives for the integration of Renewable Energy (RE) sources. This integration is crucial for the effective mitigation of climate change and the efficient management of water and energy resources. The necessity for diversifying the water sector needs [44–47], can be met by the establishment of a microgrid (MG), which serves as a solution for integrating distributed intermittent and unpredictable energy sources, using optimized models towards a flexible operation.

2.3 Simulation and optimization models of hybrid energy systems

To study the feasibility of a new project that aims to explore the hybrid solution of pumped hydropower storage with other energy sources, it is crucial to develop models to simulate the behavior of the desired HES and optimize it. Hybrid energy systems with PHS as the main energy storage mechanism increase the potential for the water-nexus realm. However, most optimization studies focus on the energy consumption. It is necessary to optimize the hybrid systems for both consumption factors, analyzing the water supply patterns and long-term reliability for applications with heavy water needs, such as urban

areas, agriculture or drinking systems [48]. Some research resources to very complex and powerful tools that simulate and optimize power systems extensively. Tools such as Simscape and Power System Analysis Toolbox (PSAT), on Matlab, can be used to assess hybrid energy systems, such as wind energy combined with pumped hydro storage [49]. This method of simulation is focused on control systems and electronic components sizing/configuration to assess the stability of the power supply in the hybrid system, to ensure the appropriate connection between energy sources.

In contrast to dedicated control and power systems toolboxes, the hybrid energy systems may also be modeled and optimized by specific algorithms, including those written in C++, Matlab, Python, and other languages. This approach typically prioritizes an examination of the energy balance and the intercommunication between system components, rather than an investigation of power control and electronic design. These algorithmic models have the advantage of high flexibility for simulation and optimization. A variety of optimization algorithms may be implemented to attain the desired performance objectives of hybrid energy systems, as enumerated below:

- Differential Evolution (DE),
- Generalized Reduced Gradient (GRG NonLinear from Solver tool),
- Genetic Algorithm (GA),
- Gradient Descent (GD),
- Machine Learning (ML)
- Non-dominated Sorting Genetic Algorithm-II (NSGA-II)
- Non-dominated Sorting Whale Optimization Algorithm (NSWOA)
- Particle Swarm Optimization (PSO)

It is not necessary for the modeling of hybrid energy solutions (HES) and optimization to be conducted using a single software or algorithm. Conversely, the utilization of multiple sources serves to augment the efficacy and prospective of the devised hybrid energy solution. Notable commercial software, such as HOMER is highly regarded for its accessibility to hybrid energy system studies, particularly those focused on energy load-based systems. [43] proposes a hybrid energy solution for small communities. This solution is based on the modeling, simulation and optimization of three different engines. HOMER, Matlab, and Excel. This versatility permits a more intricate analysis and investigation of the capabilities of each software/algorithm for studying hybrid energy systems, despite their complexity. This multifaceted approach was employed in this thesis for the modeling and deployment of hybrid energy solutions. The model developed follows similar approaches found in the presented literature, for example, the technical simulation and optimization by hourly timesteps, evaluating each energy source contributions and constraints [29].

Chapter 3

Methodology

This work aims to study the performance of pumped-hydro storage technology and evaluate its implementation with other energy sources, to analyze their integration, symbiosis and capabilities. First, pumped hydropower storage's behavior is explored in laboratory tests and in the WaterGEMS simulation software, to analyze different hydraulic parameters and energy specs associated with the PHS operation. The ultimate goal is to develop a model capable of recreating a hybrid energy system, exploring different renewable energy sources, with pumped hydropower storage (PHS) portraying a vital role. The modeled hybrid energy systems were designed to meet both energy and water needs for applications such as agriculture, industry, water treatment or small energy communities.

3.1 Experimental and simulation of PHS systems

Prior to the definition and development of the mathematical algorithmic model, it is essential to conduct an in-depth analysis of the behavior of the pumped storage system itself. Accordingly, the following Chapter 4, examines the principles of PHS through experiments conducted at the IST-Hydraulic laboratory research center (Civil Engineering Research and Innovation for Sustainability (CERIS)); and through software simulations in WaterGems. In both experimental and virtual software universes, storage capacity tests were performed to characterize the system behavior of pumped storage in the laboratory. The storage capacity tests consist of the registration of the pumped volume, energy consumption, efficiency, general hydraulic parameters, and pump performance, measured in energy per volume units.

The Chapter 4 objective in the scope of this work is to establish key parameters, serving as the primary study of the pumped hydropower storage solution to take into consideration in the design of PHS systems, especially in hybrid energy solutions, with flexible and oscillating behaviors. In the following chapters, the definition of PHS systems is based on the conclusions and knowledge retrieved from the laboratory study.

3.1.1 Laboratory pumped-storage definition

The laboratory's pumped-storage system is limited by the lower reservoir and the hydropneumatic tank. The pipeline is made of ductile iron ($C_{hazen-williams}$ =130) with a nominal diameter of 50 mm. The pumped-storage circuit in the IST-Hydraulic CERIS laboratory is depicted in Fig.3.1.

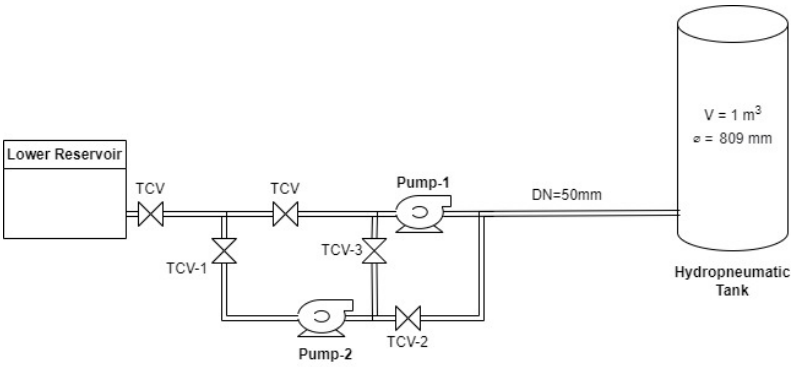

Figure 3.1: Laboratory's Pumped-Storage scheme

Its total length via pump-1 and pump-2 is 5.1 and 6 meters, respectively. The lower reservoir, Fig.3.2(a), composed of two tanks, has a total area (A^{LR}) of 1.606 m^2 and a height of 0.70 m. It is elevated from the ground 0.10 m, approximately; and the outlet pipe location, which connects the reservoir to the pumped-storage system, is installed at the bottom of the reservoir. The maximum volume of the reservoir makes up to 0.964 m^3. Due to the small volume available at the lower reservoir, it is not an infinite source, i.e. a river, nonetheless, it is sufficient for storage experiments in a lab small-scale system and defined time interval.

(a) Lower reservoir + Pumps

(b) Hydropneumatic Tank

Figure 3.2: Laboratory's pumped-storage station

The hydropneumatic tank, presented in Fig.3.2(b), has the function of simulating an upper reservoir with great elevation at a laboratory scale. Therefore, the hydropneumatic uses compressed air inside it to increase the potential energy represented through the hydraulic grade line. Table 3.1 presents the main characteristics of the hydropneumatic tank.

The pumped-storage system has two 4kW Grundfos pumps, of fixed rotational speed (imposed by the grid frequency), identified as in Fig.3.3. Further specifications of the pumps are presented in Table 3.2.

Table 3.1: Hydropneumatic Tank Carachteristics

Volume Capacity [m^3]	1
Diameter [mm]	809
Maximum Pressure [bar]	13
Compressed Gas	Air

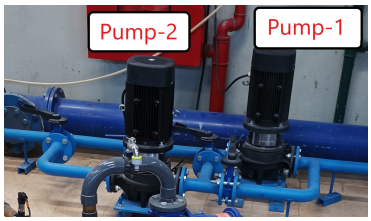

Figure 3.3: Grundfos Pumps

Table 3.2: Pumps hydraulic and electrical specifications

Nominal Flow Rate [m^3/h]	31.3	Rated Power [kW]	4
Nominal Head [m]	28.2	Frequency [Hz]	50
Shut-off Head [m]	35.8	Rated Voltage [V]	3x 380-415
Maximum Flow [m^3/h]	38	Rated Current [A]	8
Head @Max. Flow [m]	24.3	Rated speed [rpm]	2910-2930
Maximum Pressure [Bar] @140ºC	16	Motor Efficiency [%]	88.5

Additionally, the characteristic, efficiency and power performance curves of the pumps are provided by the manufacturer and presented in Figures 3.4 and 3.5, with the Best Efficiency Point (BEP) highlighted. This information is key in the simulation section 3.1.2, where it is necessary to calibrate the pump curves in the WaterGEMS model to properly recreate the conditions of the laboratory.

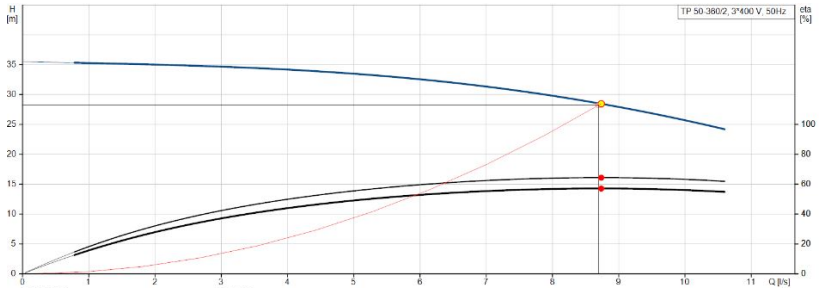

Figure 3.4: Characteristic curve

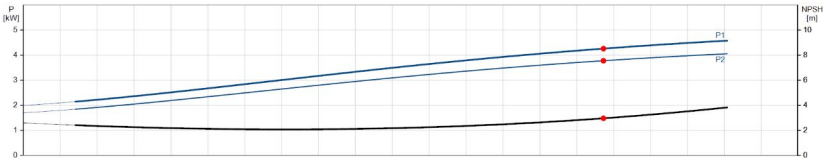

Figure 3.5: Power curve

3.1.2 Pumped Hydropower Storage simulation

The Laboratory pumped-storage system was later reproduced in the WaterGEMS software, enabling a more complex study of the process for comparison with the experimental results produced in the laboratory. With this, it is possible to enhance hydraulic circuits and bypass the limitations associated with physical experiments.

The hydraulic circuit, Fig.3.6, designed in WaterGEMS replicates the laboratory pumped-storage system. Parameters such as pipe length, material, headloss coefficients, diameter, pump characteristics, and reservoir levels were defined according to the laboratory setup, obtaining an identical virtual twin model. The pump curves provided by the manufacturer were extrapolated to the software to precisely reproduce the existing pumps in the laboratory.

As shown in Fig.3.6, the pump used for the main storage capacity simulations was **Pump2**. Additionally, the configuration of both pumps in series is simulated to explore the maximization of energy storage in the hydropneumatic tank by air compression, induced by the hydraulic head. The **lower reservoir** is set with an initial water level of 0.5m and a total area of 1.606m^2, simulating the two existent tanks in the laboratory as one single open tank in waterGEMS. The **pipelines** have a constant diameter of 50mm and the same material, ductile iron (Hazen-Williams coefficient = 130). The type of valves used in the system simulation are Throttle Control Valves (TCVs), which allows the regulation of the flow in the hydraulic circuit and adjusts the head loss coefficient according to the closure percentage of the valves. With Flow Control Valves (FCVs) it would not have been possible to manipulate this on WaterGEMS. The throttle control valves, **TCV-1**, **TCV-2** and **TCV-3**, are configured according to the manufacturer's datasheet (Sylax DN50 Butterfly valves); using a fully open discharge coefficient of 0.0036 and a calibrated valve characteristic curve, which determines the discharge coefficient variation according to the closure percentage.

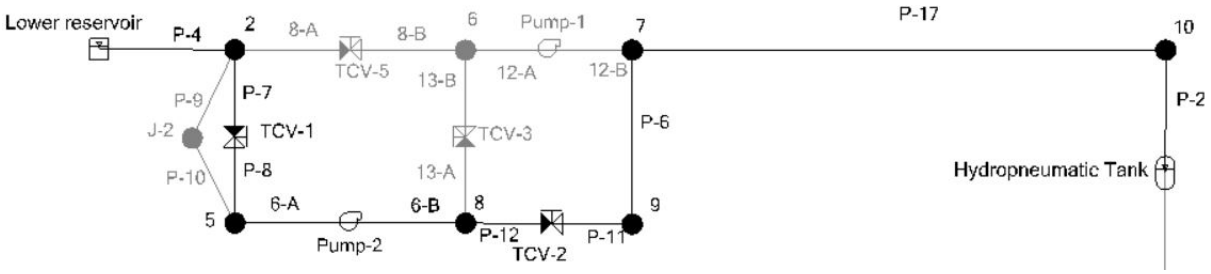

Figure 3.6: PHS system in WaterGEMS

As in the laboratory experimental tests for the storage capacity, in waterGEMS, the system was simulated for different hydraulic heads in the hydropneumatic tank, with different valve closures. The executed simulations are distinguished by the initial head in the tank, designated as H_i^H, which represents the piezometric and pressure head in the tank at the beginning of each test. The values of H_i^H are 5,

10, and 20 m, respectively. A variable closure pattern is tested in each head simulation, exploring the variation of flow and head loss induction on the pumping behavior. Therefore, three valve patterns are used for each single pump simulation: 0% and 34% closure, both fixed and one variable closure, framed linearly throughout the pumping process, starting fully open.

For the analysis of two pumps in series, the simulation starts with a single active pump, consistent with the other simulations. Nevertheless, when the hydropneumatic vessel reaches a head superior to the maximum operating head of a single pump, the second (Pump-1) is added, in series to increase the total pump head of the circuit. A fixed 0% closure setting was used throughout the simulation of the pumps in series, for **TCV-2**, when only pump-2 was in operation, and **TCV-3** when the circuit transitioned to the two pumps in series. The second path, through TCV-3, could have been used since the start of the simulation, with pump-1 deactivated. However, it may present risks to the safety of the pump due to the static resistance of the impeller and transient effects. Alternatively, both pumps in series could start in operation, but it would increase the total energy consumption by both pumps and reduce storage efficiency.

The efficiency of the pumped-storage system and the energy stored in each trial were evaluated for the laboratory and simulation results. The total control volume of the hydropneumatic tank can be divided into the control volume of air (at the top) and water (at the bottom). The variation of the gravitational energy of the water inside the tank corresponds to the elevation difference, as a consequence of the pumping process. The initial and final gravitational potential energy of water is computed with eq. (3.1) [50].

$$E_p^w = m.g.h = \rho.V^{water}.g.h = \frac{\rho.g.(V^{water})^2}{A} \cdot \frac{1}{3.6\,10^6} \tag{3.1}$$

where E_p^w is the water potential energy, in kWh; ρ is the water density, equal to 998 kg/m^3; g is the acceleration of gravity, equal to 9.8 m^2/s; V^{water} is the water volume inside the hydropneumatic tank, in m^3; A is the cross-section of the hydropneumatic tank, in m^2.

The compressed-air energy variation corresponds to the work done by the pumping process to compress the air inside the hydropneumatic, expressed by eq. (3.2) [50].

$$W = \int_{V1}^{V2} P\,dV = \int_{V1}^{V2} \frac{constant}{V^n}\,dV = \frac{P_2.V_2 - P_1.V_1}{1-n} \tag{3.2}$$

This process is considered adiabatic ($n = 1.4$), with the measured variation of volume and pressure of the air control volume defined. The compressed-air energy within the hydropneumatic vessel is calculated with eq. (3.3), both at the start and end of the experiment/simulation, which correspond to each parcel retrieved from eq. (3.2). The sum of these two energy variations, water and compressed air, results in the energy stored on the hydropneumatic vessel by the pump operation. The results of the storage efficiency

assessment are presented in section 4.2.4.

$$E^a = \frac{P.V^{air}}{\gamma^{air} - 1} \cdot \frac{1}{3.6\,10^6} \tag{3.3}$$

where E^a is the compressed air energy, in kWh; P is the air pressure inside the hydropneumatic tank, in Pa; V^{air} is the air volume inside the hydropneumatic tank, in m^3; and $\gamma^{air} = n$ is the heat capacity ratio, equal to 1.4.

3.2 Hybrid energy solutions for water-energy nexus

The subsequent stage of this work entails the modeling of hybrid energy systems. The pumped-hydro storage technology is integrated alongside other energy sources, including photovoltaic, wind, grid and batteries. The model developed was created using Solver-Excel and Python in order to enhance its flexibility, computational power and potential for optimization algorithms. In Solver, the available optimization methods are limited to two: GRG-NonLinear and Evolutionary. The LP Simplex method is not valid in this context, as the problem described by this type of model is nonlinear and of considerable iteration complexity. In Python, however, the model has an open border to multiple optimization algorithms. The developed model is presented in section 7.2.

3.2.1 Mathematical modeling

The mathematical formulation represents the logical core setup of the model, delineating the relationship and operational methodology. It is of paramount importance to define the symbiotic relation between the various energy sources and to elucidate how they function in order to satisfy the system's needs.

3.2.1.1 Timestep definition

Concerning the temporal resolution of the system, the default approach, based on existing literature, is to utilize hourly units. This entails that the model performs the computations of the presented parameters, balances, and iterations on an hourly basis. Nevertheless, should greater or lesser temporal precision be required, this can be modified to months, days, or even seconds. It is necessary to update the energy collected data, such as solar/wind generation, to respect the used time increment. The designated index for the timestep is the letter (i) in superscript, as presented in the majority of the parameters of the mathematical modeling.

3.2.1.2 Consumption needs

The objective of the hybrid system model is to provide a feasible solution for activities that require two distinct forms of demand, energy and water. The model is designed for use in different applications, such as agriculture, industry, small communities or any other context where a dual demand, water-energy nexus, is required. Moreover, the application must be suitable for the incorporation of pumped hydropower storage systems, which represents the primary objective of this thesis.

The HES must be capable of satisfying energy needs. It may resort to primary renewable energy sources, such as solar and wind, or energy storage mechanisms, for example, pumped hydro storage (PHS) and Battery Energy Storage Systems (BESSs). The objective of hydropower, in a PHS system, is to compensate for the intermittency of solar and wind energy production. However, as the reservoir volume is not infinite and there are water consumption needs, the volume that can be turbine-based is not always feasible. Accordingly, the designed system is equipped with two auxiliary energy sources: Grid-connected (Alternative A) or Stand-alone/Batteries (Alternative B). These default alternatives can be altered into other energy sources, for example, hydrogen production/storage and diesel generators. The energy demand profile may exhibit fluctuations over time or remain constant, depending on the case to be studied. The attributed symbol to energy needs is (E_c^i), for each timestep.

The other system consumption requirement comes in the form of water supply. The water outflow is calculated based on the upstream reservoir, necessitating the optimal and strategic operation of the PHS station and subsequent overall system to fulfill the water requirements in a cost- and energy-efficient manner. The symbol attributed to water consumption is (A^i), derived from the Latin word *aqua*.

3.2.1.3 Photovoltaic energy

Solar energy is a primary renewable energy source that plays a significant role in the model's design. The generated power, in conjunction with other primary sources, such as wind, is accountable for the direct management of the system's energy balance and ensures the optimal fulfillment of energy requirements. Solar energy production data can be retrieved on public databases, such as PVGIS (SARAH3), so that the solar energy parameter (S^i) can be collected and processed, in kWh. Based on the retrieved solar energy generation for a given timestep, within a determined period, plus the energy needed values, the excess solar energy available can be computed with eq. (3.4) by the denominated Solar Surplus (S_S^i). This variable is only valid if there is no other primary energy source, such as wind.

$$S_S^i = S^i - E_c^i \ , \ If \ > \ 0 \tag{3.4}$$

If the solar surplus is not greater than zero, either it fully satisfies the energy needs and there is no energy wasted, or it is insufficient to satisfy energy needs, thus requiring compensation from other secondary

sources, i.e. the PHS system (hydropower) or auxiliary alternatives.

3.2.1.4 Wind energy

Similarly, wind turbines can be integrated into the model to generate supplementary renewable energy for the system's load and energy storage mechanisms, such as PHS. Wind power production data can be obtained from a variety of data tools/libraries/APIs, such as NREL or Renewables (Ninja), through manufacturer's power curves. Additionally, it can be estimated through the wind speed and selected height. The obtained wind energy production is framed to the desired timestep and period, (W^i), in kWh. The total primary (renewables) energy surplus, of solar plus wind, (S^i_{S+W}), can be computed, with the following eq. (3.5).

$$S^i_{S+W} = S^i + W^i - E^i_c \ , \ If \ > \ 0 \tag{3.5}$$

From here onwards, solar and wind surplus are summed and presented together as renewable surplus (S^i_{S+W}), in the mathematical modeling. Nevertheless, if one of the renewable sources is not to be considered, its raw value: S^i or W^i, is set to zero.

3.2.1.5 Pumped-hydropower storage (PHS) stations

The PHS station is designed to operate in either pump or turbine mode, never both simultaneously. The mathematical principles that govern the station's operational methodology are structured in a closed-loop logic iteration process. In the event that the solar and wind energy available in a specific hour is insufficient to satisfy the energy needs, the PHS is configured for turbine mode, with the objective of producing hydropower, expressed by eq. (3.6). H^i_{need} is the required hydropower energy to fulfill the remaining energy requirements, expressed in kWh. This approach is a **load-responsive generation** method, whereby the hydropower produced is contingent upon the unmet demand quantity. An alternative methodology could be employed, particularly in the case of dams or rivers, where the hydropower output remains constant (fixed flow rate) despite fluctuations in the unmet demand. Subsequently, if the generated hydropower exceeds the requisite amount, it can be sold to the electric grid or stored in a battery system.

$$H^i_{need} = E^i_c - [S^i + W^i], \ If \ > \ 0 \tag{3.6}$$

In the event that the energy needs are fully satisfied by solar and wind energy, and a surplus of this energy exists, the PHS is set for pump mode. This is achieved by using that same surplus to pump water to the upper reservoir, where it is stored as potential energy, expressed by eq. (3.7). P^i_S is the available renewable energy to be used by the pumps, expressed in kWh.

$$P^i_S = S^i_{S+W}, \ If \ > \ 0 \tag{3.7}$$

Regarding the reversed operation, the PHS station will only turbine when the water level in the reservoir is at a sufficient level, after accounting for the hourly water allocation requirements, A^i:

$$V_R^{i-1} - A^i - V_t^i \geq V_{min} \tag{3.8}$$

The variable V_R^{i-1} corresponds to the reservoir volume at the end of the previous hour and V_t^i to the Turbine volume, both in m^3. If eq. (3.8) is fulfilled, then the hydro turbine volume set is executable; if not, then it is zero for that hour in analysis. The turbined volume is computed by the following formula, eq. (3.9), based on [4, 9, 51].

$$V_t^i = \frac{\alpha.H_{need}^i.3600.10^3}{9800.\eta_t.H_t} \tag{3.9}$$

With the variable α representing the hydropower factor, a value between 0 and 1; H_{need}^i the required hydropower energy for energy needs, in kWh; η_t the average turbine+generator efficiency; and H_t the average turbine head. The feasible hydropower energy, H^i, is then equal to the multiplication of the hydropower factor by the required hydropower, which satisfies eq. (3.8) and eq. (3.9).

When the station is operating in the pump mode, the underlying principle remains analogous. The pump is only capable of transferring water into the upper reservoir if the reservoir's volume is sufficient to accommodate the requisite increment. Furthermore, the subtraction of water allocation, when required, is also considered.

$$V_R^{i-1} - A^i + V_p^i \leq V_{max} \tag{3.10}$$

The variable V_p^i corresponds to the pumped volume, in m^3. If the maximum volume condition, outlined by eq. (3.10), is adhered to, then the set volume for pumping can be executed. If not, there is no uphill flow during that specific hour. The pumped volume, V_p^i, is a function of the total feasible energy used by the pump station, P^i. The feasible energy for pump operation can be divided into two variables: the feasible renewable energy for pump (P_{F-S}^i) and the feasible alternative energy for pump ($P_{F-A/B}^i$), in kWh. The aforementioned variables are the result of the multiplication of their available/possible energy by a factor, as presented in the expressions eq. (3.11) and eq. (3.12).

$$P_{F-S}^i = \beta.P_S^i \tag{3.11}$$

$$P_{F-A/B}^i = \gamma.P_{A/B}^i \tag{3.12}$$

The potential alternative energy variable ($P_{A/B}^i$) is deemed equivalent to the pump station's nominal power when the grid-connected, designated as the alternative A, is considered. Consequently, eq. (3.12) derives into the eq. (3.13).

$$P_{F-A/B}^i = \gamma.P_N \tag{3.13}$$

When the Battery option is considered, designated as alternative B, eq. (3.12) derives into eq. (3.14).

$$P^i_{F-A/B} = \gamma.B^{i-1} \tag{3.14}$$

where B^{i-1} represents the energy stored on the battery system at the beginning of the hour (previous timestep final storage), in kWh. Further details on the alternative B - Batteries parameters are presented in section 3.2.1.8. The pumped volume is obtained through (eq. (3.15)), based on the literature [4, 9, 51].

$$V^i_p = \frac{P^i.\eta_p.3600.10^3}{9800.H_p} \tag{3.15}$$

It can be described in more detail by eq. (3.16):

$$V^i_p = \frac{(P^i_{F-S} + P^i_{F-A/B}).\eta_p.3600.10^3}{9800.H_p} = \frac{(\beta.P^i_S + \gamma.P^i_{A/B}).\eta_p.3600.10^3}{9800.H_p} \tag{3.16}$$

The multiplier β and γ represent the solar and grid/battery factors, respectively, with values between 0 and 1; P^i_S is the solar energy available for pumping; $P^i_{A/B}$ is the possible pump station energy consumption from one of the alternatives (either A or B); η_p is the average pump+motor efficiency; and H_p is the average pump head. The total energy used for pump operation, P^i, is equal to: $\beta.P^i_S + \gamma.P^i_{A/B}$.

Energy from solar and wind farms is always prioritized for pumping versus grid/battery energy, to follow the primary objective of the project, as sustainable and green energy systems. The considered available renewable energy for the pumps must exceed 20% of the nominal pump station power (P_N) and remain below this same parameter. The technical minimum of 20% serves to ensure the generation of valid results concerning average heads and efficiency, thereby avoiding possible deviations from reality. Depending on the number of pumps used, the minimum power set determines the feasible range of rotational speed variations [52]. The minimum limit for pump operation with renewable surplus serves, firstly, to avoid low efficiency and high energy consumption, inherent to real-world scenarios. In this work, the efficiency is fixed on an average value for simplicity reasons, but in reality, it varies according to the operation point of the pump, close to the selected value. Secondly, it restricts the operating window for renewable power to protect the pump station from renewable source fluctuation instability.

If this condition is not met, P^i_{F-S} is considered null, thereby allowing the excess renewable energy to be sold to the grid. To ensure that the renewable energy is prioritized, its feasible energy for pump (P^i_{F-S}) is initially iterated, and then the feasible alternative energy for pump operation ($P^i_{F-A/B}$) is determined, taking into account the pumped volume from the renewable energy share. Grid contribution for the pump station operation is only possible if its value, plus the available renewable energy for pump (P^i_S) multiplied

by its factor (β) is less than or equal to the nominal power (P_N). This is described by eq. (3.17).

$$P^i_{F-A/B} = \gamma.P^i_{A/B} = \gamma.P_N, \quad If \quad \beta.P^i_S + \gamma.P_N \leq P_N \tag{3.17}$$

Otherwise, no grid energy can be used. The grid factor is the decisive agent in evaluating whether the grid can or not contribute to the pump station operation.

If batteries are utilized instead of the grid-connected alternative, then the $P^i_{A/B}$ variable is indicative of the battery energy available at the inception of specific timestep (i), (B^{i-1}). γ is the decisive factor of how much battery energy is consumed by the pump station, yielding a feasible value to be used ($P^i_{F-A/B}$). Nevertheless, the nominal pump power must be respected in this alternative, through eq. (3.18).

$$P^i_{F-A/B} = \gamma.P^i_{A/B} = \gamma.B^{i-1}, \quad If \quad \beta.P^i_S + \gamma.B^{i-1} \leq P_N \tag{3.18}$$

3.2.1.6 Reservoir volume

The upper reservoir volume status is modeled at every timestep, wherein it represents the total volume at the conclusion of the selected time interval. Accordingly, the reservoir volume computation is performed subsequent to the assessment of the water consumption and hydro turbine/pumped volume parameters. At the start of the simulation period, the reservoir is assigned a fixed initial volume (V^0_R), while the subsequent timestep volumes (V^i_R) are iterated, in m^3, through eq. (3.19).

$$V^i_R = V^{i-1}_R - A^i - V^i_t + V^i_p \tag{3.19}$$

At any time during the simulation, the volume at the reservoir must respect the specified minimum and maximum limits. The eq. (3.19), considers two ports: (i) one of which can serve as an inlet or outlet. This refers to the pipeline used by the PHS station, which may operate in pump or hydro turbine mode, resulting in a change in the designation of this port; (ii) the other port is designated as a permanent outlet port, corresponding to the water consumption pipeline, and serves to connect the reservoir to a specific water consumption network, such as irrigation fields or other industrial applications, such as cooling units.

3.2.1.7 Alternative A: Grid-connected

When there is an excess of primary energy, whether not utilized for energy needs or by the pump station, it can be sold to the grid, resulting in a profit according to the tariff, which may vary on a monthly basis. The energy surplus (E^i_+), expressed in kWh, available for sale, is computed by eq. (3.20).

$$E^i_+ = S^i_{S+W} - P^i_{F-S} \tag{3.20}$$

The hourly profits (R^i), in €, can be calculated with eq. (3.21).

$$R^i = E^i_+ . T^i_S \tag{3.21}$$

T^i_s corresponds to the sell price, in €/kWh, depending on the month and period of the day/hour selected.

In scenarios where the primary energy and the hydropower produced are insufficient to meet the energy needs of the system, the variable of energy deficit emerges. There is the option to import from the grid the energy that is in deficit, E^i_-. It is calculated by eq. (3.22), in kWh. The grid energy used for pumping, $P^i_G = P^i_{F-A/B}$, is incremented, so it can be considered in the cost calculation.

$$E^i_- = [E^i_c - S^i - W^i - H^i,\ If\ >\ 0] + P^i_G \tag{3.22}$$

The hourly purchase costs (C^i), in €, can be calculated with eq. (3.23).

$$C^i = E^i_- . T^i_B \tag{3.23}$$

T^i_b corresponds to the hourly price of buying energy from the grid, in €/kWh, which only varies according to the month of computation.

3.2.1.8 Alternative B: Batteries

The second default alternative, a battery energy storage system (BESS), serves as an auxiliary energy storage mechanism for ensuring the system requirements are met when the primary/renewable sources are insufficient or there is a lack of the necessary installed power. It presents a stand-alone option for hybrid system solutions. The battery plant needs to have a defined maximum storage capacity (B_{max}), that can guarantee the supply of energy when solar, wind and hydropower are insufficient to meet energy demands or pump operation. Furthermore, it must account for the typical range of surplus renewable energy not used by the pumps and that can be stored in the batteries for subsequent use. The accurate and appropriate sizing of the batteries is a critical determinant of the self-sufficiency of the hybrid system as a stand-alone option. The amount of energy stored by the batteries at each timestep is represented, in kWh, by the symbol B^i.

The energy that can be charged, B^i_c, to the battery system is equal to the energy surplus, as described in eq. (3.20). The battery may discharge energy, designated as B^i_d, to the PHS system. This serves to complement the surplus of solar and wind energy to increase pumping capacity or satisfy the remaining energy needs. The energy required (discharged) from the batteries to the system is calculated by eq. (3.24).

$$B^i_d = B^i_e + B^i_p = [E^i_c - S^i - W^i - H^i,\ If\ >\ 0] + [P^i_{F-A/B}] \tag{3.24}$$

B_e^i represents the energy needed from the batteries for energy needs, in kWh; and B_p^i is the feasible battery energy to be used for pump operation, in kWh. To model the hourly battery storage capacity (B^i) the following computation method is used in eq. (3.25).

$$\begin{cases} B^i = B^{i-1} + B_c^i - B_p^i, & B^{i-1} + B_c^i - B_d^i < 0 \\ B^i = B^{i-1} + B_c^i - B_d^i, & 0 < B^{i-1} + B_c^i - B_d^i < B_{max} \\ B^i = B_{max}, & B^{i-1} + B_c^i - B_d^i > B_{max} \end{cases} \tag{3.25}$$

The stored energy in the battery system must never exceed the defined maximum storage capacity (B_{max}). Hereby, the system may not always discharge the required amount of energy deficit at a specific hour. This limitation justifies the reliability parameter pertaining to energy needs.

3.2.2 Model development for single and multi-objective optimization

Given the system's extensive versatility and complexity, stemming from the management of different energy sources, demands and constraints, it is imperative to identify the most optimized solution. Even minor alterations to the operation strategy over the course of the defined period can result in considerable discrepancies from optimal outcomes, which may have adverse effects on the economic assessment. Consequently, once the input data has been defined in the simulation model and the preliminary results have been calculated, several optimization iterations are conducted for each configuration, to improve results, in accordance with the specific defined optimization approach.

In this study, both single and multi-objective optimization techniques are investigated, in Solver tool (MS-Excel) and Python, respectively. The multi-objective criteria optimization algorithm employs the NSGA-II method, which is capable of selecting two objective functions and seeking the best solution to both criteria. It used the open-source framework/library, pymoo, to construct the multi-objective optimization algorithm with a pre-defined assembly for the NSGA-II method. Figure 3.7, summarizes the energy sources in play and their relationship, following the model defined in section 3.2.1. It is important to mention that the illustrated logic defining the model uses the upper reservoir for fulfilling water needs. Nevertheless, as the model possesses significant flexibility and customization potential, the water needs can be disassociated from the storage reservoir and directly accounted for as an energy consumption parameter. This is the scenario analyzed by the second case study presented in this thesis. Additionally, for the optimization configuration, the decision variables, objective function(s) and constraints can be modified and setup according to the user's goals for a certain hybrid energy system and application.

The integration of optimization methods in the model is fundamental to enhance the obtained solutions. Throughout the chapter concerning the large-scale case study, which explores different optimization algorithms and configurations to analyze their differences, it is clear the impact that one optimization method has on the final results and what consequences it originates on the economic assessment.

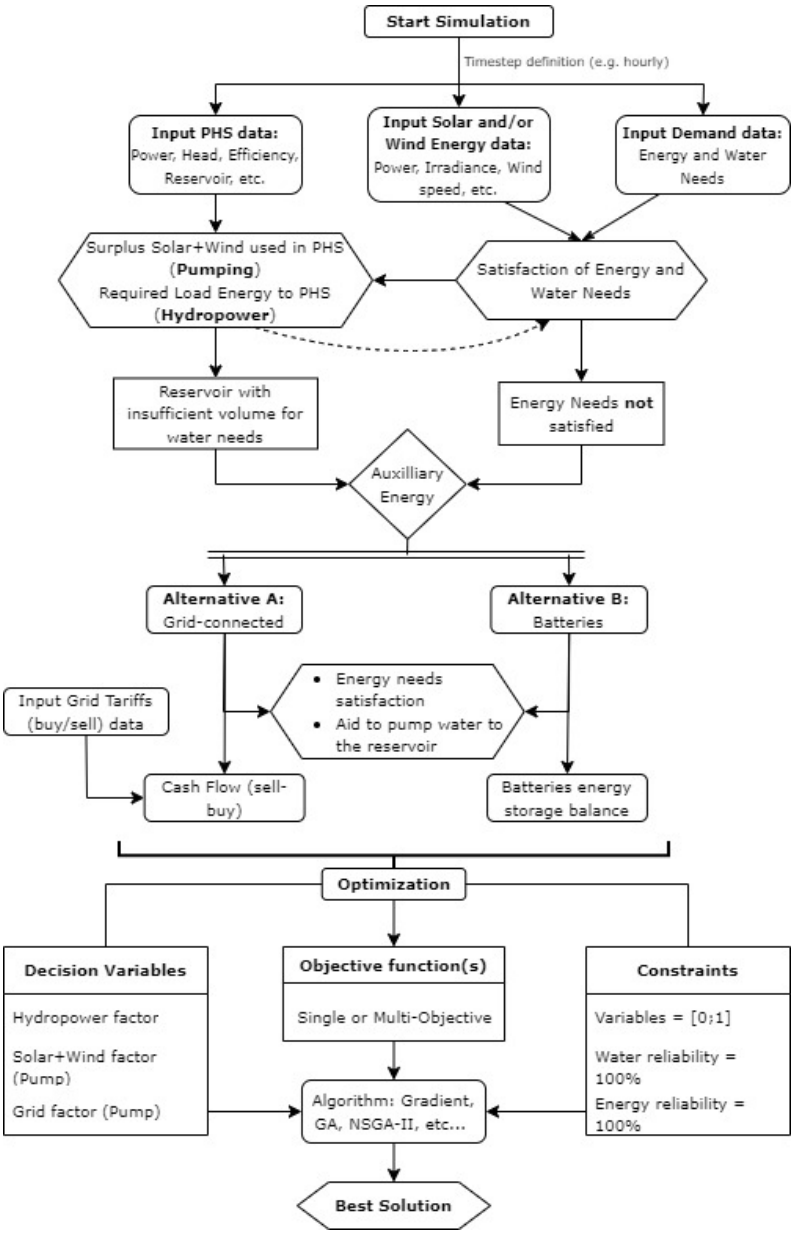

Figure 3.7: General Model for a Hybrid Energy System

3.3 Model deployment - Irrigation system

An irrigation system is used to analyze and simulate a hybrid system for large-scale applications. The input data collection and results are presented in detail in Chapter 5. The chosen irrigation field, the Genil Margen Izquierda Irrigation System, is located in Andalusia, in Southern Spain. The complex hybrid energy system uses agricultural activity to dictate its operational status and optimization approach. For the model deployment, it is necessary to define the energy sources used, before simulation and

optimization. Three scenarios have been defined; the first scenario, referenced as the main scenario (**Scenario 1**) uses solar, PHS and grid energy. The second scenario (**Scenario 2**) increments wind energy to the first scenario, hence, it possesses solar, wind, PHS and grid sources. The third and final scenario (**Scenario 3**), exploits the other presented auxiliary alternative, batteries, instead of the conventional national grid. Scenario 3, represents a hybrid off-grid renewable solution, maintaining solar and PHS sources while increasing wind power according to the optimization results. For the modeling of the irrigation system, the season was considered to begin on March 1 and end on September 30, with a timestep (i) of one hour. The **current approach** scenario for the irrigation system uses only grid power to meet its energy needs and to operate the pumps to deliver water to the upper reservoir. The irrigation system is immensely dependent on the reservoir balance throughout the season. Therefore, it is fundamental to satisfy the water needs for the irrigation activity and ensure the best operation strategy for the PHS system.

3.3.1 Optimization configuration

Using the Solver toolbox, with the implementation of the model in MS-Excel, depicted by figures 1A.1(a), A.2 and A.3, a single objective function optimization was performed, through the Non-Linear method of Generalized Reduced Gradient (GRG), which seeks better results through gradient patterns, making it very dependent on the initial settings for the decision variables. This provokes results that are mostly local best solutions. However, the multistart option was selected to improve the accuracy of the GRG Non-Linear method. The multistart option combines the fast computational power of the GRG method with the complexity and precision of the Evolutionary method in Solver, based on GA. With the multistart option, the optimization process has a higher probability of achieving a global solution.

The population size was set to 200, with no initial seed set; the convergence requirement was left unchanged from the default 0.0001. The decision variables are the hydropower factor (α), the grid factor (γ) and the solar factor (β). Set as constraints, all of these variables must take values between 0 and 1. In addition, a constraint of the total number of hours of no water consumption was set to zero, to enforce the satisfaction of the water needs, on the period of defined consumption. The model can optimize different parameters, according to the preferences and objectives of the project.

Regarding the optimization definition of the Solver for each water allocation, three initial optimizations were performed, for different objective functions, labeled as OPT1, OPT2 and OPT3 throughout this work. **OPT1**: Maximize the lifetime cash flow; **OPT2**: Minimize the consumption of grid energy used for pump operation; **OPT3**: Maximize the hydropower production. The cash flow is the difference between revenues (selling excess energy to the grid) and costs (buying energy from the grid). For scenario 3, it is necessary to add a second constraint, similar to the water needs reliability, but for the energy needs consumption, since with the replacement of the grid by batteries, the energy demand also becomes

susceptible to be satisfied or not. Additionally, for scenario 3, a different optimization configuration was adopted, **OPT4**: Minimize battery storage capacity, expressed in kWh. The goal of this objective function is to minimize the required battery capacity to be installed for the system to be self-sufficient and independent from the grid while ensuring minimal initial investment costs.

A multi-objective optimization algorithm was also developed in Python, **NSGA-II**, with two objective functions: Maximize hydropower production and Minimize consumption of grid energy used for pump operation. The NSGA-II algorithm was used to optimize the hybrid system applied to the case study for scenarios 1 and 2, listing 2 in the appendix. The objective functions were chosen to meet the project objective of reducing grid consumption and implementing a pumped hydropower storage system. Initially, the algorithm was designed to assign a decision variable to each hour and each factor, i.e. hydropower, grid and solar, with a total of about twenty-five thousand variables, which critically increases the computational time and requires an unnecessary complexity. Therefore, an approximation identical to the one used in Solver, i.e. variables allocated to periods of the day/month, is used to reduce the number of decision variables. Thus, 315 variables were used in the Python algorithm to manipulate the energy balance during the year. It corresponds to 105 variables for each factor, creating three matrices of 21x5, where the rows are periods of the month, i.e. months separated in three: 1-10, 11-20 and 21-30/31, and the columns refer to periods of the day, taking into consideration the period division of the grid tariffs used for the case study. The number of generations was set to 10 and the population size to 250 in order to produce sufficient solutions without increasing the optimization time. The biased initialization approach was adopted in this work, to improve the results from the NSGA-II algorithm. Since the simulation results could be obtained first and independently, an initial solution could then be used as a guide for the Python code. This helped to obtain better solutions that were able to satisfy the constraints. The biased initialization definition can be seen in Fig.2 from line 8 to 103.

3.3.2 Economic assessment

Once the results for different water allocations have been obtained and optimized, the annual energy and economic balance can be evaluated. For the selected case study, a lifetime analysis of 25 years is performed, assuming a constant water allocation each year. Regarding the economic aspect, the annual cash flow can be calculated using the following expression, eq. (3.26).

$$Cash\ Flow(n) = \sum_{i=1}^{k} Profits(i) - \sum_{i=1}^{k} Costs(i) \tag{3.26}$$

The cash flow corresponds to the total annual difference between profits and costs, where n represents the year under consideration; Profits(i) and Costs(i) are the hourly profits and costs, respectively. k is the total number of hours in the studied year. The defined cash flow corresponds to the balance between

grid sales (profits) and grid purchases (costs). However, in most cases, large photovoltaic investments in Spain are not allowed to sell energy to the grid for the first five years, in case they are subsidized by State/Commission funds. Therefore, the cash flow(n) in the first five years is only composed of the total annual cost portion. Thus, the cash flow part of the net present value (NPV) can be defined by eq. (3.27).

$$NPV_{CF} = CF_{[1-5]}.\frac{1-(1+r)^{-N1}}{r} + \frac{CF_{[6-25]}.\frac{1-(1+r)^{-N2}}{r}}{(1+r)^{N1}} \tag{3.27}$$

where the NPV_{CF} corresponds to the cash flow parcel of the net present value, in €; CF_{1-5} is the yearly cash flow on the first five years, in €; CF_{6-25} is the yearly cash flow after year 5, in €; r is the discount rate, equal to 10%; N1 corresponds to the first period of years, 5; and N2 to the rest of the lifetime, 20 years.

It is necessary to consider initial investment, operation and maintenance (O&M) costs, and taxable CO_2 emissions. The irrigation system already has a pumping station, so there are no required investments regarding new pumps, reservoirs, pipelines, or significant valves. However, the conversion to Variable Speed Drive (VSD)/Variable Frequency Drive (VFD) pump operation is being considered because the energy coming from the photovoltaic panels and/or wind turbines is intermittent and rapidly changing. A traditional Fixed Speed Drive (FSD) pump could still operate with renewable energy integration but in a much more restrictive and inefficient strategy. Since a fixed rotational speed pump would have only a single characteristic curve, it would greatly reduce the operating window, which would be determined solely by the intersection with the hydraulic system's curve. This performance is in line with the current approach of powering the pumps, only from the grid, at a fixed frequency, and only adjusting the power supplied, through the substation or through hydraulic valve control to manipulate the system curve.

Power control with hydraulic valves is subject to transient conditions and material wear, which can significantly increase costs over the life of the project; in an environment of fluctuating power supply and constant demand oscillation as it is characterized by the hybrid solution. Power control with a VSD/VFD mechanism can be done with suited electronic controllers, which despite their higher initial investment, are more robust and precise to the transient characteristics of renewable systems.

Therefore, the choice of variable speed drive (VSD) pumps for the hybrid solution is clear to match its flexibility and operation to the fluctuating renewable source and demand, maximizing efficiency and minimizing energy consumption for the desired flow. The conversion of fixed speed drive (FSD) pumps to VSD, with the implementation of control systems, requires an initial investment. In addition, for the main scenario, scenario 1, the initial investments were the implementation of PV panels, inverters and turbines for hydropower generation. In scenario 2, the wind turbine component must be added, as well as the BESS component in scenario 3. Grid operation and maintenance costs have not been included as valid

and consistent values could not be obtained. Nonetheless, their impact is minimal when comparing the grid-connected scenarios (1 and 2) with the off-grid solution (scenario 3). Table 3.3 presents the overall economic parameters used in the economic evaluation of the irrigation case study.

Table 3.3: Economic parameters of the irrigation system

Solar Energy	[10, 53]
Installed PV Capacity	9,000 kW
C_{inv}_PV	850 €/kW
O&M_PV	8.5 €/kW/year
Inverters (DC/AC) x26	GW350K-UT 1500 Series
DC Power	350 kW
C_{inv}_Inverter	8,000 €
O&M_inverter	1%
Subsidies	50 %
Wind Energy	[37, 54, 55]
Model Turbine	Vestas V110-2.0 MW
Nº of Turbines	2 (scenario 2)
Installed Capacity	4,000 kW (scenario 2)
C_{inv}_WT	1,200 €/kW
O&M_WT	15 €/kW/year
Subsidies	50%
PHS (Pumped Hydropower Storage)	[18, 53, 54]
Turbine Station Installed Capacity	1,000 kW
C_{inv}_Hydro	1,500 €/kW
O&M_Hydro	20 €/kW/year
Pump Station Installed Capacity	7,400 kW
C_{inv}_VSD/VFD (Pumps alterations)	740,000 €
O&M_Pump	10 €/kW/year
Reservoir Capacity	261,000 kWh
BESS (Battery Energy Storage System)	[56]
C_{inv}_BESS	300 €/kWh
O&M_BESS	15 €/kWh/year
Additional parameters	
Lifetime of the project	25 years
Interest rate - r	10%

A major difference between the current approach (grid plus the pumping station) and the proposed hybrid solution is the environmental impact and the impact on sustainability and grid independence. The hybrid system can be off-grid or significantly independent of it, cutting drastically on the contribution to carbon emissions. Recently, most EU countries have taxed these emissions, which increases the costs included in the economic analysis projected over a lifetime. In this study, the carbon emissions tax is attributed to the grid energy consumption, to account for the electricity produced by non-renewable sources that supply it. The annual cost derived from CO2 emissions can be calculated by eq. (3.28).

$$EC_{CO2}(n) = Grid\ Energy\,.\,CO_2\ factor\,.\,Emissions\ Tax \tag{3.28}$$

EC_{CO2}(n) corresponds to the annual costs derivative from CO_2 emissions, in €; Grid Energy is the total annual energy consumed by the system, in kWh; the CO2 factor is the relation value between energy and

kilograms of carbon dioxide emitted, equal to 0.331 kgCO2/kWh [54]; and the emissions tax corresponds to the value defined by the government/authorities to penalize the emissions associated with the electric grid, equal to 0.1162 €/kgCO2 [54].

Finally, the total net present value for a 25-year lifetime can be determined, in €, by eq. (3.29), where the variable (N) corresponds to the total lifetime of the project, which is 25 years.

$$NPV = NPV_{CF} - Initial\ Inv. - O\&M.\frac{1-(1+r)^{-N}}{r} - EC_{CO2}.\frac{1-(1+r)^{-N}}{r} \tag{3.29}$$

Additionally, the levelized cost of energy (LCOE) can be computed through the parameters presented in this section. This metric is crucial to analyze the viability of a project for an extended period. The formula to obtain the LCOE is listed below, in eq. (3.30):

$$LCOE = \frac{Total\ Costs}{Total\ Generated\ Energy} \tag{3.30}$$

A comparison with the current approach scenario (100% grid as an energy source), was conducted to evaluate the potential of the new hybrid solution, for each scenario and optimization. This comparison is based on the economic metrics presented. However, the technical and social parameters should not be neglected as the hybrid solution stands out as a better solution.

3.4 Model deployment - Small energy community

As a second deployment test, the model was utilized to analyze a small energy community, to be presented and analyzed in Chapter 6. It may be entirely isolated from the national electric grid (i.e., stand-alone) or grid-connected. In the latter case, synchronization is required to enable imports/exports between the microgrid and the outside grid network. In this case study, a small community in the northern part of Portugal, Marruge, was selected as the site for the setup of the implementation of a small hybrid energy solution. As with the irrigation system, the model's iteration algorithm is set to an hourly timestep. Two approaches were delineated for this study: stand-alone and grid-connected. The selected location permits the examination of a grid-connected configuration, as it is neither an island nor an exceedingly remote community.

The **Stand-alone (SA)** configuration employs solar and wind energy as the primary renewable energy source, integrating PHS as an energy storage and production mechanism. Furthermore, a scenario with a battery energy storage system (BESS) is presented. The **Grid-connected (GC)** setup implements solar or wind with PHS. The grid-connected solutions were validated based on two criteria: a minimum yearly grid independence of 80%, i.e. low dependence, and a positive grid balance, defined as energy exports minus imports.

The primary objective is to develop a reliable and cost-effective solution for a small-scale energy community. Accordingly, in both the stand-alone and the grid-connected setups, the evaluation encompasses a range of energy source configurations and installed capacities. The sole optimization method employed was the minimization of the overall installed power capacity of the HES, designated as **OPT5**. The optimization was conducted using the Generalized Reduced Gradient Non-linear method of the Solver tool, in MS-Excel. The optimization was established with the multistart approach, a population equal to 250 and a convergence value of 0.0001, as shown in Fig.1A.1(b).

The economic parameters utilized in the small energy community case study are largely consistent with those employed in the previous case study, with a few notable exceptions, particularly concerning the inclusion of considerations related to inverters and state subsidies. For this analysis, the subsidies are not considered, as well as the costs associated with the hydraulic circuit of the PHS, including reservoirs, pipelines and valves, as every analyzed system configuration possesses an identical circuit. The economic parameters defined for the small-scale analysis are summarized in Table 3.4.

Table 3.4: Economic parameters of the small energy community

Solar Energy	[10, 53]
C_{inv}_PV	850 €/kW
O&M_PV	8.5 €/kW/year
Inverter (DC/AC) - 100kW	Huawei SUN2000-100KTL-M3-AFCI-H4
Inverter (DC/AC) - 40kW	Huawei SUN2000-40KTL-M3-H4
Inverter (DC/AC) - 50kW	Huawei SUN2000-50KTL-M3
C_{inv}_Inv.100/40/50	3,414 € / 2,177 € / 1,861 €
O&M_inverter	1%
Wind Energy	[37, 54, 55]
C_{inv}_WT	1,200 €/kW
O&M_WT	15 €/kW/year
PHS (Pumped Hydropower Storage)	[18, 53, 54]
C_{inv}_Hydro	1,500 €/kW
O&M_Hydro	20 €/kW/year
C_{inv}_Pump	950 €/kW
O&M_Pump	9.5 €/kW/year
Reservoir Capacity	2,173 kWh
BESS (Battery Energy Storage System)	[56]
C_{inv}_BESS	300 €/kWh
O&M_BESS	15 €/kWh/year
Additional parameters	
Lifetime of the project	25 years
Interest rate - r	10%

The carbon dioxide emissions tax is calculated using the same factors employed in the large-scale case study. The grid balance cash flow, for the grid-connected setup, is constant throughout the entire lifetime, due to the absence of state subsidies. Accordingly, the net present value of the cash flow is computed by eq. (3.31). The total project's NPV and LCOE are obtained with eq. (3.29) and eq. (3.30), respectively.

$$NPV_{CF} = Cash\ Flow. \frac{1-(1+r)^{-25}}{r} \tag{3.31}$$

Chapter 4

Laboratory and Simulation Results of PHS Systems

4.1 Experimental storage capability characterization

In the laboratory experiments, Pump-1 was singularly used, and the **TCV-1** valve was handled to control the flow, located upstream of the pump inlet, as shown in Fig.4.1.

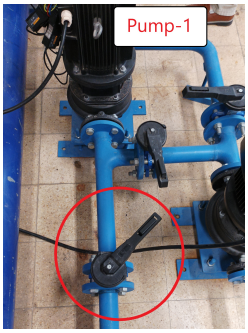

Figure 4.1: Butterfly Control Valve

The bottom reservoir, composed of two tanks with the same volume and height, has an initial water elevation of 0.5 meters, to its base. For each trial, the initial hydraulic grade line (HGL) in the lower reservoir is identical; i.e. 0.5m, excluding the difference between the floor and the base of the tanks, as the rest of the system is also located at the same height from the floor. The storage capacity test was divided into multiple trials, each with two control input parameters: initial pressure in the hydropneumatic tank and closure stage of the valve (fixed % Closure). In each trial, the valve closure percentage was fixed throughout the experiment. Table 4.1 presents the registered results. With them, the pumped volume can be computed, plus the average flow in each trial as well. In the pumped-storage system in the laboratory, the flow is estimated as the average value, resulting from the division of the pumped volume by the measured timestep, as described in eq. (4.1).

$$Q_{avg.} = \frac{\Delta V}{\Delta t} = \frac{A^{LR}(Z_i^{LR} - Z_f^{LR})}{\Delta t} \tag{4.1}$$

P_i^H is the initial pressure in the hydropneumatic tank; H_i^H is the initial head in the hydropneumatic tank

(pressure head plus elevation); P_f^H is the final pressure in the hydropneumatic tank (immediately before closing the system); Z_i^H is the initial water elevation in the hydropneumatic tank; Z_i^{LR} is the initial water elevation in the lower reservoir; and Z_f^{LR} is the final water elevation in the lower reservoir.

Table 4.1: Experimental results for Storage Capability Test

Trial	P_i^H [bar]	H_i^H [m]	P_f^H [bar]	Z_i^H [m]	Z_i^{LR} [m]	Z_f^{LR} [m]	%Closure
Hydropneumatic Tank at $H_i^H \approx 5m$							
1	0.5	6.41	3.40	1.30	0.5	0.325	0
2	0.5	6.46	3.40	1.35	0.5	0.325	34
3	0.5	6.46	0.75	1.35	0.5	0.470	67
Hydropneumatic Tank at $H_i^H \approx 10m$							
4	1.0	11.57	3.40	1.35	0.5	0.365	0
5	1.0	11.57	3.40	1.35	0.5	0.365	34
6	1.0	11.54	1.20	1.32	0.5	0.485	67
Hydropneumatic Tank at $H_i^H \approx 20m$							
7	2.0	21.66	3.35	1.22	0.5	0.405	0
8	2.0	21.66	3.35	1.22	0.5	0.405	34

The computed values derived from the results of Table 4.1 are presented in Table 4.2.

Table 4.2: Computed pumped volume and average flow of Storage Capability Test

Trial	$\triangle V^{LR}$ [m^3]	$\triangle t$ [s]	$Q_{avg.}$ [m^3/s]	$Q_{avg.}$ [l/s]	V_i^H [m^3]	V_f^H [m^3]
Hydropneumatic Tank at $H_i^H \approx 5m$						
1	0.28105	46.75	0.00601	6.01	0.56540	0.84645
2	0.28105	59.35	0.00474	4.74	0.59110	0.87215
3	0.04818	(109)	0.00044	0.44	0.59110	0.63928
Hydropneumatic Tank at $H_i^H \approx 10m$						
4	0.21681	44.60	0.00509	5.09	0.59110	0.80791
5	0.21681	55.80	0.00389	3.89	0.59110	0.80791
6	0.02409	(84)	0.00029	0.29	0.57568	0.59977
Hydropneumatic Tank at $H_i^H \approx 20m$						
7	0.15333	36.80	0.00417	4.17	0.52430	0.67763
8	0.15333	49.9	0.00307	3.07	0.52430	0.67763

Trials **3** and **6** have their time delta in between parenthesis because the flow was so low, due to the high percentage of closure of the valve, that it would require an extensive period to achieve the maximum head of the pump while it operates under stress before the flow turned to zero.

With the average flows, it is possible to obtain the average pump head through the pump curves sourced by Grundfos manufacturer. Although the maximum flow, in each trial, was slightly higher than the average flow, and the flow towards the end of the period was approximately zero, the average flow allows the estimation of the pump head, pump efficiency, and pump power. With the estimated pump power and efficiency, it is possible to compute the total energy cost, across the registered period and divide it by the total pumped volume to measure the pump storage capacity, in kWh/m^3. Table 4.3 summarizes the results of the storage capability test, with crucial parameters to study pumped-storage systems.

From Table 4.3, it is clear that with the decrease of the average flow, derived by the valve closure,

the storage performance worsens, as the required energy to pump a cubic meter of volume increases. When the flow is near zero, the energy cost per pumped volume exponentially rises, to a scale ten times superior to the average values.

Table 4.3: Pump and energy results

Trial	$Q_{avg.}$ [l/s]	$H_{p,avg.}$ [m]	$\eta_{p,avg.}$ [%]	$P_{p,avg.}$ [kW]	$P_{total,avg.}$ [kW]	Energy [kWh]	E/V [kWh/m^3]
Hydropneumatic Tank at $H_i^H \approx 5m$							
1	6.01	32.55	59.6	3.203	3.615	0.0470	0.167
2	4.74	33.64	54.5	2.894	3.275	0.0540	0.192
3	0.44	35.30	8.5	1.777	2.074	0.0628	1.303
Hydropneumatic Tank at $H_i^H \approx 10m$							
4	5.09	33.41	55.9	2.972	3.360	0.0398	0.183
5	3.89	34.24	49.0	2.645	3.003	0.0465	0.214
6	0.29	35.40	6.1	1.754	2.049	0.0478	1.985
Hydropneumatic Tank at $H_i^H \approx 20m$							
7	4.17	34.06	51.0	2.727	3.093	0.032	0.209
8	3.07	34.62	42.9	2.423	2.763	0.038	0.248

4.2 Storage capacity simulation

With the hydraulic circuit replicated in WaterGEMS, presented in 3.1.2, the storage capacity analysis was performed to compare results with the empiric parameters obtained in the IST/Hydraulic-CERIS laboratory. It is divided into three different hydropneumatic heads, each with three methods of valve closure operation.

4.2.1 Hydropneumatic head: 5 meters

For 5 m of head in the hydropneumatic tank, the component's parameters throughout time are presented in Fig.4.2. The pump head and flow evolution confirm the results obtained in the lab's experiment, in which the pump reaches a limit and cannot pump more volume to the hydropneumatic vessel due to the maximum possible pump head.

Table 4.4 presents the cumulative energy results for each valve pattern, which are successfully similar to the values obtained in the laboratory experiments.

Table 4.4: Energy storage capacity, $H_i^H = 5m$

Valve Pattern	Volume Pumped [m^3]	Energy [kWh]	Storage performance [kWh/m^3]
0% Closure	0.293	0.044	0.152
34% Closure	0.293	0.057	0.193
Variable Closure	0.293	0.046	0.155

The simulations in WaterGEMS align with the laboratory results, where the computed average parameters confirm this, as presented by Table 4.5, with the percentage difference to experimental results.

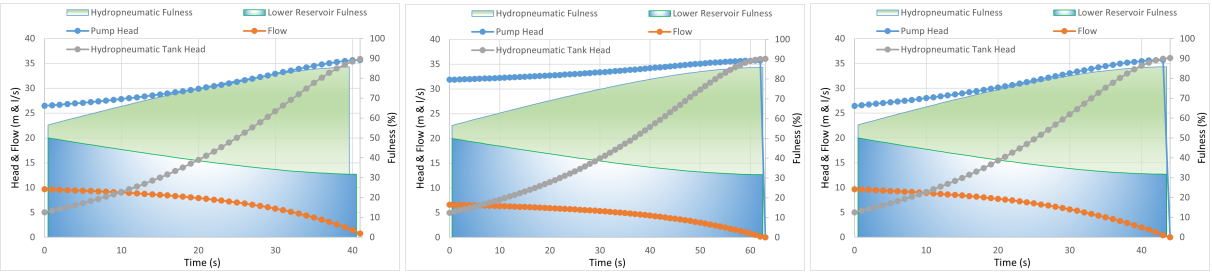

(a) Fixed - 0%Closure **(b)** Fixed - 34%Closure **(c)** Variable closure - 0% to 100%

Figure 4.2: Circuits evolution for $H_i^H = 5m$

Table 4.5: Average pump results, $H_i^H = 5m$

Valve Pattern	$Q_{avg.}$ [l/s]	$H_{p,avg.}$ [m]	$\eta_{p,avg.}$ [%]	$P_{p,avg.}$ [kW]
0% Closure	6.98 (+16%)	30.55 (-6%)	57.89 (-3%)	3.38 (+5.5%)
34% Closure	4.65 (-2%)	33.63 (+0%)	50.44 (-7%)	2.87 (-1%)
Variable Closure	6.66	30.91	56.36	3.31

4.2.2 Hydropneumatic head: 10 meters

For 10 m of head in the hydropneumatic tank, the pump curve intersects the system curve with a lower initial flow than 5 m. Table 4.6 presents the energy results obtained for 10 m of head in the hydropneumatic vessel.

Table 4.6: Energy storage capacity, $H_i^H = 10m$

Valve Pattern	Volume Pumped [m^3]	Energy [kWh]	Storage performance [kWh/m^3]
0% Closure	0.246	0.041	0.165
34% Closure	0.246	0.051	0.211
Variable Closure	0.246	0.044	0.179

Additionally, Table 4.7 indicates the computed average hydraulic parameters, associated with the pump performance, with the percentage difference to experimental results. Both the energy and hydraulic results obtained for a 10 m head in the hydropneumatic tank are similar to the experimental data (Table 4.3), with slight differences induced by the use of average parameters. The head losses in joints, curves and connections, induce common small discrepancies due to the scale effects associated with the lab size facilities.

For 10 m of head in the hydropneumatic tank, the systems' curve evolution through time, for each valve pattern, is presented in Fig.4.3. It is possible to visualize the effect of closing the valve during operation; as the valve closes, the headloss coefficient greatly increases, overshadowing the flow reduction with the

pump head increase. This leads to the system curves narrowing to the vertical asymptote as it progresses in time.

Table 4.7: Average pump results, $H_i^H = 10m$

Valve Pattern	$Q_{avg.}$ [l/s]	$H_{p,avg.}$ [m]	$\eta_{p,avg.}$ [%]	$P_{p,avg.}$ [kW]
0% Closure	5.86 (+15%)	31.91 (-4%)	55.04 (-2%)	3.17 (+6.6%)
34% Closure	3.97 (+2%)	34.17 (-0.2%)	46.91 (-4%)	2.71 (+2.4%)
Variable Closure	5.12	32.65	50.68	2.99

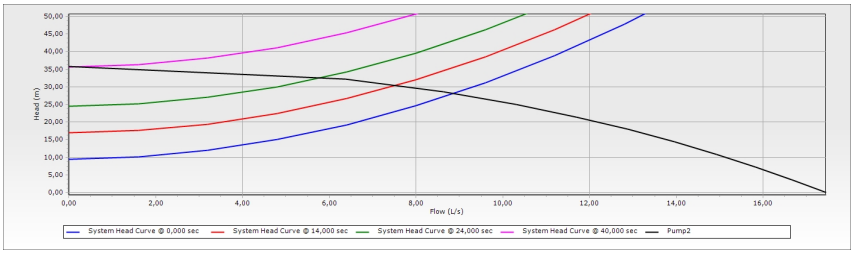

(a) Fixed - 0%Closure

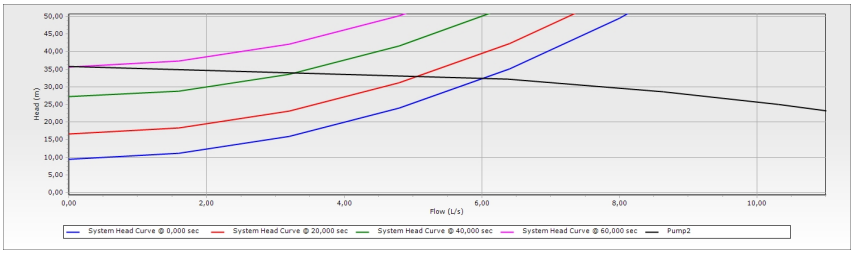

(b) Fixed - 34%Closure

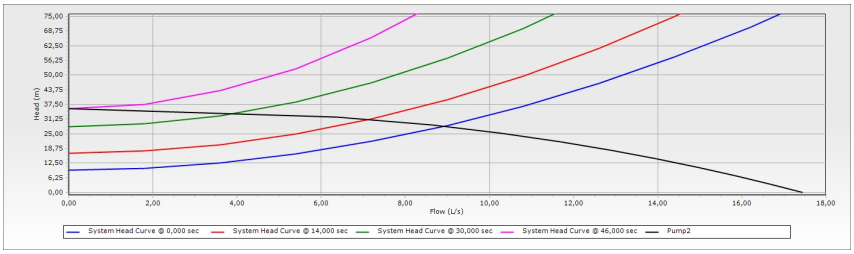

(c) Variable closure - 0% to 100%

Figure 4.3: System curve evolution, $H_i^H = 10m$

4.2.3 Hydropneumatic head: 20 meters

Similar to previous hydropneumatic heads, with 20 m, the pump can not deliver more water flow into the upper reservoir, once its head reaches 36 meters, approximately. Fig.4.4 presents the hydraulic results for a permanent fully open valve. As the initial hydraulic head in the hydropneumatic tank is much superior

to previous simulations, the system curve's origin point is higher, resulting in a start operation point with a lower flow value. Nevertheless, the maximum pump head point is reached sooner than the other two heads, as shown in Fig.4.5; that presents the system curves for a variable valve closure, reinforcing the previously stated phenomenon that the system curves get more vertical with the closure of the valve and subsequent increase of the head losses.

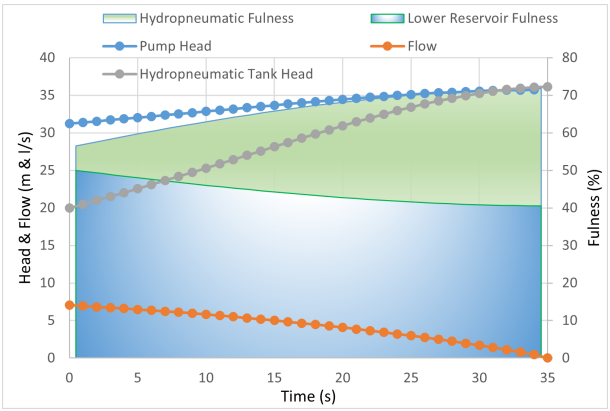

Figure 4.4: Circuits evolution for $H_i^H = 20m$

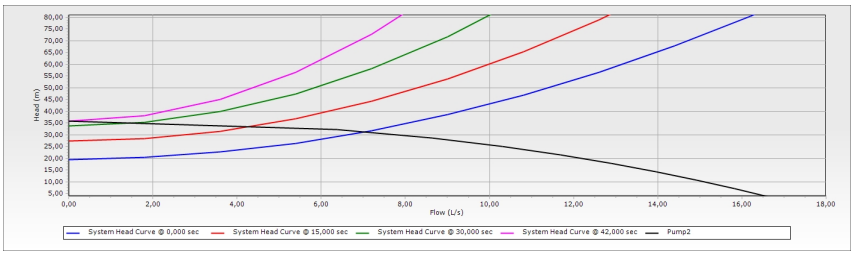

Figure 4.5: System curve evolution, $H_i^H = 20m$

The pump energy performance and associated average hydraulic parameters are presented in Tables 4.8 and 4.9, respectively.

Table 4.8: Energy storage capacity, $H_i^H = 20m$

Valve Pattern	Volume Pumped [m^3]	Energy [kWh]	Storage performance [kWh/m^3]
0% Closure	0.152	0.031	0.201
34% Closure	0.246	0.040	0.264
Variable Closure	0.246	0.035	0.229

Table 4.9: Average pump results, $H_i^H = 20m$

Valve Pattern	$Q_{avg.}$ [l/s]	$H_{p,avg.}$ [m]	$\eta_{p,avg.}$ [%]	$P_{p,avg.}$ [kW]
0% Closure	4.22 (+1%)	33.82 (-1%)	48.12 (-5%)	2.79 (+2%)
34% Closure	2.81 (-8%)	34.97 (+1%)	38.31 (-11%)	2.41 (-1%)
Variable Closure	3.45	34.33	41.34	2.58

Figure 4.6 illustrates the progression of pump performance through time until reaching the maximum operation point and the flow becomes null.

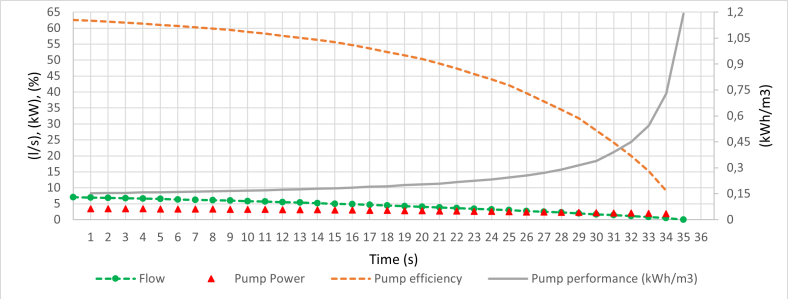

Figure 4.6: Pump's performance through time, $H_i^H = 20m$

4.2.4 Storage efficiency - empirical versus simulation results

The data presented in Table 4.2, allows for a general evaluation of the storage efficiency for the laboratory experiments. The potential energies obtained for each trial, where E_p^w is the water gravitational potential energy and E_p^a is the compressed air energy, in kWh, are calculated at the start and end point with eqs. 3.1) and (3.3), and resultant energy stored in the hydropneumatic tank are presented in Table 4.10. The final column presents the storage efficiency of each trial, calculated by dividing the stored energy by the energy consumed by the pump.

Table 4.10: Laboratory: energy storage results

Trial	E_i^w [kWh]	E_f^w [kWh]	E_i^a [kWh]	E_f^a [kWh]	E_{stored} [kWh]	$\eta_{storage}$ [%]
Hydropneumatic Tank at $H_i^H \approx 5m$						
1 (0%)	0.00169	0.00379	0.0151	0.0363	0.0233	49.6
2 (34%)	0.00185	0.00402	0.0142	0.0303	0.0183	33.9
3 (67%)	0.00185	0.00216	0.0142	0.0188	0.00491	7.8
Hydropneumatic Tank at $H_i^H \approx 10m$						
4 (0%)	0.00185	0.00345	0.0284	0.0454	0.0186	46.7
5 (34%)	0.00185	0.00345	0.0285	0.0453	0.0184	39.6
6 (67%)	0.00175	0.00190	0.0295	0.0333	0.00395	8.3
Hydropneumatic Tank at $H_i^H \approx 20m$						
7 (0%)	0.00145	0.00243	0.0660	0.0784	0.0134	41.8
8 (34%)	0.00145	0.00243	0.0660	0.0761	0.0111	29.2

Concerning the software simulations, Table 4.11 presents the corresponding results. In WaterGEMS the point at which the pump surpasses its maximum operating head and the flow is null is considerably more precise than that achievable through empirical measurement. Consequently, the valve closure pattern does not impact the potential energy evaluation, as the start and end values are equal for each valve pattern. However, the pump's energy consumption is subject to variation based on the valve pattern, which consequently affects storage efficiency. The storage efficiency values obtained from the simulation

of pumped storage are quite similar to the empirical results. The average simulation deviation (absolute) from the empiric efficiencies is 2.46%. The small margin of deviation is attributed to the simulation energy results being computed with the total incremental values.

Table 4.11: Simulation: energy storage results

H_i^H	E_i^w [kWh]	E_f^w [kWh]	E_i^a [kWh]	E_f^a [kWh]	E_{stored} [kWh]	$\eta_{storage}$ [%] - 0%/34%/Var.
5m	0.00169	0.00390	0.0139	0.0345	0.0228	51.9 / 40.0 / 49.6
10m	0.00169	0.00348	0.0286	0.0459	0.0191	46.6 / 37.5 / 43.4
20m	0.00169	0.00272	0.0582	0.0689	0.0117	37.7 / 29.3 / 33.4

In contrast, the storage efficiencies yielded from the laboratory trials are based on average power results and the time length of each experiment. Additionally, the volume calculation in the hydropneumatic vessel for the experimental analysis was based on measured heights in the laboratory with associated reading uncertainties. The final pressure gauge in the hydropneumatic tank is also difficult to precisely capture in the appropriate timeshot since it varies along the storage process and after. Nonetheless, the energy results and efficiency deducted from both scenarios converged, demonstrating the same pump behavior and storage capacity.

4.2.5 Pumps in series

The analysis of pumped storage with two pumps in series uses the preceding results obtained for a single pump and varying initial hydropneumatic head with a fixed 0% closure (TCV-2). Subsequently, the simulation is continued with two pumps in series until the maximum total pump head is reached. This strategy was implemented with the objective of enhancing storage efficiency by reducing the overall pump energy consumed. If both pumps were to be initiated in series, the resulting energy consumption would be approximately doubled, due to the low positive slope of the power curve, as illustrated in Fig.3.5. The use of pumps in series is advantageous for hydropneumatic vessels as it allows the generation of higher air compression pressures, which in turn create greater hydraulic heads and thus maximize energy storage. In the three simulations, the final hydraulic head achieved was 72 m, corresponding to an air gauge pressure of approximately 7 bar, approximately, for an initial hydropneumatic head of 5, 10 and 20 m. This threshold is the result of the summation of the two pumps' maximum operating pump head, head losses (which are nearly negligible due to the low flow rates near the maximum point) and elevation difference.

Figure 4.7 depicts the hydraulic head evolution through the circuit with the two pumps connected in series, via TCV-3. It corresponds to the final timestep before achieving a null flow rate. The individual pump heads are identical, comprising half of the total pump head. Nevertheless, it is crucial to monitor the suction head, particularly in the case of **Pump-2**, to prevent the occurrence of cavitation pressures. Since the series connection was implemented solely after a single pump (pump-2) reached its maximum

capacity, the throttle control valve (TCV-3) could also be maintained in a permanently open position. In the event that both pumps were in operation, TCV-3 would have been slightly closed to induce head losses on the discharge of the first pump, in order to avoid the formation of cavitation.

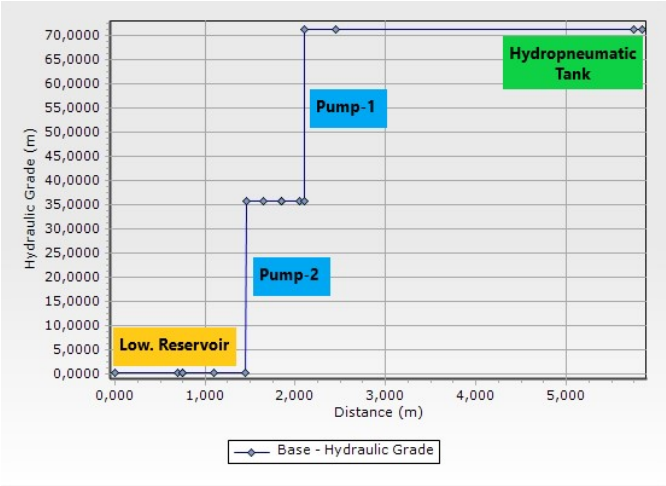

Figure 4.7: Circuit's hydraulic head with pumps in series, WaterGEMS

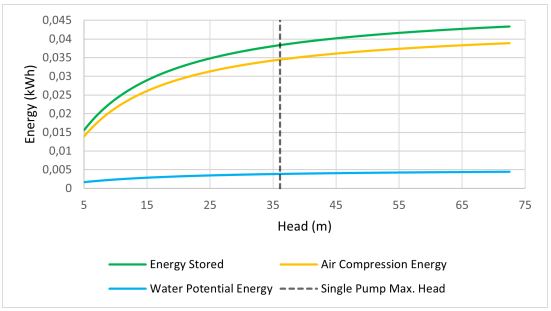

(a) H_i^H =5 m

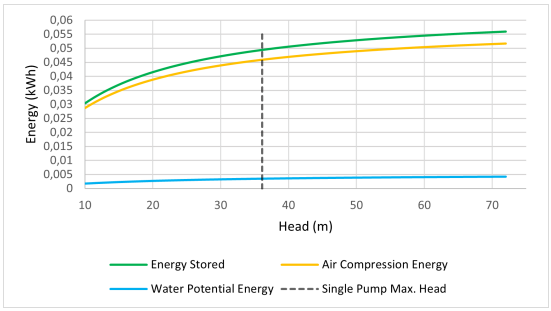

(b) H_i^H =10 m

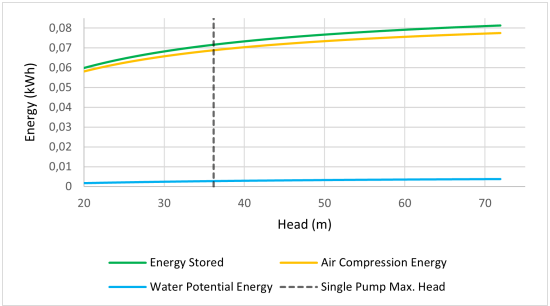

(c) H_i^H =20 m

Figure 4.8: Energy stored in the hydropneumatic vessel, pumps in series

The extension of the storage capacity analysis with two pumps connected in series increases the feasible hydraulic head on the hydropneumatic vessel. The air compression is the main contributor, whereas the water level exhibits a slight increase. Figure 4.8 illustrates the evolution of energy stored as a function of the hydropneumatic head (H^H), which continuously increases throughout the simulation runtime, for each initial hydropneumatic head (H_i^H).

The overall storage performance, as indicated by the ratio of energy consumption to the pumped volume in the hydropneumatic tank, slightly increases in comparison to the values obtained for a single pump and a fixed 0% closure, as detailed by Table 4.12.

Table 4.12: Pumped-storage performance, full runtime

H_i^H [m]	Volume pumped [m^3]	Energy [kWh]	Storage performance [kWh/m^3]
5	0.355	0.065	0.182
10	0.328	0.067	0.204
20	0.275	0.071	0.257

Although the initial head simulations achieved identical air pressures, of approximately 7 bar, the final compression energy of the air differed due to the disparate volumes of air involved. The simulation with an initial head of 20 m presents the highest compression energy stored, as it possesses a superior air volume at the common final pressure. Nevertheless, the total variation of compressed-air energy is greater for the lowest initial hydropneumatic head, due to the significantly low initial pressure. Consequently, the pumps must perform superior compression work for the 5 m head. This deduction extends to the overall energy stored (E_{stored}), which corresponds to the variation between the final and initial energy (water/air) parcels. Table 4.13 presents the energy results for each initial hydropneumatic head. Despite the work demanded being higher for a head of 5 m, the storage efficiency is the best because the system curve intersects the overall pump curve at superior flow rates, thereby increasing efficiency.

Table 4.13: Energy storage results, pumps in series

H_i^H [m]	ΔE_{water} [kWh]	ΔE_{air} [kWh]	E_{stored} [kWh]	$\eta_{storage}$ [%]
5	0.00279	0.0250	0.0277	43
10	0.00253	0.0231	0.0256	38
20	0.00205	0.0193	0.0214	30

In comparison to the single pump simulation, the series connection demonstrated an increase of the energy stored of 22, 34 and 83% for an initial hydropneumatic head of 5, 10 and 20 m, respectively. I.e. the total energy stored inside the hydropneumatic vessel, with two pumps in series, is equal to 122, 134 and 183% of the energy stored with a single pump in operation (Pump-2), for each initial hydropneumatic head simulation and a fixed fully open valve (TCV-2 and TCV-3).

Chapter 5

Irrigation System - large-scale case study

5.1 Data Collection

Before the model deployment, it is necessary to collect the input data and process it to set the model with the desired energy sources and consumption parameters, according to the analyzed scenario, as presented in Fig.5.1.

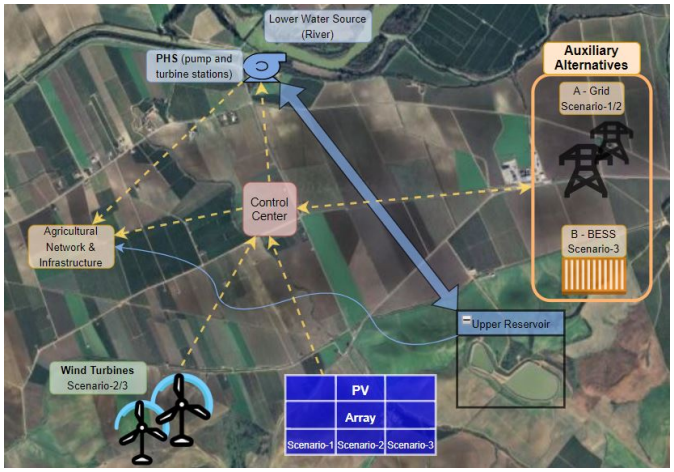

Figure 5.1: Satellite scheme of the system's configuration

5.1.1 Energy needs

The energy needs (E_c^i), correspond to energy requirements for the operation of the agricultural activity. It corresponds to every energy consumed by the field's activity, that is not directly related to the PHS station operation. It accounts for control systems (crucial in a hybrid system), auxiliary equipment (as the irrigation extends for 24h), operation of the irrigation network (pumps, hydrants, valves) and water recycling. The attributed energy consumption values were based on historical data from a nearby irrigation field, Valle Inferior, in which energy consumption was extrapolated to the scale of this case study. It is considered constant throughout the month, solely varying in accordance with the month of the irrigation

season. Table 5.1 presents the energy demand according to the irrigation month and required water allocation.

Table 5.1: Hourly energy consumption per month for each water allocation

Month	800 m3/ha [kWh]	1000 m3/ha [kWh]	3000 m3/ha [kWh]	6000 m3/ha [kWh]
March	215	269	807	1614
April	315	394	1181	2362
May	376	470	1411	2822
June	583	741	2222	4444
July	645	807	2420	4840
August	520	650	1949	3898
September	278	347	1042	2084

5.1.2 Water needs

The irrigation area in the study has a wide variety of crops, mainly citrus trees and corn, which require different amounts of water every season. For simplification purposes, the hourly water needed for irrigation is considered constant throughout the month. Nevertheless, it varies according to the irrigation month, i.e. in the peak of summer and crop growth, the water spent for irrigation is higher than at the beginning of the season (lower temperatures and crops have just been planted) or the end of the season (temperatures decreasing, as evapotranspiration; and crops are being harvested). The presented expression, eq. (5.1), determines the hourly water irrigation volume attributed to a specific month (A_m^i).

$$A_m^i = \frac{Water\ allocation\ .\ Irrigation\ area\ .\ Month\ share}{Total\ hours\ of\ the\ month} \tag{5.1}$$

Every annual season has a predetermined maximum water restriction that can be used by the irrigation system, which farmers must obey, as this imposition prevents the risk of increasing droughts and further environmental damage to the surrounding ecosystem and watershed. For this study, the irrigation season was defined to start on the 1st of March and end on the 30th of September. Based on the real values of recent years, this study analyzes the system operation for water allocations of 800, 1000 and 3000 and 6000 m3/ha. The total area of the irrigation fields is approximately 6000 ha. Therefore, the irrigation volume for each month is presented in Table 5.2, according to each water allocation and designated monthly share.

The current approach scenario uses the pump station for pumping water to the upper reservoir that only serves for irrigation; therefore, the allocation limit is assigned to the volume that could be pumped. However, this study implements new hybrid energy solutions. Since the PHS station either serves to pump or turbine water, it is no longer limited by this restriction. The allocation limit is only applied to the reservoir's outlet that feeds the irrigation pipeline network i.e., the water that is discharged downstream through the turbines and back to the Guadalquivir river does not count for the water allocation limit.

Table 5.2: Hourly water allocation for each month

Month	Share [%]	800 m3/ha [m3]	1000 m3/ha [m3]	3000 m3/ha [m3]	6000 m3/ha [m3]
March	7	451.61	564.52	1,693.55	3,387.10
April	10	666.67	833.33	2,500.00	5,000.00
May	15	967.74	1,209.68	3,629.03	7,258.07
June	20	1,333.33	1,666.67	5,000.00	10,000.00
July	22	1,419.36	1,774.19	5,322.58	10,645.16
August	18	1,161.29	1,451.61	4,354.84	8,709.68
September	8	533.33	666.67	2,000.00	4,000.00

During the off-season months, the water and energy needs are null. At the beginning of January, the water volume pumped to the upper reservoir is accounted for, plus the associated energy consumption for the pump station operation. Therefore, when the season starts, on the 1st of March, the reservoir is approximately full.

5.1.3 Photovoltaic energy production

Solar power data was retrieved from the online tool PVGIS-SARAH3 [57], for the year 2020, with the precise coordinates, PV rated power and parameters of the PV array: monocrystalline silicon, peak power = 9000 MWp, optimum slope = 33º, azimuth = 0º and system losses = 14%. From the collected solar data, the hourly energy production from the photovoltaic plant (S^i), in kWh, can be obtained. The studied region is highly advantageous for solar energy exploration, as seen by Fig.5.2.

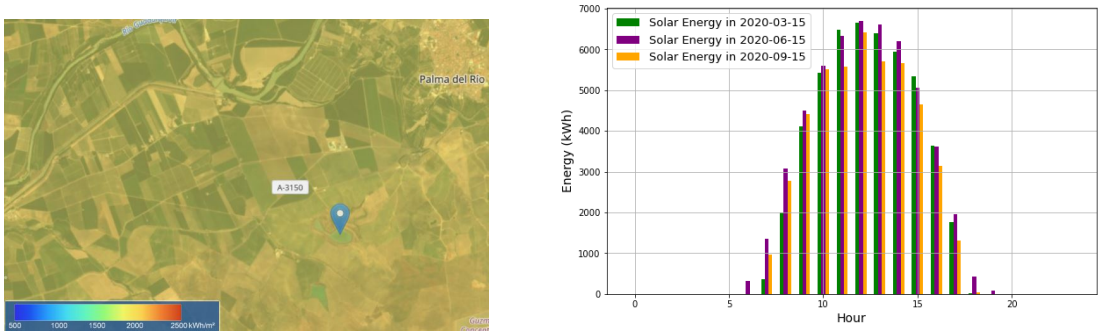

(a) Irradiation satellite map of the site

(b) PV energy production

Figure 5.2: Solar data from PVGIS web tool

5.1.4 Wind energy production

Regarding the scenarios that explore the implementation of wind energy, alongside the photovoltaic; the Vestas V110-2.0 MW wind turbine was selected, with a hub height of 110 meters and rated power of

2,000 kW. With the web tool renewables.ninja [58], the hourly energy production of a single turbine was obtained from the manufacturer's power curve and wind speed profile, Fig.5.3. It is then integrated into the model and scaled following the total number of turbines for the selected scenario.

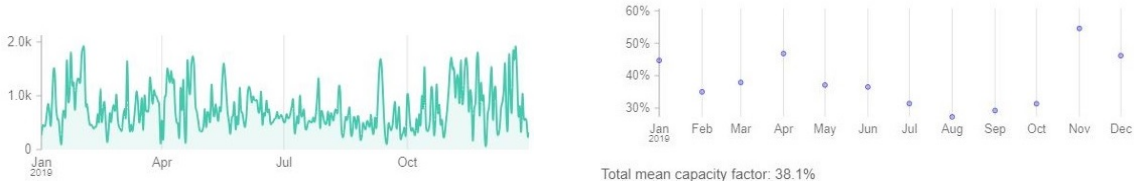

(a) Daily mean **(b)** Monthly capacity factor

Figure 5.3: Wind energy production pattern of a singular 2MW turbine

One scenario implements two wind turbines, 4 MW, and another, as will be detailed in the results section, the number of wind turbines varies with the water allocation needs, to enhance the OPT4 optimization, which minimizes the installed battery capacity. The energy data collected from the web tool for a single turbine was projected to the selected number of turbines in each scenario, to obtain the total wind energy power, each hour.

5.1.5 Pumped Hydropower Storage system

The PHS station uses excess renewable energy to pump water from the Guadalquivir River to an upper reservoir, enabling storage of water/energy; so that in periods of renewable scarcity, water is discharged down the penstock to generate the necessary hydropower. The water pumped upstream must be sufficient to satisfy the water needs for irrigation, every hour, A^i. The pump/turbine station is located 5 m above the river height and the upper reservoir is 89 m above it, when at maximum level. The total pumping capacity is 4.500 l/s with a nominal power of 7.4 MW. Head losses were simulated, for the pipeline characteristics with various flow values, to estimate the average pump head required for the system, equal to 100.14 m, by adding the average value of head losses as a function of various water flows. The average pump efficiency, 60%, was computed by eq. (5.2), to respect the maximum flow and nominal pump power. These conditions are achieved by 4 parallel centrifugal VSD pumps, maximizing the possible pumping flow, to the total 4.500 l/s.

$$\eta_p = \frac{\rho.g.Q.H}{P} \tag{5.2}$$

Regarding the powerhouse, the average turbine head follows the same principle. It is equal to 80.1 m, with the average head losses and reservoir level variation discounted. The average turbine efficiency was set to 76%. The overall rated power of the hydropower is determined in the results chapter, never surpassing

a maximum of approximately 1 MW, for each water allocation and optimization method. Nevertheless, assuming a nominal power of 1 MW for a single turbine, with a net head of 80.1 m and a maximum flow of 1.5 m^3/s (from section section 5.2), the Francis type would be the most appropriate. However, the load required for the hydropower is highly variable, as is the flow. For most of the simulation time, the hydropower is far from the nominal power and the maximum flow. Therefore, the most suitable turbine type for this application is the Turgo turbine, which ensures high stable efficiency for oscillating flows [59]. The single pipeline of 1200 mm in diameter and a total length of approximately 3.5 km serves for both the pump and turbine operation. Hence, the system can never do both operation modes simultaneously.

The man-made reservoir, Fig.5.4, has a total potential energy of 261 MWh, eq. (3.1). The water needs are discounted from this reservoir, enabling pressurized irrigation. Throughout the simulation of the irrigation system, the reservoir volume is responsible for feeding the crops with the necessary water volume and in the intermediate, to function as a component of the PHS system. The minimum and maximum reservoir volumes are 118,231.16 and 1,078,627 m^3, respectively. The minimum volume was arbitrated as the estimated volume of the reservoir when it is at a minimum of 1 m of water depth (h_R^i). The reservoir shape was approximated by a rectangular prism with a resultant area (A_R) of 118,231.16 m^2, determined via satellite measurement.

Figure 5.4: Upper reservoir for the PHS and water needs

5.1.6 Battery station

For the scenario wherein the grid is replaced with batteries, presenting an off-grid solution, the required parameters are the total storage capacity of the battery plant and the definition of the initial energy stored on it. Although the nominal storage capacity of the battery plant depends on the water allocation configuration and resultant optimization value, the initial energy stored, in kWh, was permanently set as zero. The batteries chosen for the battery energy storage system (BESS) are lithium-ion. The economic parameters for the BESS were attributed based on this selected category.

5.1.7 Grid tariffs

The scenarios that use the national electric grid require the input of purchase and feed-in tariffs to allow its accountability on the economic assessment. The used tariffs for the model simulation and optimization are presented in Fig.5.5, with purchasing and selling prices, respectively.

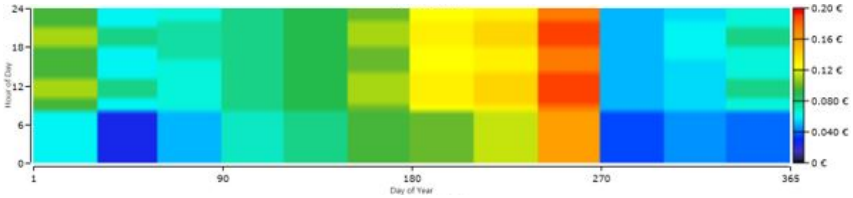

(a) Purchase price

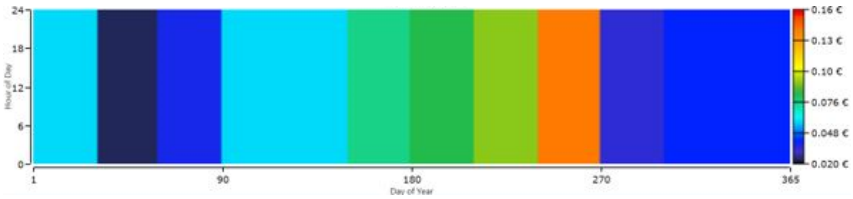

(b) Sell price

Figure 5.5: Grid tariffs

5.2 Results and Discussion

This section presents the irrigation system case study results for the three defined scenarios and water allocations of 800, 1000, 3000 and 6000 m^3/ha.

5.2.1 Scenario 1 - PV+PHS+Grid

An extensive analysis was made for scenario 1, where the three optimization objective functions were tested for each water allocation, in Solver, thus facilitating a comprehensive comparison between the algorithms and approaches. Furthermore, the NSGA-II optimization algorithm, in Python, was used for 3,000 and 6,000 m3/ha water allocations. In contrast, for the other two water needs, it does not justify its utilization as the system can be self-sustainable without using grid energy for the pump's operation.

5.2.1.1 Water allocation: 800 m3/ha

The total results for a single year, for a water allocation of 800 m3/ha, plus the lifetime (25 years) cash flow are present in Table 5.3. Reminder, the lifetime cash flow considers no selling of solar excess to

the grid in the first five years, as it is described in eq. (3.27). Further yearly balances are presented in Fig.A.4.

Table 5.3: Scenario 1: Main results, 800 m3/ha

Optimization method:	**OPT1**	**OPT2**	**OPT3**
Turbine Volume [m^3/year]	6,503,314.808	6,503,314.808	6,503,314.808
Pumped Volume [m^3/year]	11,553,481.970	11,553,941.630	11,553,941.630
Hydropower [kWh/year]	1,077,716.323	1,077,716.323	1,077,716.323
Solar Energy for Pump [kWh/year]	5,249,196.2	5,249,405.0	5,249,405.0
Grid Energy for Pump [kWh/year]	0.0	0.0	0.0
Grid Energy [kWh/year]	0.0	0.0	0.0
Solar Excess to Grid [kWh/year]	8,335,480.0	8,335,271.0	8,335,271.0
Lifetime Cash Flow [€]	2,527,096.0	2,477,787.0	2,477,787.0

The overall results for 800 m3/ha are quite identical, and equal for OPT2 and OPT3, as all the optimization methods followed the same path and obtained the "one" solution for system operation. The three optimizations with Solver used a hydropower factor equal to 1 in all periods, reaching the maximum required hydropower generation. OPT1 explored a little bit more the profit by selling excess solar energy to the grid, hence the slightly higher cash flow. For 800 m3/ha, OPT3 did not produce a different perspective for the system, as all Solver optimizations were capable of maximizing the hydropower. Since the water allocation is quite low and the system is flexible to this amount, the grid energy for the pump is zero for all optimizations, as the hydropower and solar energy are sufficient for satisfying energy and water needs. The solution variables for OPT2 and OPT3 are the same, yielding identical results.

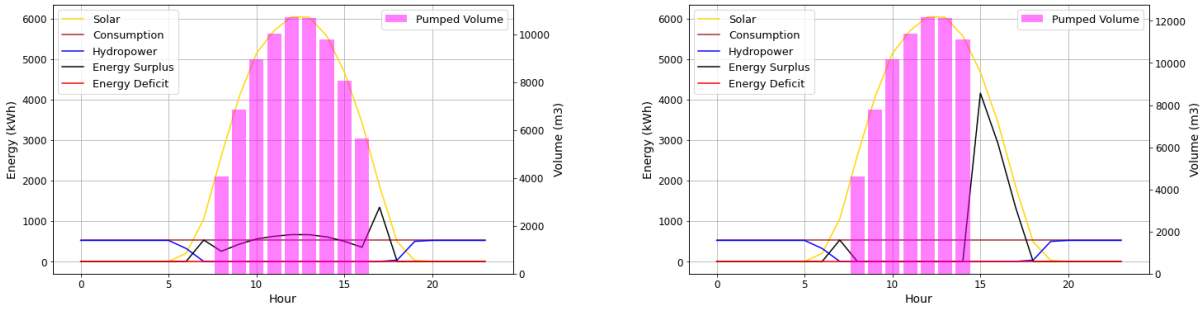

(a) OPT1 **(b)** OPT2 & OPT3

Figure 5.6: Energy Balance on 1st of August, 800 m^3/ha

Figure 5.6 represents the energy balance of different sources and the demand, throughout 24 hours, enhancing the symbiosis between the different subsystems, required to operate in harmony to fully satisfy the energy needs. It can be noticed, in both graphs, that at night, hydropower (blue) is responsible for assuring energy consumption needs, whereas during the day, this mission is carried by solar-produced energy (yellow). The variable "Energy Deficit" corresponds to grid energy required to buy, either for pumping or to satisfy energy needs, which remains at zero. Whenever the solar energy is in excess,

after consumption and usage for pumping water by the PHS subsystem, it can be sold to the grid, seen as the variable “Energy Surplus”; prominent at mid-day if the solar factor allows it or at the beginning and ending of solar production, where the power generation is quite low and not suitable for operating the pumps. Therefore, the system prefers to not use low-power solar energy to pump water, instead, it can be sold. In Fig.5.6(b), there is a high peak of solar energy surplus, sold to the grid, accompanied by no pumped volume to the upper reservoir. This occurrence is due to the reservoir maximum volume restraint, which forbids the system to pump water uphill and the solar surplus available cannot be used by the PHS. The storage level of the reservoir every hour is important for the operation of the system and highly influential on the energy balance obtained after optimization. Figure 5.7 illustrates the fullness of the uphill reservoir throughout the season, for each optimization method.

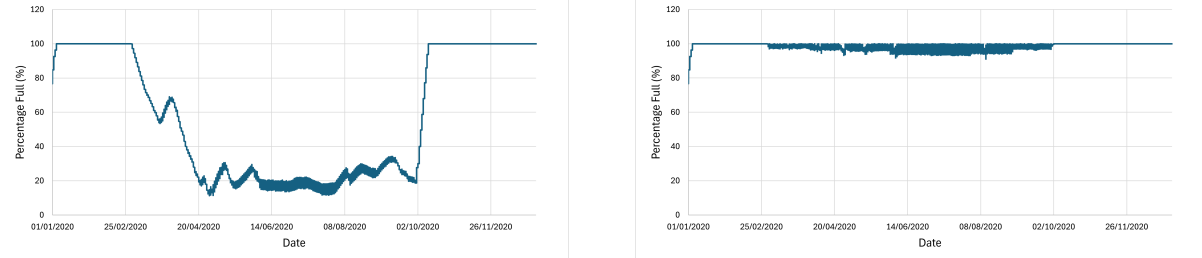

(a) OPT1 **(b)** OPT2 & OPT3

Figure 5.7: Reservoir capacity throughout the year, 800 m^3/ha

The symbiosis between solar generation, reservoir fulness, and the possible pumped volume at each hour, can also be seen in the plot, Fig.5.8(a), for the maximizing lifetime cash flow optimization method (OPT1). In every optimization method the water reliability was easily fulfilled, assuring a 24h irrigation throughout the whole defined season. Not only for the 800 m3/ha water allocation but for every allocation, the water reliability sought in the optimization methods was 100%. As the study is defined for an irrigation field, it is crucial to comply with the main objective: satisfying the water needs, and subsequent energy requirements. Additionally, the energy needs must also be always satisfied, to ensure the proper operation of the agricultural activity. The pie chart, Fig.5.8(b), represents the shares of solar, hydropower, and grid energy sources to fulfill energy requirements by the system. It corresponds to the three optimization configurations in Solver.

Finally, the yearly energy balance is shown in Fig.5.9, for the case of lifetime cash flow maximization (OPT1). For 800m3/ha, this optimization configuration presents the best solution, as for energy parameters, all methods have identical results, but, ultimately, this obtains the best cash flow. ”Grid In” corresponds to energy sold to the grid and ”Grid Out” to energy purchased from the grid.

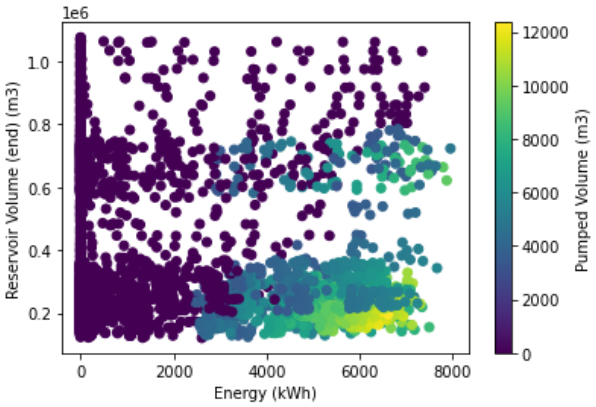

(a) Solar and PHS relation

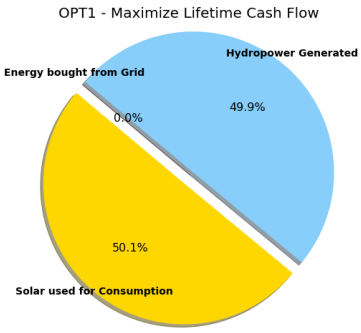

(b) Energy Needs distribution by source, 800 m^3/ha

Figure 5.8: Energy sources symbioses

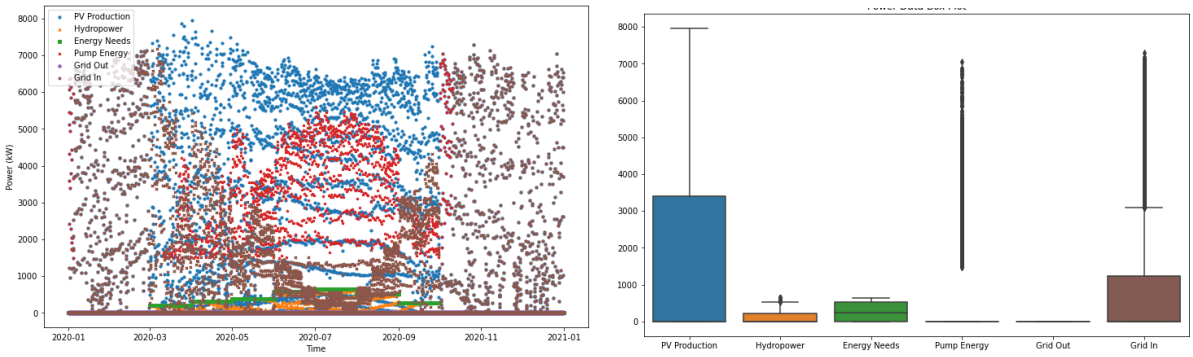

(a) Yearly energy balance

(b) Yearly energy statistics

Figure 5.9: Energy balance, 800 m^3/ha - OPT1

5.2.1.2 Water allocation: 1000 m3/ha

Table 5.4 presents the total results for a single year, for 1000 m3/ha water allocation, plus the lifetime (25 years) cash flow. Further yearly balances are presented in Fig.A.5.

In contrast to 800 m^3/ha, for a water allocation of 1000 m^3/ha, the system can no longer be independent from the grid assistance. It can still guarantee complete irrigation satisfaction (water reliability = 100%) by solely filling the upper reservoir with solar surplus energy powering the pump station, as yielded by OPT1 and OPT2. In this configuration, the grid usage solely corresponds to the energy needed to satisfy the rest of the energy needs, not fulfilled by solar or hydropower energy. OPT1, which aims to maximize the lifetime cash flow, uses less hydropower, which in one way increases grid usage, but also enables for more solar energy to be sold, as the water volume required in the reservoir throughout the season becomes less rigid. The total yearly solar excess from OPT1 is 10,493,562 kWh whereas for

OPT2 is 6,814,492 kWh. Although costs from grid purchase are much inferior in OPT2, in comparison to OPT1, the profit difference between methods is much higher, hence the greater cash flow for OPT1.

Table 5.4: Scenario 1: Main results, 1000 m3/ha

Optimization method:	**OPT1**	**OPT2**	**OPT3**
Turbine Volume [m^3/year]	11,398.1	8,111,511.0	8,277,052.0
Pumped Volume [m^3/year]	6.261.798,6	14,359,433.2	14,526,279.7
Hydropower [kWh/year]	1,888.9	1,344,223.4	1,371,656.5
Solar Energy for Pump [kWh/year]	2,844,978.6	6,524,049.0	6,050,773.8
Grid Energy for Pump [kWh/year]	0.0	0.0	549,080.0
Grid Energy [kWh/year]	1,369,768.0	27,433.0	549,080.0
Solar Excess to Grid [kWh/year]	10,493,562.0	6,814,492.0	7,287,767.0
Lifetime Cash Flow [€]	2,050,599.0	1,667,899.0	1,395,290.0

Regarding maximizing hydropower generation, OPT3, the solution is similar to OPT2, but with the increase of hydropower, due to a greater turbine volume, it is needed to also compensate with grid energy to power the pumps and ensure the reservoir has enough volume for every water requirement. Therefore, the cash flow is the lowest for OPT3.

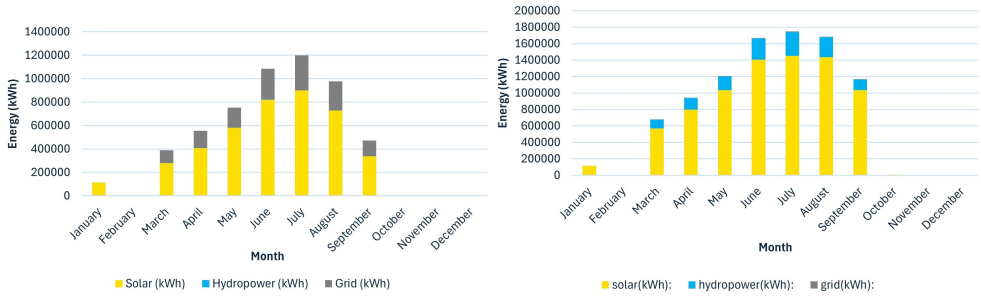

(a) OPT1

(b) OPT2

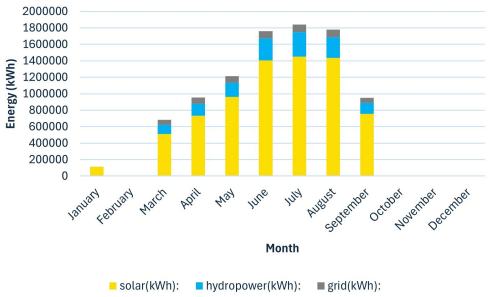

(c) OPT3

Figure 5.10: Monthly energy consumption by source, 1000 m^3/ha

The total energy consumption each month by source (needs + pump station) is shown by Fig.5.10, in which the main traces of each optimization method are present: OPT1 - less hydropower to be able to sell more solar energy and require less pumped volume; OPT2 - increase in solar consumption to

diminish grid consumption, aided by a compensation of hydropower on energy needs; OPT3 - increase in grid consumption to boost the hydropower maximization.

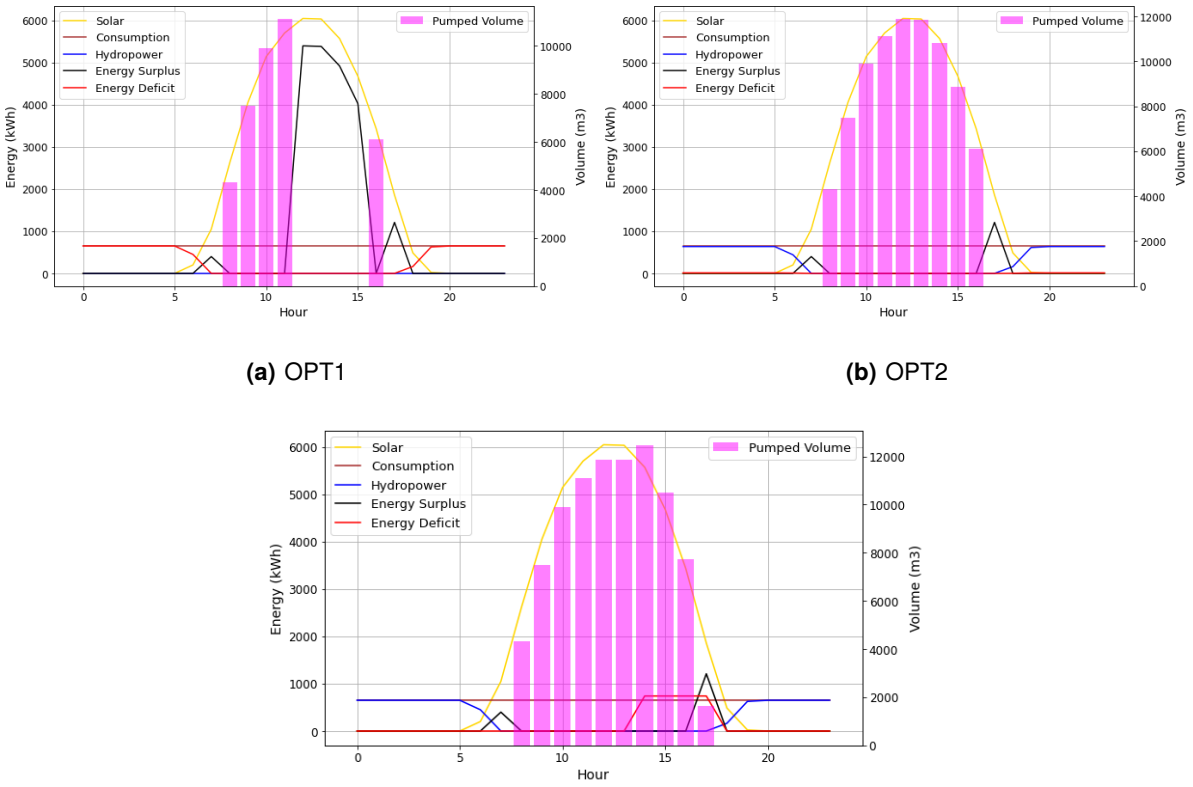

(a) OPT1

(b) OPT2

(c) OPT3

Figure 5.11: Energy balance on 1st of August, 1000 m^3/ha

Figure 5.11 represents the energy balance on a selected day (1st of August) for every Solver optimization method. Characteristic traces of each configuration can be visualized for 24h period. For OPT1, there is a higher dependence on grid assistance. For OPT2, a more balanced system. In OPT3, it is visible the influence provoked by the increase in hydropower generation; and the need to aid the pump operation with grid energy ("Energy Deficit" variable). Figure 5.12 illustrates the hourly average water flow in the reservoir PHS port for OPT1. When positive, it means the PHS is in pump mode, if negative it is in turbine mode. The monthly profile increases its peak in the summer months, due to higher water needs. However, every month follows an identical trendline of pumping water to the upper reservoir in the morning hours, at the first sunlight period; and either pump or turbine in the afternoon, according to the system's requirements, i.e. reservoirs fulness and energy/water needs. During night hours and late evening, the PHS runs in turbine mode, producing hydropower.

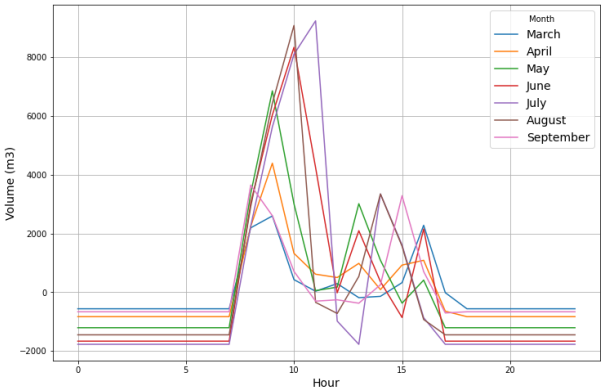

Figure 5.12: Reservoir's average hourly water flow, 1000 m^3/ha - OPT1

5.2.1.3 Water allocation: 3000 m3/ha

The total results for a single year, for 3000 m3/ha water allocation, plus the lifetime (25 years) cash flow are presented in Table 5.5.

Table 5.5: Scenario 1: Main results, 3000 m3/ha

Optimization method:	**OPT1**	**OPT2**	**OPT3**	**NSGA-II**
Turbine Volume [m^3/year]	1,915,870.0	3,301,640.0	5,705,169.0	3,700,615.9
Pumped Volume [m^3/year]	20,166,447.2	21,552,595.3	23,954,453.2	21,893,512.0
Hydropower [kWh/year]	317,494.1	547,141.2	945,449.3	612,989.0
Solar Energy for Pump [kWh/year]	4,133,361.2	5,027,692.2	5,490,393.7	4,516,647.7
Grid Energy for Pump [kWh/year]	5,029,040.0	4,764,490.0	5,393,046.0	5,430,426.2
Grid Energy [kWh/year]	9,219,036.0	8,724,839.0	8,955,087.0	9,324,927.6
Solar Excess to Grid [kWh/year]	6,940,262.0	6,045,931.0	5,583,229.0	6,556,975.2
Lifetime Cash Flow [€]	-7,598,476.0	-7,818,833.0	-8,325,705.0	-7,943,661.7

The leap from 1000 m3/ha water allocation to 3000 m3/ha is quite prominent. From 800 m3/ha to 1000 m3/ha it was noticeable a slight increase in grid usage, depending on how intensively explored were the renewable sources, especially hydropower. Now, the water volume for irrigation is very high and the system no longer can operate the PHS sub-system entirely on solar energy. Additionally, the feasibility of turbine water downhill to generate power for energy needs is lower and more restricted to small amounts and periods. Regarding the NSGA-II optimization, the Python algorithm found the best solution with a maximum of 99.7% water reliability. Nevertheless, the algorithm counts with a biased initialization to help the GA method find solutions that satisfy the constraint of water reliability (=100%). Figure 5.13 presents the energy balance for the same selected day (1st of August) for 3000 m3/ha water allocations, for each optimization method. A major difference in comparison to the energy balances of previous water allocations is the augmentation of the "Energy Deficit" variable, i.e., the energy bought from the grid, to fulfill the leftover energy needs or to power the pumps of the PHS subsystem to increase the stored water volume in the reservoir.

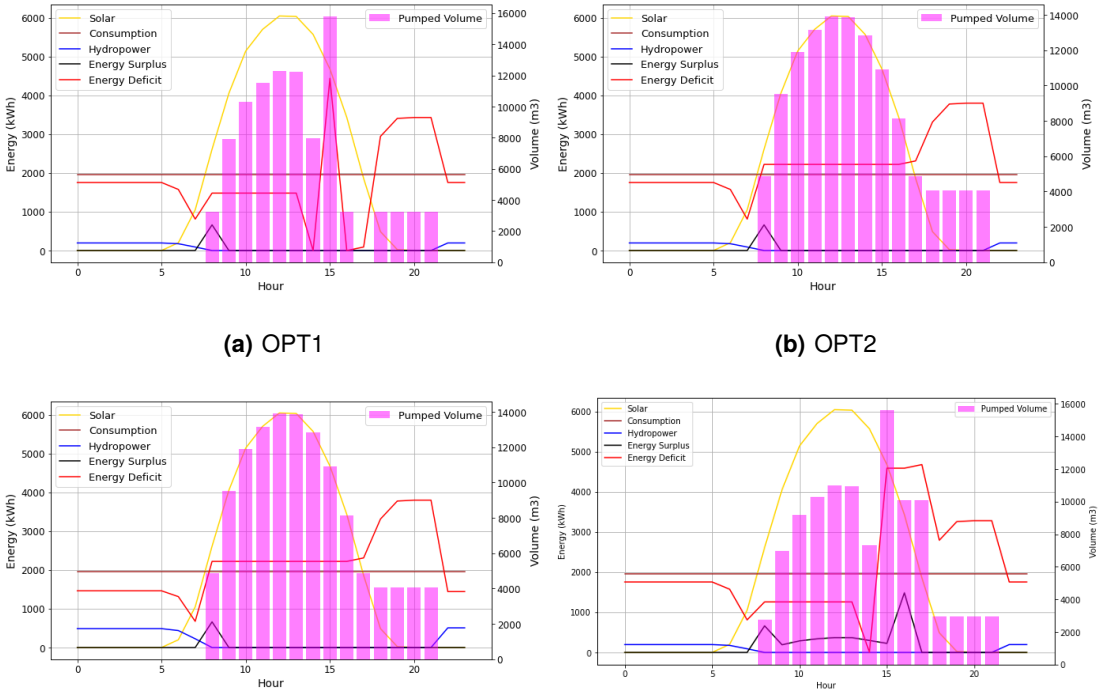

(a) OPT1

(b) OPT2

(c) OPT3

(d) NSGA-II

Figure 5.13: Energy balance on 1st of August, 3000 m^3/ha

On the other hand, the “Energy Surplus”, available to sell to the grid, is much inferior. At 3000 m3/ha water allocation, every opportunity to pump water uphill and store it for safekeeping for irrigation is prioritized. Logically, the contribution of grid energy to the satisfaction of energy needs and the operation of the pumping system is much higher, in comparison to the previously analyzed water allocation, 1000 m3/ha. Figure 5.14 illustrates this phenomenon for OPT1. Further yearly balances for the other optimization methods are presented in Fig.A.6.

It is the significant increase in grid energy dependence that causes the solutions for 3000 m3/ha water allocation to originate such negative cash flows. For 1000 m3/ha, with the OPT1 optimization configuration, the system is not pumping water uphill 85% of the hours of the defined irrigation season (1st of Mar. till 30th of Sept.), despite not using grid energy. But, for 3000 m3/ha and the same optimization configuration, the system is not pumping water only at 44% of the hours of the total irrigation season. Additionally, the first water need (1000 m3/ha + OPT1) only uses around 2.8 GWh of solar energy for pump operation; whereas for a water need of 3000 m3/ha, it uses approximately 4.1 GWh of solar energy to power the pumps. The solar contribution for the PHS increased, but still, it was not sufficient for the 100% energy and water reliability at a 3000 m3/ha water allocation. Regarding the reservoir’s average hourly water flow, the contrast between 3000 m3/ha, Fig.5.15, and 1000 m3/ha, Fig.5.12, is evident, especially the water inflow during night hours and late afternoon, to ensure higher water/energy needs.

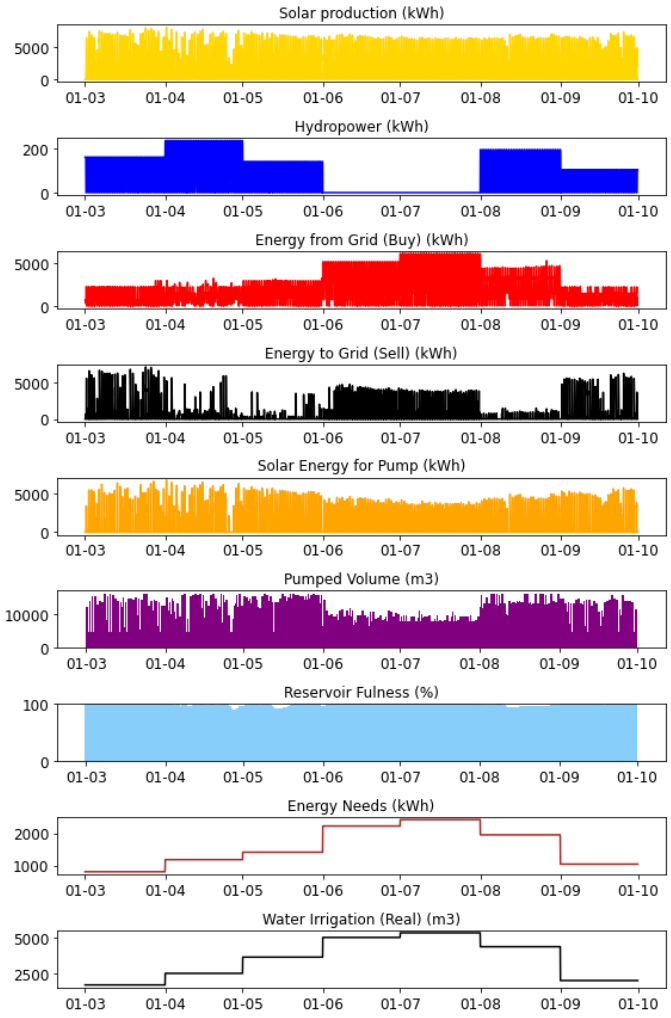

Figure 5.14: Yearly Balance, 3000 m^3/ha - OPT1

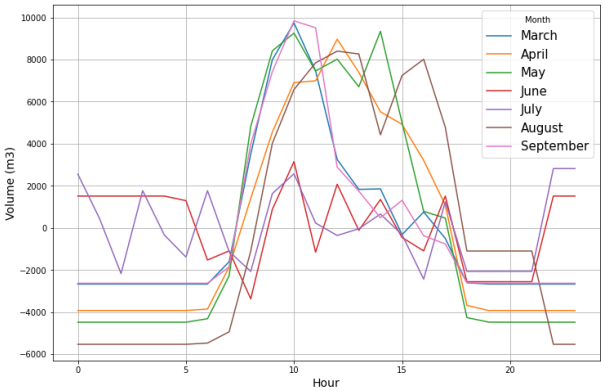

Figure 5.15: Reservoir's average hourly water flow, 3000 m^3/ha - OPT1

5.2.1.4 Water allocation: 6000 m3/ha

The total results for a single year, for 6000 m3/ha water allocation, plus the lifetime (25 years) cash flow are presented in Table 5.6. Further yearly balances are presented in Fig.A.7.

Table 5.6: Scenario 1: Main results, 6000 m3/ha

Optimization method:	**OPT1**	**OPT2**	**OPT3**	**NSGA-II**
Turbine Volume [m^3/year]	891,098.2	295,154.0	933,858.0	6,301,779.0
Pumped Volume [m^3/year]	37,141,485.4	36,546,008.6	37,184,241.5	34,279,223.0
Hydropower [kWh/year]	147,671.0	48,912.3	154,757.0	1,044,281.0
Solar Energy for Pump [kWh/year]	3,259,265.2	3,018,760.9	2,920,753.0	1,516,573.4
Grid Energy for Pump [kWh/year]	13,615,556.0	13,585,512.0	13,973,494.0	14,057,810.6
Grid Energy [kWh/year]	23,421,659.0	23,490,374.0	23,772,511.0	22,967,303.7
Solar Excess to Grid [kWh/year]	5,159,513.0	5,400,018.0	5,498,026.0	6,902,205.2
Lifetime Cash Flow [€]	-22,973,973.0	-23,250,284.0	-23,505,846.0	-21,649,585.3

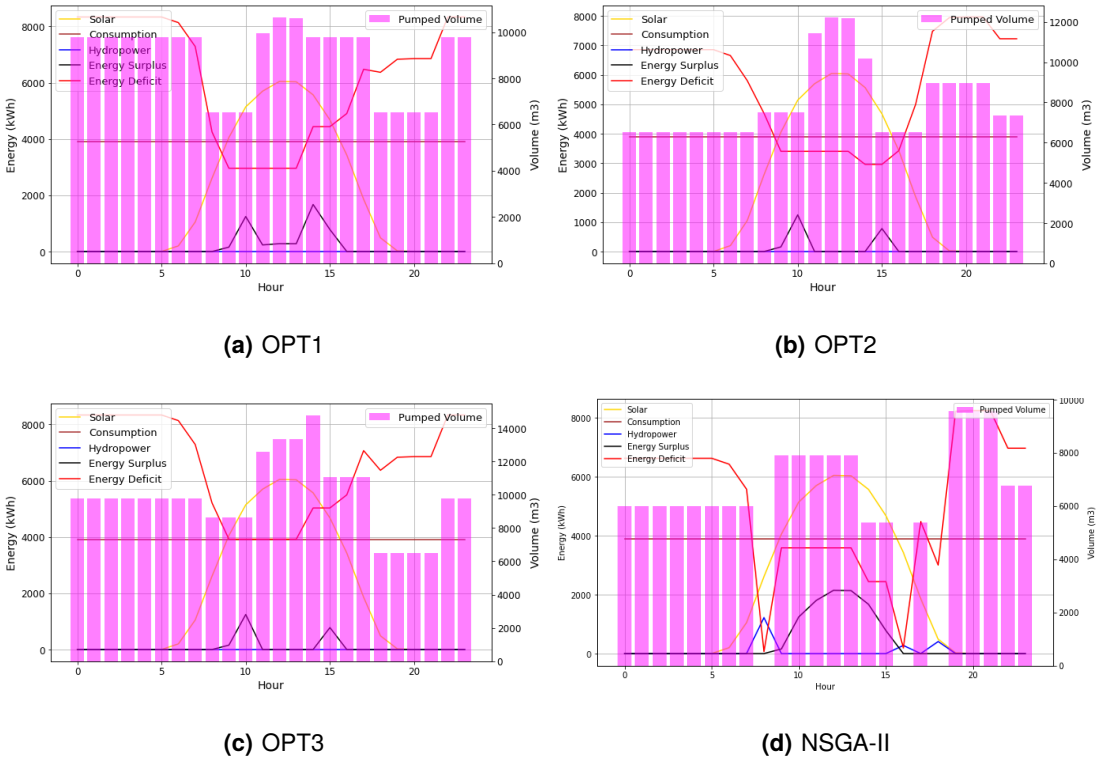

(a) OPT1 **(b)** OPT2

(c) OPT3 **(d)** NSGA-II

Figure 5.16: Energy balance on 1st of August, 6000 m^3/ha

For a water allocation of 6000 m3/ha, the importance of using the grid as an auxiliary to renewables increases to its peak. Most solar energy is primarily consumed for energy needs. On the first of August, Fig.5.16, it is easily noticeable that the pump schedule is no longer limited to sunny hours. This is due to the hydropower generation being almost nonexistent, opening the possibility to pump water during the night, or throughout the day. This is one of the reasons why grid usage also increases significantly, as the

system prefers to pump water during the night as the used tariffs are less punishable during those hours. For 6000 m3/ha of water allocation, hydropower generation, with the system's characteristics, is mostly undesirable as it requires high volumes of water to produce the needed energy for the load demand.

During the optimization process, for this irrigation volume, it was more difficult to achieve a diverse range of solutions, as the slightest modification to the energy balance would immediately compromise the water reliability. That's why, from all the water allocations studied, 6000 m3/ha presents the most similar results for each optimization method. As an exception, the NSGA-II optimization in Python, could not obtain a feasible solution, capable of ensuring 100% of water needs. The yielded "best" solution has a water reliability of 79,4%, which corresponds to a significant absence of water fulfillment throughout the season. The algorithm is chosen to maximize hydropower to the extent that the reservoir could never be able to store enough water volume for both hydropower and water consumption. Nevertheless, the multi-objective optimization results, in Python, present a new view of the system for such a great water allocation, in terms of hydropower capabilities, as the maximum power was approximately 4.5 MW. Although a biased initialization was used in the algorithm, with solutions obtained previously with GRG Non-Linear (Solver), the algorithm still could not find a solution with 100% water reliability.

5.2.2 Scenario 2 - PV+Wind+PHS+Grid

Regarding scenario 2, in which the wind energy source is added to the previous scenario (2x2MW wind turbines), the model was deployed and optimized with OPT1 (Maximizing lifetime cash flow) for each water allocation, and with the NSGA-II algorithm for 3000 and 6000 m^3/ha.

5.2.2.1 Water allocation: 800 m3/ha

Table 5.7 presents the total results for a single year, for 800 m3/ha water allocation, plus the lifetime (25 years) cash flow. Reminder, the lifetime cash flow considers no selling of solar excess to the grid in the first five years, as it is described in eq. (3.27). Further yearly balances are presented in Fig.8A.8(a).

Table 5.7: Scenario 2: Main results, 800 m3/ha

Optimization method:	**OPT1**
Turbine Volume [m^3/year]	425,761.0
Pumped Volume [m^3/year]	5,475,570.8
Hydropower [kWh/year]	70,556.2
Renewable Energy for Pump [kWh/year]	2,487,764.8
Grid Energy for Pump [kWh/year]	0.0
Grid Energy [kWh/year]	0.0
Renewable Excess to Grid [kWh/year]	22,446,033.0
Lifetime Cash Flow [€]	7,308,106.1

In comparison to scenario 1 results, the implementation of wind turbines immensely contributed to excess energy sold to the grid, increasing the lifetime cash flow by almost 300%, plus it diminished the

hydropower dependency to satisfy energy needs leftovers. As in scenario 1, the current scenario does not rely on grid assistance to fully ensure water and energy requirements. Therefore, for this small water allocation, 800 m^3/ha, the scenario 2 solution can be presented as an off-grid solution.

5.2.2.2 Water allocation: 1000 m3/ha

Table 5.8 presents the total results for a single year, for 1000 m3/ha water allocation, plus the lifetime (25 years) cash flow. Further yearly balances are presented in Fig.8A.8(b). The water allocation of 1000 m^3/ha follows the same trend as the previous amount. It can still reproduce a system fully independent from the grid (off-grid solution) with the same pattern results: low hydropower requirements and high excess renewable energy for sale. The lifetime cash flow increased 330% in comparison to scenario 1 yielded value with OPT1.

Table 5.8: Scenario 2: Main results, 1000 m3/ha

Optimization method:	**OPT1**
Turbine Volume [m^3/year]	753,252.0
Pumped Volume [m^3/year]	7,002,158.7
Hydropower [kWh/year]	124,827.5
Renewable Energy for Pump [kWh/year]	3,181,353.0
Grid Energy for Pump [kWh/year]	0.0
Grid Energy [kWh/year]	0.0
Renewable Excess to Grid [kWh/year]	21,266,641.0
Lifetime Cash Flow [€]	6,738,222.0

5.2.2.3 Water allocation: 3000 m3/ha

The total results for a single year, for 3000 m3/ha water allocation, plus the lifetime (25 years) cash flow are presented in Table 5.9. The yearly energy and water balance for OPT1 is stated in Fig.5.17. The yearly balances of the NSGA-II optimization, in Python, are shown in Fig.9A.9(a).

Table 5.9: Scenario 2: Main results, 3000 m3/ha

Optimization method:	**OPT1**	**NSGA-II**
Turbine Volume [m^3/year]	649,022.6	642,414.7
Pumped Volume [m^3/year]	18,899,804.0	18,890,557.9
Hydropower [kWh/year]	107,554.7	106,459.0
Renewable Energy for Pump [kWh/year]	6,725,713.1	6,363,455.1
Grid Energy for Pump [kWh/year]	1,861,203	2,219,260.0
Grid Energy [kWh/year]	3,153,867.7	3,513,020.6
Renewable Excess to Grid [kWh/year]	13,596,921.0	13,960,124.8
Lifetime Cash Flow [€]	284,781.0	-17,200.0

For 3000 m^3/ha, the scenario 2 solution required assistance from the electric grid, just as in scenario 1. However, the quantity required to be purchased from the grid, to satisfy all the system's energy/water

needs, is much inferior, yielding a significantly higher lifetime cash flow regarding grid purchases/sales. Wherein scenario 1, the lifetime cash flow reached -8 M€; in scenario 2 it is positive. With the implementation of wind turbines, the system has more flexibility as the energy available from wind generation is almost constant throughout the day and night, complementing the PV energy, which does not produce energy during night hours. Therefore, the PV+Wind variable can satisfy most energy needs during 24 hours, making the system less dependent on hydropower or grid energy to fulfill the night energy needs, as seen by Fig.5.18.

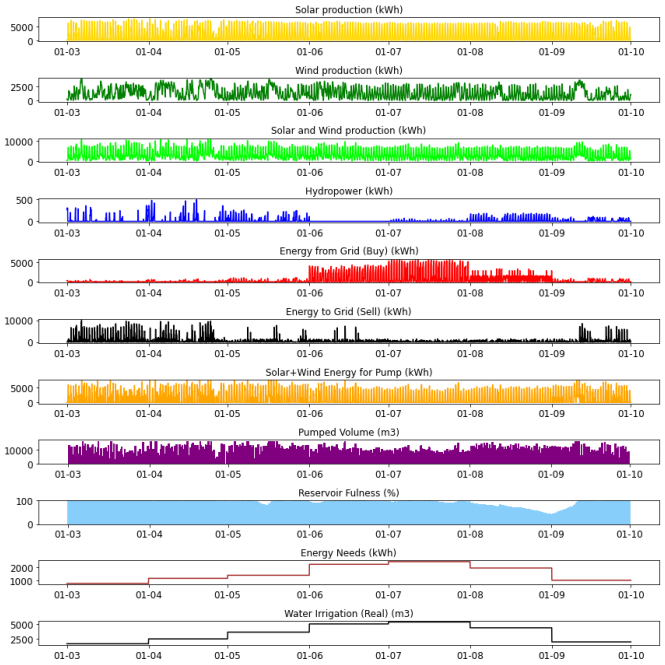

Figure 5.17: Scenario 2: yearly balance, 3000 m^3/ha - OPT1

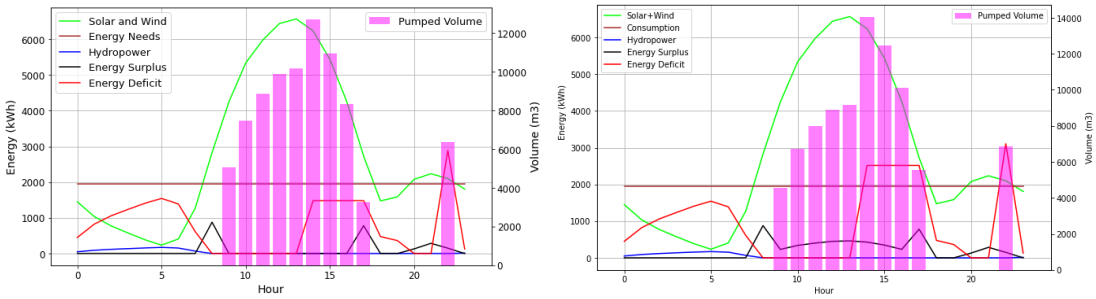

(a) OPT1 **(b)** NSGA-II

Figure 5.18: Energy balance on 1st of August, 3000 m^3/ha

Therefore, with less obligation to hydropower volume, the reservoir and its system are more resilient and capable of ensuring water needs. Additionally, the grid costs to fulfill energy needs, drastically

decrease. This is verified by the significant difference in grid energy usage in both scenarios. Moreover, regarding the performance of the NSGA-II algorithm, for scenario 2, it was better at obtaining more feasible solutions (100% water reliability), than for scenario 1.

Figure 5.19 presents the yearly energy balance with the NSGA-II optimization method and the Pareto front obtained by plotting all of the feasible solutions yielded by the algorithm, that completely ensure water and energy needs. The statistical box plots emphasize the scenario advantage with wind implementation, that reproduces an almost null average grid energy import. Nevertheless, Fig.5.19 helps in the visualization of the abilities of the NSGA-II algorithm, despite it still being quite dependent on the biased initialization, which corresponds to OPT1 results, hence the similarities. However, the algorithm could still yield better solutions, distinct from OPT1 results, if the number of generations is increased and the size of the populations. The significant increase in computational power and run time must be considered.

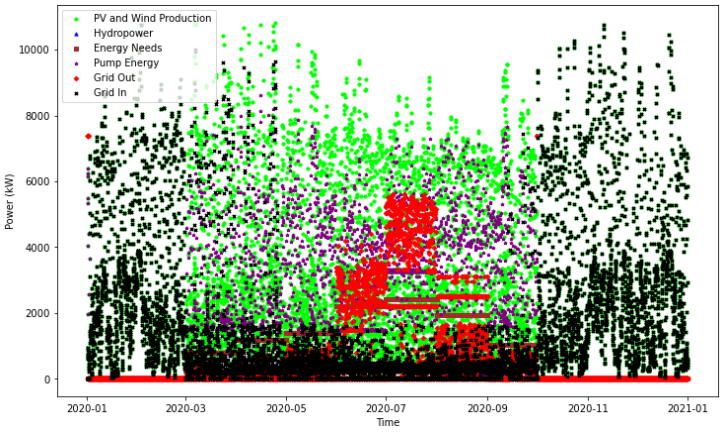

(a) Yearly energy balance

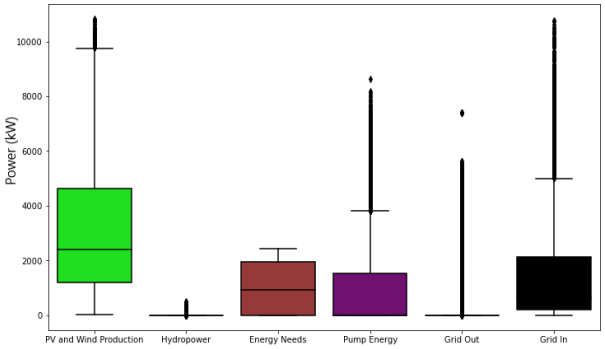

(b) Yearly energy statistics

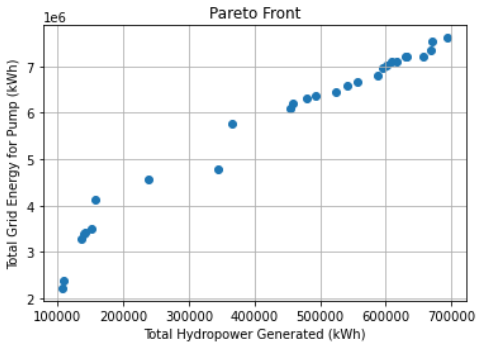

(c) Pareto Front

Figure 5.19: NSGA-II results, 3000 m^3/ha

5.2.2.4 Water allocation: 6000 m3/ha

In Table 5.10 the total results for a single year, for 6000 m3/ha water allocation, plus the lifetime (25 years) cash flow are presented. Further yearly balances are presented in Fig.8A.8(c) and Fig.9A.9(b). For the

Table 5.10: Scenario 2: Main results, 6000 m3/ha

Optimization method:	**OPT1**	**NSGA-II**
Turbine Volume [m^3/year]	502,332.8	4,955,047.4
Pumped Volume [m^3/year]	36,752,296.8	33,145,319.1
Hydropower [kWh/year]	83,245.6	821,145.0
Renewable Energy for Pump [kWh/year]	5,345,139.7	2,068,313.5
Grid Energy for Pump [kWh/year]	11,352,858.0	12,990,893.9
Grid Energy [kWh/year]	16,738,534.2	17,638,670.9
Renewable Excess to Grid [kWh/year]	10,945,068.0	14,222,840.6
Lifetime Cash Flow [€]	-14,775,600.0	-14,319,842.8

highest water needs studied, scenario 2 reproduces a similar behavior as scenario 1. The increase in both water and energy needs makes the system immensely dependent on grid assistance, creating a lifetime cash flow of -14 M€, prominently lower in comparison with the results obtained for 3000 m^3/ha. The NSGA-II optimization could not find solutions that ensure the water reliability constraint, yielding a solution with 83% water needs satisfaction; slightly higher than scenario 1. The unfulfillment of this requirement can be explained by the algorithm's randomly chosen path. From the two objective functions, the maximization of hydropower was the elected one, as the NSGA-II results yielded a higher total hydropower generation, illustrated by Fig.5.20, while slightly increasing grid energy for pump, in comparison to OPT1, which possesses the opposite mission.

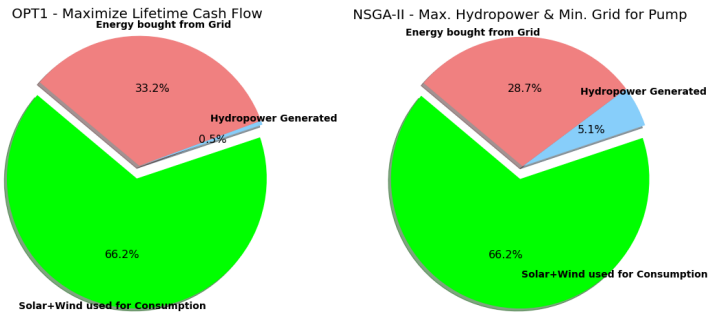

(a) OPT1 **(b)** NSGA-II

Figure 5.20: Energy sources distribution for energy needs, 6000 m^3/ha

5.2.3 Scenario 3 - PV+Wind+PHS+BESS

As for scenario 3, where the grid is replaced by a battery station, the model was deployed and optimized with OPT4, which minimizes battery installed capacity, for each water allocation. The lowest studied

water need does not require a battery energy storage system (BESS), even without wind turbines, as it can be deducted by the results in section 5.2.1.1, where no grid energy is required and hydropower can fulfill the rest of energy needs not satisfied by solar energy.

5.2.3.1 Water allocation: 1000 m3/ha

For 1000 m^3/ha, the optimization was carried out for a system with no wind turbines, but still assured water and energy reliabilities (100%) with a yielded battery station capacity of 2 MWh, rounded up. Table 5.11 presents the yearly results with OPT4. Without wind energy, the system can still generate the total required hydropower energy, proved by the battery energy for the pump equal to the total battery energy to discharge. Further details on the yearly energy and water balance are present in the Appendix folder, by Fig.10A.10(a).

Table 5.11: Scenario 3: Main results, 1000 m3/ha

Optimization method:	**OPT4**
Turbine Volume [m^3/year]	8,277,052.1
Pumped Volume [m^3/year]	14,527,689.8
Hydropower [kWh/year]	1,371,656.5
Renewable Energy for Pump [kWh/year]	6,211,500.9
Battery Energy for Pump [kWh/year]	388,994.0
Battery Energy to Discharge [kWh/year]	388,994.0
Renewable Excess to Charge [kWh/year]	7,127,040.0

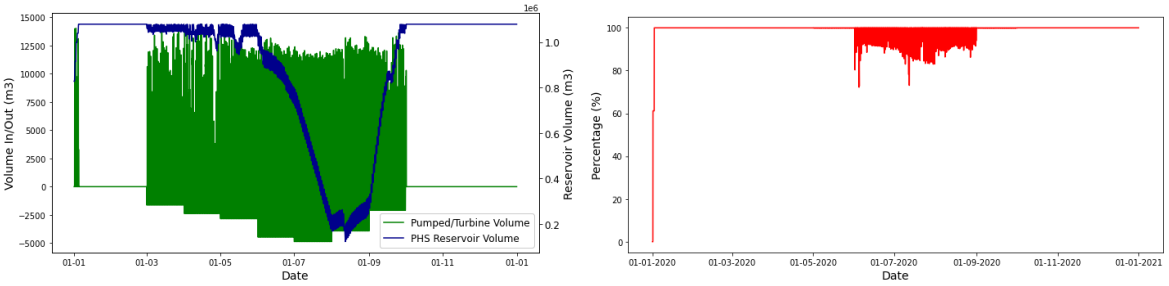

(a) Reservoir fulness **(b)** BESS state of charge

Figure 5.21: Reservoir and BESS hourly state of charge, 1000 m^3/ha

Figure 5.21 presents the state of charge of both the water reservoir and the BESS station, throughout the year. For this water allocation, the off-grid solution with a BESS of 2 MWh is quite robust and flexible to the demand. Although the reservoir fulness nearly drops to its minimum, the system's optimization is attributing the maximum hydropower generation share possible, hence the significant drop.

5.2.3.2 Water allocation: 3000 m3/ha

For 3000 m^3/ha, the off-grid solution has more difficulty to satisfy its needs, mainly energy consumption. A first optimization (OPT4) with 2 wind turbines, equal to scenario 2, was carried out. However, the minimum yielded BESS capacity was 18 MWh, 123% the installed solar and wind capacity, to fully satisfy water and energy needs. This result is inappropriate and an over-dimension of the BESS station. Therefore, the number of wind turbines was increased to four, to seek the minimization of BESS capacity, below the sum of solar and wind combined maximum power. The best solution obtained was 8 MWh of battery capacity, i.e. 47% of the installed solar and wind power. Although the water reliability constraint is met for this value, the energy reliability is 97.4% (132 unsatisfied hours out of 5136). This small unsatisfaction of the energy needs, i.e. 2.6%, can be neglected. The obtained capacity is appropriate to the PHS characteristics as it has a higher capacity than the nominal power of the pumps, just as the DC peak power (equal or slightly below the maximum energy capacity), crucial for the optimal pump operation. Table 5.12 presents the yearly results with OPT4. Further details on the yearly energy and water balance are present in the Appendix folder, by Fig.10A.10(b).

Table 5.12: Scenario 3: Main results, 3000 m3/ha

Optimization method:	**OPT4**
Turbine Volume [m^3/year]	1,293,590.1
Pumped Volume [m^3/year]	19,543,834.7
Hydropower [kWh/year]	214,371.2
Renewable Energy for Pump [kWh/year]	8,879,524.1
Battery Energy for Pump [kWh/year]	0.0
Battery Energy to Discharge [kWh/year]	502,159.2
Renewable Excess to Charge [kWh/year]	23,117,594.0

Figure 5.22 presents the state of charge of both the water reservoir and the BESS station, throughout the year. The vulnerability of the battery performance can be visualized by the regular oscillation between completely charged and fully discharged throughout the consumption period. This behavior is not ideal, as it positions the system under constant stress and less reliability to not satisfy water/energy needs.

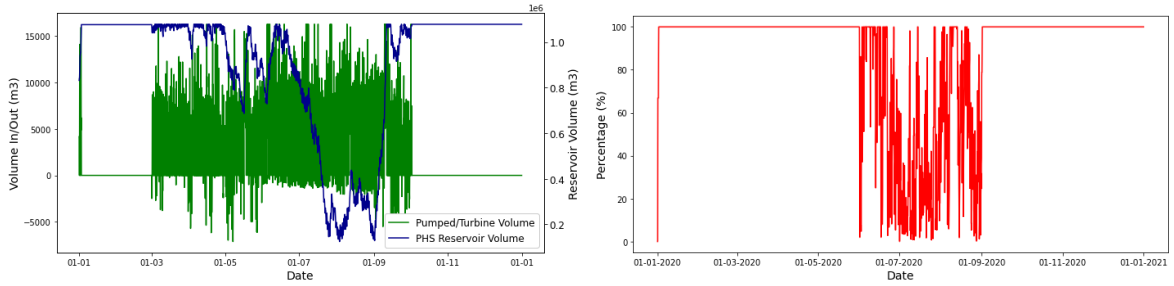

(a) Reservoir fulness **(b)** BESS state of charge

Figure 5.22: Reservoir and BESS hourly state of charge, 3000 m^3/ha

5.2.3.3 Water allocation: 6000 m3/ha

Regarding the highest water allocation, 6000 m^3/ha, the off-grid solution with batteries post-optimization could not yield any feasible solutions, or near enough. Both water and energy reliability parameters stood around 80% and 90%, respectively, in many iterations. These results are infeasible. An unrestricted increase in the number of wind turbines does not stand as a solution, as the excess renewable energy, not used on energy needs or pumping, requires to be stored in the BESS. However, it is unrealistic to implement a battery capacity of 20 MWh or above for this case study, not solely due to its costs but to its size and characteristics. Various optimization trials were made with six, seven and eight wind turbines, but no feasible solutions were obtained, even with battery capacities of 16, 20 and 22 MWh.Therefore, for 6000 m^3/ha, it was concluded that scenario 3 does not stand as an appropriate solution for the analyzed agricultural field.

5.2.4 Economic comparison

In this section, the economic results for each scenario and water allocation are presented and compared to evaluate the solution's performance during a lifetime. Each scenario is primarily compared with the "current approach" which consists solely of the grid energy to power the pump station and to satisfy energy needs.

5.2.4.1 Scenario 1 - PV+PHS+Grid

Starting with the initial investment in scenario 1, it is necessary to account for the photovoltaic farm and the PHS stations (hydropower implementation and VSD/VFD pumps). Hence, with 9 MW of PV peak power installed, the initial investment associated with solar energy (PV and inverters) is 3,929,000 €, considering 50% state subsidies. With the required 1 MW installed power of hydropower, its initial investment is 1,500,000 €. The total PHS initial investment is 2,240,000 €. The total initial investment of scenario 1 is 6,169,000 €.

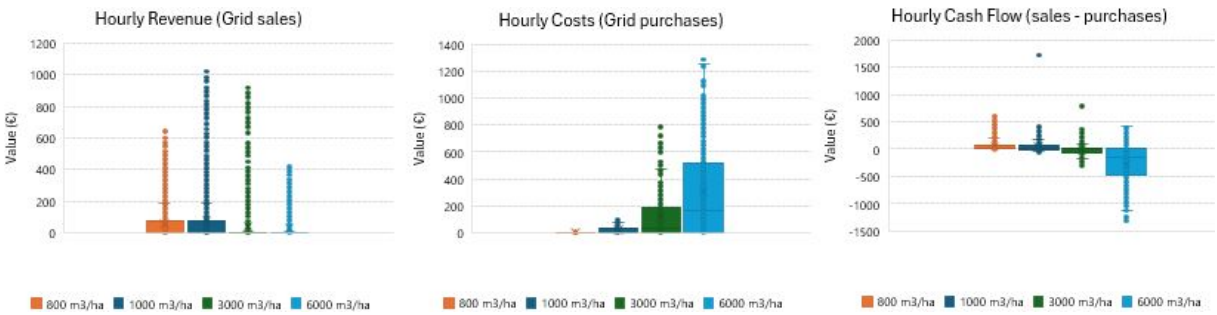

Figure 5.23: Hourly grid revenue, sales and cash flow with OPT1

Proceeding to the operation and maintenance costs, the yearly values are the following ones: 78,580 €/year from solar, 74,000 €/year from the pump station and 20,000 €/year from the turbine station. As for the cash flow, associated with the grid balance, Fig.5.23 presents the range of yearly values for each water allocation, with OPT1 (Maximize the lifetime cash flow). The lifetime cash flow of each water allocation and optimization method is present in their respective results sections, computed through eq. (3.27).

Regarding the environment component, Fig.5.24 shows the yearly produced mass of CO_2 by the system. For 1000 m^3/ha, the scenario 1 solution reduced CO_2 emissions, associated with grid usage, by 88%; while for 3000 m^3/ha, it reduced by 45%. The yearly carbon emissions tax is presented in the Table 5.13, computed through eq. (3.28).

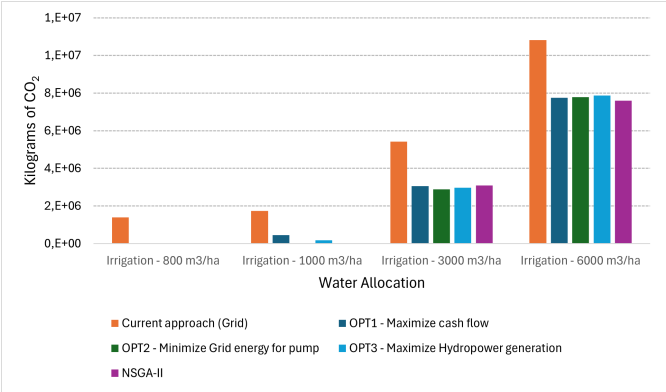

Figure 5.24: Produced mass of carbon dioxide

Table 5.13: Yearly CO2 emissions taxation for each water allocation and optimization

Solution:	800 m3/ha [€]	1000 m3/ha [€]	3000 m3/ha [€]	6000 m3/ha [€]
OPT1	0.0	52,684.3	348,940.0	900,848.5
OPT2	0.0	1,055.1	335,576.5	903,491.5
OPT3	0.0	21,118.8	344,432.4	914,343.1
NSGA-II	-	-	358,657.2	883,373.0
100% Grid	162,470.5	202,454.9	630,276.5	1,256,579.8

Ultimately, the net present value (NPV) for scenario 1 configurations is summarized in Fig.5.25. In every water allocation and optimization method, the hybrid solution proposed by scenario 1 yielded a higher NPV than the current approach, for a lifetime of 25 years. The main reason for this is the significantly lower consumption and dependence on grid energy and secondly the CO2 emissions taxation. This result is an important feature for the feasibility of the project.

On average, the current approach (solely grid as an energy source) uses four times more grid energy. For the lower water allocations, 800 and 1000 m3/ha, the difference is considerably more pronounced. About the remaining water allocations, 3000 and 6000, the difference gets thinner, but mainly due to the high energy needs and the logic behind each model design; Energy needs are primarily satisfied by solar energy. Therefore, if the energy demand is high, the solar energy available will be mainly consumed.

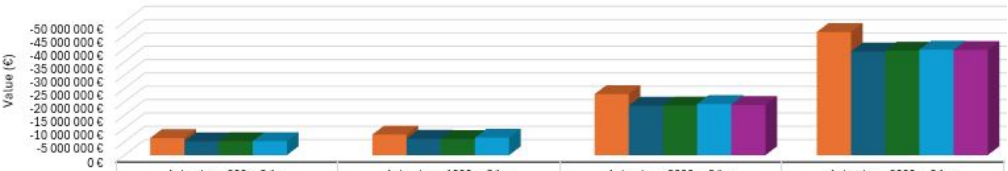

	Irrigation - 800 m3/ha	Irrigation - 1000 m3/ha	Irrigation - 3000 m3/ha	Irrigation - 6000 m3/ha
Current Approach (Grid)	-6394 154 €	-7740 413 €	-22886 040 €	-46168 712 €
OPT1 - Max. Lifetime cash flow	-5208 419 €	-6163 134 €	-18552 568 €	-38886 527 €
OPT2 - Min. Grid energy for pump	-5257 728 €	-6077 194 €	-18600 390 €	-39186 828 €
OPT3 - Max. Hydropower	-5257 728 €	-6531 922 €	-19187 647 €	-39540 890 €
NSGA-II			-18811 843,03 €	-39441 796,20 €

Figure 5.25: Net Present Value - Scenario 1 versus Current Approach

The values attributed to energy needs may be considered to be somewhat inflated, but the intent is to explore the limits, capabilities, and sizing of the hybrid solution. It was prudent to slightly exceed the energy requirements, taking into account the topography of the area, which increases the energy consumption by the water-nexus system network. To evaluate the influence of the energy need values, a single iteration optimization for 6000 m3/ha of water allocation was performed, with half the energy needs predefined. This configuration was able to double the solar energy used by the pump station and decreased the lifetime cash flow from -23M€ to -14.4M€ (OPT1), primarily due to the reduction of grid consumption. It is a significant decrease, revealing a disadvantage of the developed model; it firstly consumes the generated solar energy for energy needs and then manages it for the PHS. Which then requires an auxiliary from the grid to comply with 100% water needs reliability. Nonetheless, this strategy was preferred, as the energy needs correspond mainly to the energy consumed by the irrigation network; i.e., the operation of pumps, valves, control devices, and hydrants, present in the irrigation network distributed throughout the 6000 hectares that deploy water to the crops.

Regarding the levelized cost of energy (LCOE), computed by eq. (3.30), is an economical index parameter corresponding to the ratio between a system's costs and the energy generated by it, during a lifetime. Therefore, for twenty-five years, the following LCOEs for each water allocation on scenario 1 are 0.02, 0.03, 0.05, and 0.11 €/kWh, in ascending order. The results were obtained through the fraction of the overall costs (initial investments, O&M, carbon dioxide taxes, and grid purchases) by the summed generated energy of solar and hydropower (the grid is not included as it is an auxiliary and external source of the system). The LCOE for each optimization technique ends up yielding the same value, apart from OPT2 and OPT3 for 1000 m3/ha, which results in 0.02 €/kWh.

5.2.4.2 Scenario 2 - PV+Wind+PHS+Grid

For scenario 2, the lifetime grid cash flows balance (presented in Tables 5.7, 5.8, 5.9 and 5.10) are higher than scenario 1, for every water allocation. Implementing wind turbines into the system allows it to be more independent from the grid and produce more excess renewable energy that can be sold to the electric grid, increasing the cash flow. This characteristic is the main advantage, economically wise, of

scenario 2 versus scenario 1. Regarding initial investments, scenario 2 differs from the first scenario in the possession of wind turbines. Hence, with two selected wind turbines of 2 MW Table 3.3, the total initial investment is 8,569,000 €. As for O&M costs, from Table 3.3, the sum of it yields 232,580 € every year.

The previous economic elements are equal for each water allocation and optimization. As for the carbon emissions tax and the final net present value, it is presented in Table 5.14, computed by eq. (3.28) and eq. (3.29), respectively. Scenario 2 is capable of completely avoiding carbon emissions, associated with the electric grid, for the two lowest water needs, and up to 80% for 3000 m^3/ha.

Table 5.14: Scenario 2: Yearly CO2 costs and Lifetime NPV

Water Allocation:	800 m3/ha	1000 m3/ha	3000 m3/ha	6000 m3/ha
Yearly Carbon Dioxide Emissions Tax [€/year]				
OPT1	0.0	0.0	121,304.7	643,800.9
NSGA-II	-	-	135,118.5	678,422.1
Net Present Value [€]				
OPT1	-3,372,031.9	-3,941,915.7	-11,496,444.5	-31,299,544.4
NSGA-II	-	-	-11,923,814.0	-31,158,045.2

The net present values obtained in scenario 2 are significantly higher than in scenario 1. Despite the superior initial investment and O&M costs, two factors contribute to this occurrence: lower carbon dioxide taxes and greater cash flow balance. Concerning the levelized cost of energy (LCOE), the lifetime energy generated from solar, wind, and hydropower is approximately 678.2 GWh in each water allocation. The computed LCOE, eq. (3.30), for 800, 1000 and 3000 m^3/ha is equally 0.02 €/kWh, as for 6000 m^3/ha it is 0.05 €/kWh, independently of the optimization method (OPT1 or NSGA-II).

5.2.4.3 Scenario 3 - PV+Wind+PHS+BESS

Scenario 3, as an off-grid solution, does not possess the cash flow variable in the economic assessment. Additionally, there is no carbon dioxide impact derived from grid consumption and subsequent taxation, saving up to 5.4 10^6 kg of CO_2, annually, for 3000 m^3/ha. It is solely needed to account for initial investments and yearly operation and maintenance costs. Concerning initial investments, it is not equal for each studied water allocation, due to different installed capacities for the wind energy production and the battery energy storage system. For 800 m^3/ha, which requires either no wind turbines and batteries, post-optimization, it is not justified to make an economic assessment, as it consists of scenario 1 configuration, but without the grid sales possibility. This negatively impacts the economic results for scenario 3 - 800 m^3/ha, which would be more expensive than scenario 1.

Proceeding to the other water allocations with feasible solutions for an off-grid BESS hybrid system, 1000 and 3000 m^3/ha; their configurations slightly differ in the number of wind turbines and installed battery capacity, yielded by OPT4 optimization. In 1000 m^3/ha, no wind turbines were selected and the

installed capacity for the BESS is 2 MWh. This results in a total initial investment of 6,769,000 € and O&M of 202,580 €/year. As for 3000 m^3/ha, there are four wind turbines and a yielded through optimization battery capacity of 8 MWh. Additionally, the system's management reaches a peak hydropower of 1.2 MW through the season. Therefore it is required to account for an extension of hydropower, from 1 MW to 1.5 MW, altering its initial investment. Consequently, the total initial investment is 14,119,000 € and the O&M costs are 422,580 €/year. The initial investment of solar and wind energy maintains the 50% state subsidies, considered in previous scenarios, despite the inability to sell excess renewable energy to the electric grid. From Fig.3.29, the net present values for both water allocations can be computed, where the variables NPV_{CF} and EC_{CO2} are null. For 1000 m^3/ha, the NPV is -8,608,426.4 €, and for 3000 m^3/ha is -17,956,026.4 €.

Regarding the LCOE of scenario 3, for 1000 m^3/ha it is equal to 0.02 €/kWh and for 3000 it is equal to 0.018 €/kWh. The energy balance in the BESS is not considered in the energy generation parcel. Nonetheless, the obtained LCOE for scenario 3 is equal to scenario 2, despite the significant discrepancy in the NPV, due to the increase in wind turbine installed capacity, which subsequently increases the system's energy generation. This compensates for the higher costs in scenario 3. However, scenario 2 also has significant costs, if the revenue from grid sales is neglected.

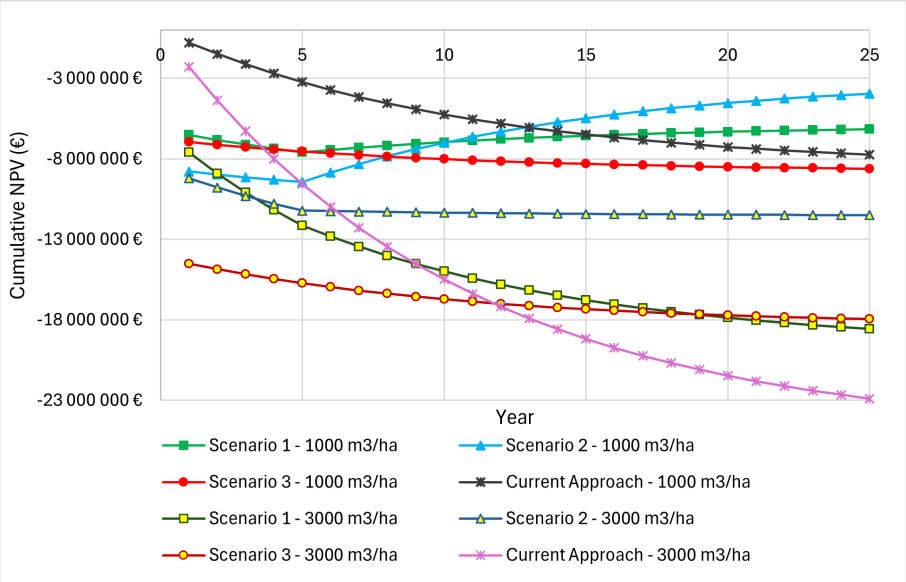

Figure 5.26: Hybrid Scenarios payback NPV comparison through lifetime, OPT1(4)

Ultimately, Fig.5.26 presents the NPV evolution of each scenario through the entire lifetime, for 1000 and 3000 m^3/ha, with OPT1 for scenarios 1 and 2 and OPT4 for scenario 3. For a water allocation of 1000 m^3/ha, scenarios 1 and 2 overcome the current approach (100% grid) by years 16 and 13, respectively. Scenario 3 never surpasses the current approach scenario for twenty-five years. Scenario 2 overcomes scenario 1 in year 11. For 3000 m^3/ha, scenario 2 overcomes scenario 1 in year 4 and the current

approach in year 7. Scenario 3 slightly overcomes scenario 1, for 3000 m^3/ha, at year 19. However, it is an exception, as scenario 3 possesses an inferior NPV throughout its lifetime, versus scenarios 1 and 2, for 1000 m^3/ha, and versus scenario 2, for 3000 m^3/ha. Scenario 2 is the hybrid solution with the most attractive NPV, surpassing other scenarios and the current approach with clear distinction.

5.3 HOMER model comparison

In addition to the developed algorithmic model, the case study's irrigation field was simulated and optimized with widely commercial software, HOMER PRO, for the scenario 1 hybrid solution [60]. The comparison has been made with the single optimization objective of maximizing the net present value. The economic evaluation of the HOMER model results did not include the cost of carbon emissions. Henceforth, the simulation/optimization work developed in the software is referenced as HOMER, as the developed algorithmic model may be referred to as HY4RES or just the model. The HOMER's diagram system is presented in Fig.5.27.

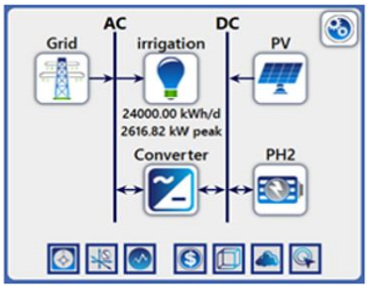

Figure 5.27: HOMER developed model's diagram

The HY4RES model, designed with an algorithm that accounts for both the energy and water demands, ensures their fulfillment and reliability assessment. However, the HOMER software is built to analyze energy systems, not considering a water consumption need. Although it can simulate pumped hydropower storage systems, it is solely restricted to an energy-based analysis. Therefore, HOMER can not ensure 100% water needs reliability.

For a lower water allocation, 1000 m^3/ha, HOMER yielded an energy balance presented in Fig.5.28(b), in which the grid purchases are null throughout the year. Placing the HY4RES results, for the same water allocation, side by side, Fig.5.28, evidences the differences between the designed model and the commercial software. From the HY4RES model, it was proved that to entirely ensure water needs, the system had to consume from the electric grid to ensure energy needs. In HOMER, with the absence of water constraints, the optimization process uses hydropower to fulfill the rest of the energy needs not covered by solar energy. Nonetheless, the reservoir's fullness is steadily at its maximum levels, therefore it is unlikely that the water needs were not met, or are near 100% reliability.

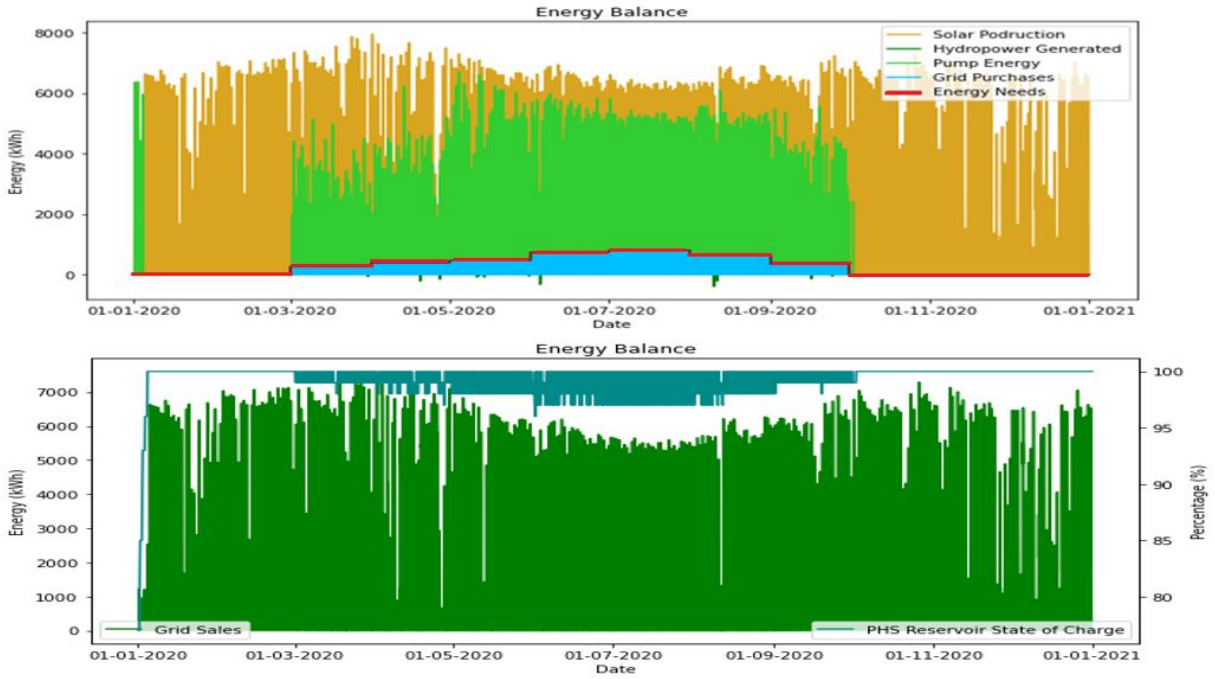

(a) OPT1 - HY4RES Model

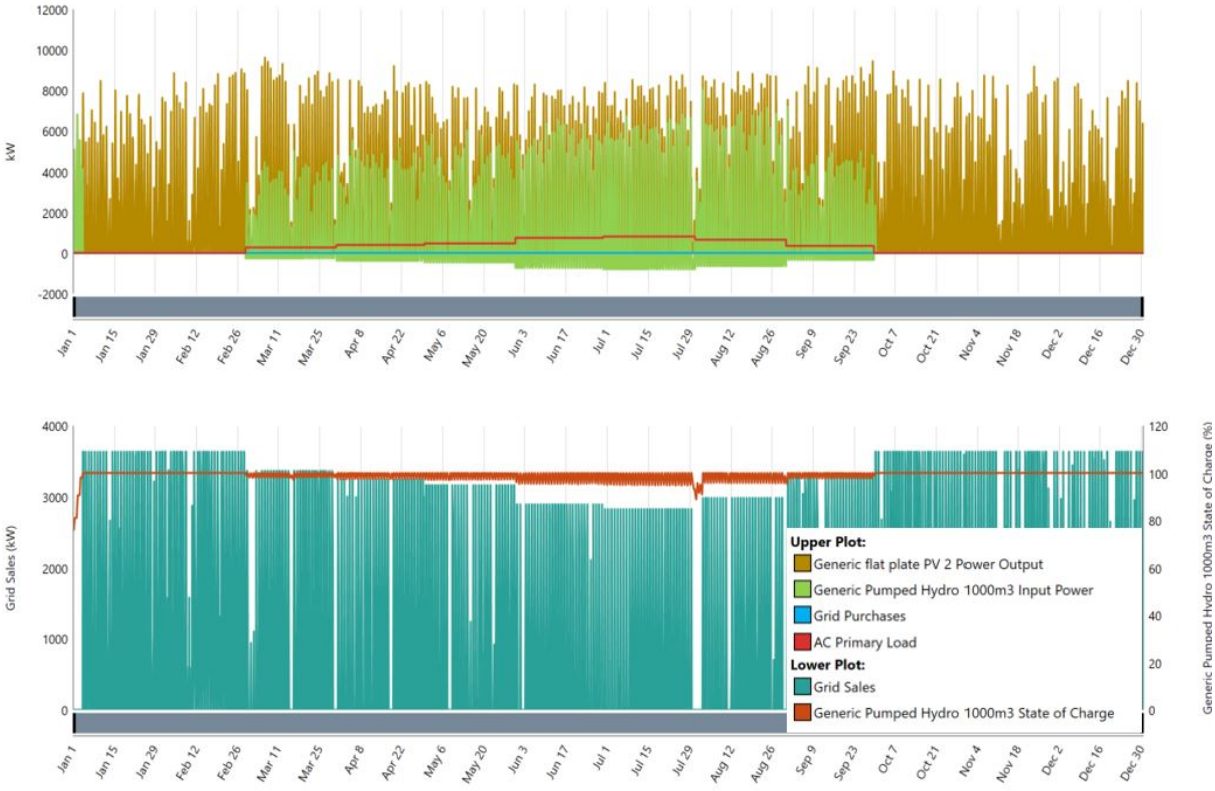

(b) HOMER

Figure 5.28: Model VS. HOMER, 1000 m^3/ha

Additionally, the obtained NPV and LCOE with HOMER were 3.6 M€ and 0.039 €/kWh. The levelized cost of energy is almost identical to the one obtained with the developed model. But, as for the net present value, there is a difference of approximately 2.4 M€. This discrepancy is justified, apart from small adding parameters, by the non-consideration of carbon dioxide emissions tax by HOMER economic evaluation, plus the absence of grid purchases.

However, with a higher water need, of 3000 m^3/ha, the HOMER results are more distant and unfeasible in comparison to the developed HY4RES model, as shown in Fig.A.11 (Appendix). It shows the energy balance produced with HOMER and HY4RES. Comparing both obtained results, it is possible to see the lower grid purchases, as the software chooses to solely buy grid energy to satisfy energy needs, without considering the additional pump energy required to store sufficient water volume in the reservoir. Thus, the reservoir in the HOMER software ends up at a regular minimum level throughout the season, not fully ensuring water needs. The monthly solar energy generation and grid imports for 3000 m^3/ha are illustrated in Fig.5.29. Although both models follow the same pattern, with a peak in both energy sources in the summer months, the HY4RES results reveal that the system requires approximately twice the grid energy required by the HOMER model. Assessing the hydropower generation, HOMER reaches a peak of approximately 2 MW power in July, whereas the HY4RES model never surpasses 1 MW. This is due to the minimum reservoir limit and water needs, permanently enforced in the HY4RES model.

Regarding the economic assessment, the obtained NPV and LCOE by HOMER are 8.5 M€ and 0.07 €/kWh, respectively. The NPVs differ by 10 M€, which is a significant discrepancy between the model's results for the same water allocation. However, the reason remains the same as to 1000 m^3/ha. The model requires higher grid consumption to ensure the energy and water needs, which greatly increases costs and the final NPV. For 3000 m^3/ha, the grid consumption in the model is 4.5 times the grid energy consumed in the optimized results with HOMER. Subsequently, the CO_2 emissions costs, resulting from the grid consumption, not accounted for with HOMER, singularly add 3.2 M€ to the HY4RES model's computed NPV.

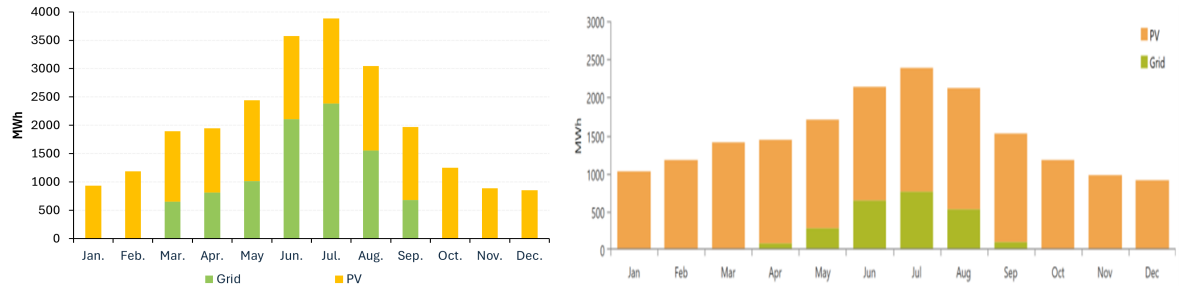

(a) OPT1 - HY4RES Model

(b) HOMER

Figure 5.29: Model VS. HOMER - Monthly PV production and Grid purchases, 3000 m^3/ha

Chapter 6

Energy Community - small-scale case study

6.1 Data Collection

This section presents the input data for the small-scale energy community case study setup, followed by the subsequent results section.

6.1.1 Load

The annual energy consumption profile of the small energy community of Marruge, in Tondela, Portugal, is presented in Fig.6.1, wherein the months of January, February and December are distinguished by a markedly elevated consumption pattern. The maximum load recorded was 43.68 kW, in February.

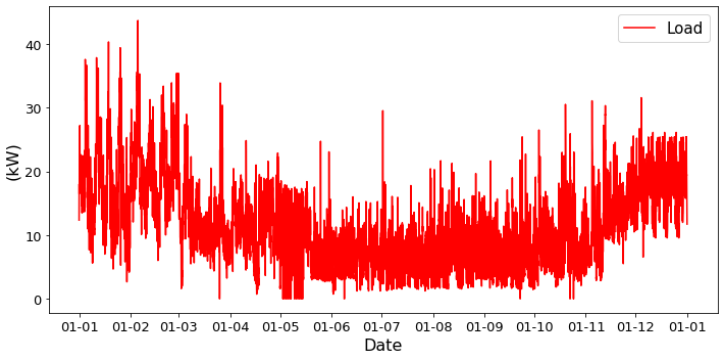

Figure 6.1: Microgrid's yearly load profile

6.1.2 Photovoltaic energy production

The solar power production data was obtained from the online tool PVGIS for a peak power of 1 kWp and subsequently scaled up in accordance with the proposed setup and configuration. The selected module was of the monocrystalline silicon module type with an optimized slope and azimuth orientation of 32 and -5 degrees, respectively.

6.1.3 Wind energy production

The wind power generation (W^i), in kW, was estimated by eq. (6.1), for standard wind speed limits: cut-in speed (u_{ci})=2 m/s, rated speed (u_r)=10 m/s and cut-out speed (u_{co})=25 m/s [61]. The hourly wind speed at a height of 50 m (u^i), was retrieved from PVGIS solar data, in m/s.

$$W^i(u^i) = \begin{cases} 0 & u^i \leq u_{ci} \\ P_r \frac{u^i - u_{ci}}{u_r - u_{ci}} & u_{ci} \leq u^i \leq u_r \\ P_r & u_r \leq u^i \leq u_{co} \\ 0 & u^i \geq u_{co} \end{cases} \tag{6.1}$$

6.1.4 Pumped Hydropower Storage system

The site for the PHS plant has a gross head of 80 m. The average pump and turbine efficiencies (water+electric) are set to 70% and 80%, respectively. In order to ascertain the optimal average pump and turbine heads, the model was initially run with the gross head value to retrieve the typical flow range of the hydraulic circuit with various PHS installed capacities. Given a flow rate range of 30 to 65 l/s, the optimal diameter for the length of a 350 m single pipeline, constructed from cast iron, is 200 mm (flow velocity does not exceed 3 m/s). Based on this, it is feasible to calibrate the average pump and turbine heads. The average pump and turbine heads have been defined as 82 and 77 m, respectively. The PHS system was modeled with two reservoirs, the bottom and upper water storage tanks, with a maximum and minimum volume of 10,000 and 1,000 m^3, respectively. The designed HY4RES model applies to reservoirs as both the starting and ending nodes of the hydraulic circuit. This is because the total volume of water, which is equal to the capacity of a single reservoir, remains constant. Accordingly, the mathematical algorithm presented remains valid for this setup, with the volume of the lower reservoir equal to its maximum volume minus the current volume of the upper reservoir. The case study could also use a smaller hydropneumatic tank, or a combination of several, to produce hydropower with the intermediate storage of potential energy and compressed air, as seen in the laboratory Chapter 4. However, the transient conditions of hydropneumatic vessels can not be accurately simulated with the defined model.

6.1.5 Grid tariffs

Concerning the grid-connected setup solutions for the small energy community system, the import and export tariffs must be defined. The grid cash flow highly depends on the type of energy contract and the price market fluctuation. Nevertheless, a fixed (simple tariff) purchase and sale price of 0.22 and 0.08 €/kWh were defined, respectively.

6.2 Results and discussion

A total of four solutions were assembled: two stand-alone and two grid-connected solutions, which combine different renewable energy sources and energy storage mechanisms. The following section presents their technical capabilities and assesses their economic comparison, obtained by the defined optimization method, OPT5, that minimizes the total installed capacity of the small energy community.

6.2.1 Stand-alone setup - SA

The stand-alone setup examines two solutions that are entirely independent of the external electric grid: PV+Wind+PHS (**SA1**) and PV+Wind+PHS+BESS (**SA2**). These solutions save up to 32 tons of CO_2 emissions, that would be associated with electricity consumption from the grid or non-renewable sources.

6.2.1.1 SA1 - PV+Wind+PHS

The fundamental configuration of the off-grid system, designated as SA1, employs the combination of solar and wind energy sources, with the supplementation of pumped hydropower storage system. The optimization method, defined as OPT5, which minimizes the required installed capacity, while adhering to the 100% grid independence constraint, yielded the power installments for each energy source, as presented in Table 6.1. In the absence of an external grid, the peak winter months require the installation of supplementary power sources to meet the increased demand for energy. Accordingly, the power installed yielded by the optimization generates three times the total consumption energy, in case all the energy sources are permanently connected throughout the year.

Table 6.1: SA1 - PV+Wind+PHS power installment results

Source:	PV	Wind	Pump	Turbine	Total
Power [kW]	40	120	20	40	220

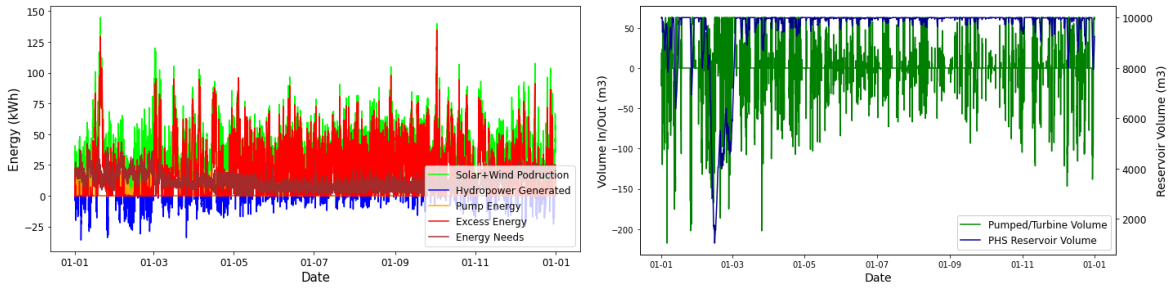

(a) Energy Balance

(b) Water Balance

Figure 6.2: SA1 - PV+Wind+PHS yearly balance

Figure 6.2 illustrates the energy and water balances throughout the year, with particular emphasis on the excess energy (i.e., wasted) generated by the system during periods of low or average demand. The combination of wind and solar energy markedly augments the system's capacity to meet the demand. While the optimized power installations may be deemed excessive for the average consumption load, it is nevertheless imperative to guarantee sufficient capacity during peak months. The issue of wasted energy can be addressed by either deactivating primary renewable sources or, ultimately, connecting the microgrid to the national grid for exclusive exportation.

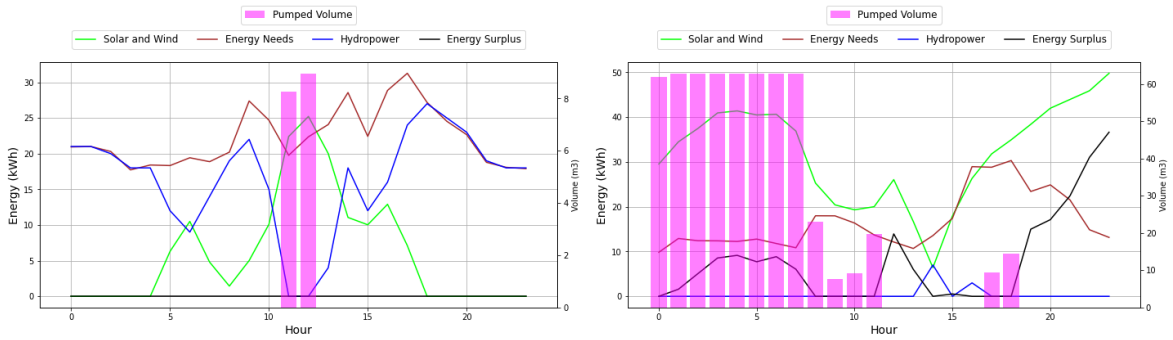

(a) February 12 **(b)** November 12

Figure 6.3: SA1 - PV+Wind+PHS daily balance

Figure 6.3 presents the daily balance on two distinct days. The consumption profile on February 12 is significantly greater than on November 12. The high energy demand requires more hydropower generation to satisfy the unmet consumption by solar and wind energy sources. Subsequently, the month of February is characterized by the balance presented, wherein the pumped volume is restricted to a few hours, permanently decreasing the reservoir's stored volume, and hydropower is highly required to fulfill the energy needs. On the contrary, for months of lower demand, such as presented by Fig.6.3(b), the installed power of solar and wind is enough to completely fulfill the energy load, with its surplus being used to pump significant volumes of water for storage. Regarding the installed pump power, it is significantly lower than the renewable sources as the average renewable surplus is approximately 20 kW. This is due to the prominence of wind energy which causes an inferior but stable surplus of energy, while solar energy tends to create peaks of surplus.

6.2.1.2 SA2 - PV+Wind+PHS+BESS

The second stand-alone solution designated SA2, introduces a battery energy storage system (BESS) to investigate its influence on the system's behavior and ascertain whether it is advantageous by reducing the necessary power installations of other energy sources. The optimized power results are presented by Table 6.2.

Table 6.2: SA2 - PV+Wind+PHS+BESS power installment results

Energy:	PV	Wind	Pump	Turbine	Battery	Total
Power [kW]	55	100	35	40	40	270

Figures 6.4 and 13A.13(a) (Appendix) show the annual balance with the integration of a battery energy storage system. The incorporation of the BESS into the stand-alone setup resulted in a slight decrease in the solar and wind energy sources. However, the total power installation increased, due to an increase in pump power resulting from the optimization preference for installing more solar energy. The surplus energy generated from solar sources exceeds that from wind sources. Consequently, a higher pump nominal power is required to enable its usage in the pumped-storage process, as the solar surplus is characterized by higher peaks than wind surplus due to their distinct generation patterns. The BESS system plays a relatively inferior role in the SA2 solution. Even if its storage capacity were to increase to a hypothetical 1 MWh the power installation of the other energy sources would not undergo a notable reduction. During the winter months, maximum loads occur over consecutive hours, for consecutive days, which presents a challenge for the performance of an electric battery, under the power ranges of the presented small energy solution. Ultimately, the electric battery served to boost the pumped-storage system to ensure enough stored water volume to produce hydropower, when energy needs were not fulfilled by the primary renewables. The scale of the PHS system can endure longer periods of high energy demand, without oversizing the required installed capacity, in comparison to batteries.

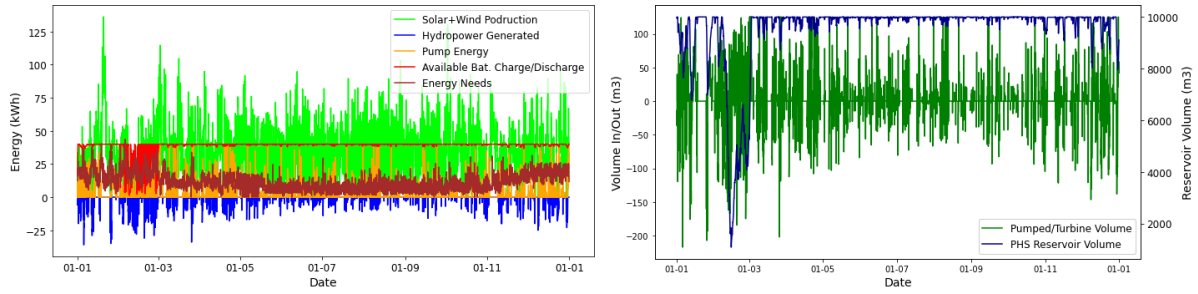

(a) Energy Balance

(b) Water Balance

Figure 6.4: SA2 - PV+Wind+PHS+BESS yearly balance

6.2.2 Grid-connected setup - GC

The grid-connected setup explores a small energy community solution that maintains synchronization with the national electric grid. Nevertheless, to prevent the grid from unduly influencing the system's operation and deviating it from the intended purpose of a microgrid, it is essential to establish two validation criteria. The solution must be at least 80% independent from it and have more energy export than import.

6.2.2.1 GC1 - PV+PHS+Grid

The initial grid-connected configuration, designated as **GC1**, integrates solar energy with pumped hydropower storage. The optimized results yielded a required photovoltaic peak power of 95 kW, with a nominal pump and turbine power of 65 and 40 kW, respectively. The installed power thus satisfies both criteria for the system to be considered a valid small community solution for this case study. If this configuration was to be entirely independent of the external grid, it would necessitate 330 kW of PV and 180 kW of pump power, thereby increasing the initial investment by more than double. Figures 6.5 and 13A.13(b) (Appendix) illustrate the annual balance of the grid-connected solar power solution with PHS.

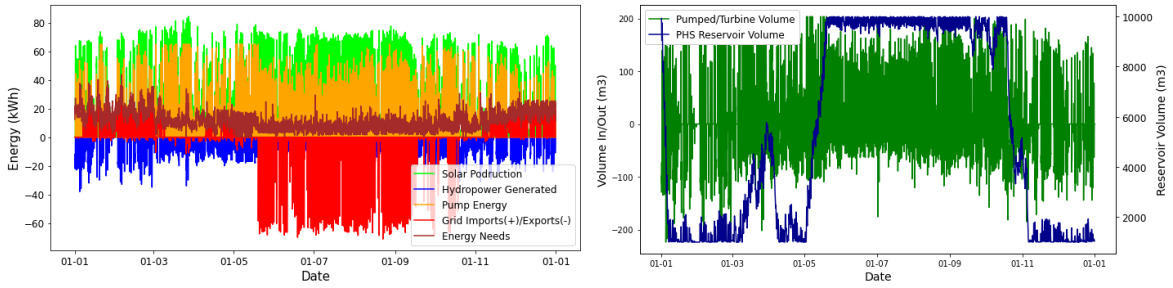

(a) Energy Balance **(b)** Water Balance

Figure 6.5: GC1 - PV+PHS+Grid yearly balance

In comparison to the stand-alone configurations, the grid-connected setup with solar power is more suitable for meeting the total load demand, with a total solar energy production of 134 MWh for an annual energy consumption of 97 MWh. In the stand-alone setup, both configurations demonstrated a primary renewable energy production level that was approximately three times greater than the demand. The import of grid energy is permitted solely during the peak winter months.

6.2.2.2 GC2 - Wind+PHS+Grid

The second configuration for a grid-connected solution, designated as **GC2**, involves the integration of wind energy with pumped hydropower storage, as opposed to the integration of solar energy in the previous solution (GC1). The optimization yielded a requisite wind power installation of 65 kW, with a nominal pump and turbine power of 20 and 40 kW, respectively. The obtained installed power demonstrates a grid independence of 91.7%, with a positive grid balance wherein exports are twice the imported energy required. To be fully independent from the grid it would require a wind power installation of 205 kW and a pump power of 65 kW, representing a doubling of the initial investment. Figure 6.6 illustrates the yearly energy and water balance for the second grid-connected configuration, constituted by wind energy and pumped hydropower storage. This solution stands as the optimal choice regarding installed power ver-

sus energy needs. The annual wind energy production is 123 MWh, with a grid energy requirement of only 9.5 MWh to satisfy the load demand.

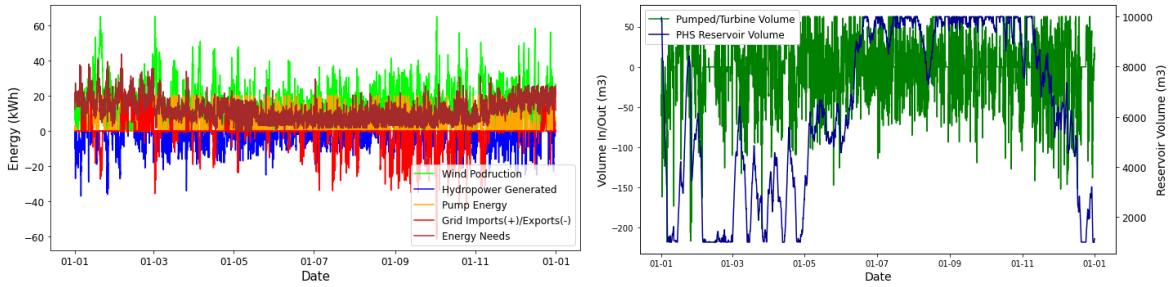

(a) Energy Balance **(b)** Water Balance

Figure 6.6: GC2 - Wind+PHS+Grid yearly balance

Figure 6.7 compares SA1 and GC2, which correspond to the best technical solutions for stand-alone and grid-connected configurations, respectively. The stand-alone solution, SA1, is characterized by grid independence but with significant excess energy due to oversized power installed to fulfill peak load months, during winter. The grid-connected solution, GC2, is characterized by a precise power installment, tuned to the required load, that results in lower excess energy. However, grid energy purchases are required during peak winter months.

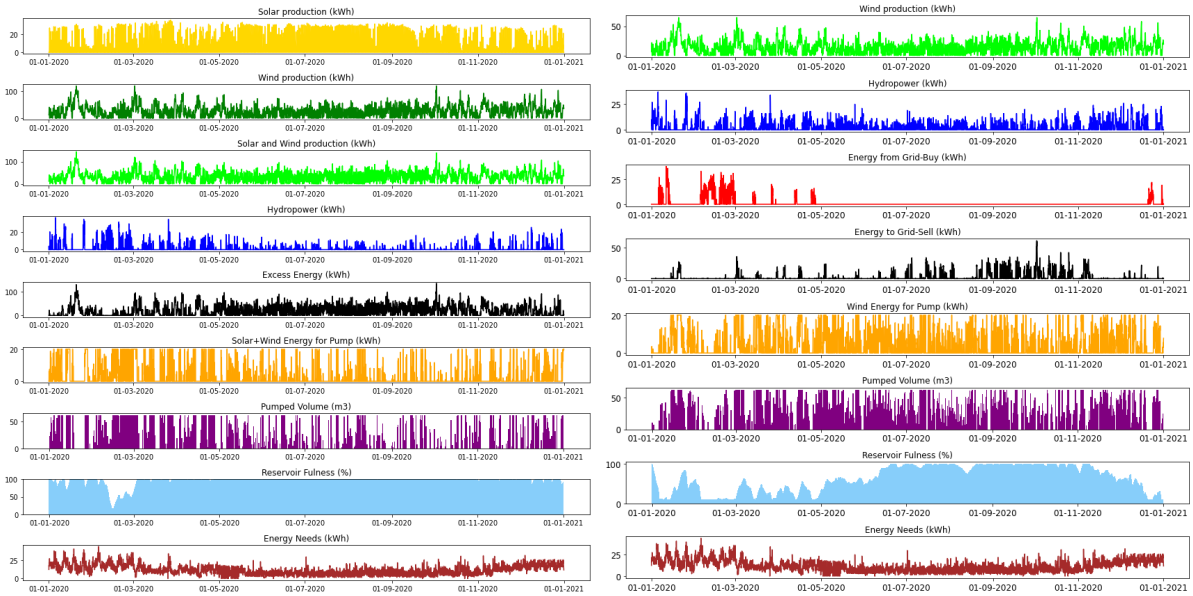

(a) SA1 - PV+Wind+PHS **(b)** GC2 - Wind+PHS+Grid

Figure 6.7: Stand-alone versus grid-connected

6.2.3 Economic assessment

Under the specified economic parameters delineated in Table 3.4, the requisite initial investment and annual operation and maintenance costs are summarized in Table 6.3. In the case of a grid-connected setup, the installation costs of the grid on the small energy system and its synchronization with the national grid's frequency are not necessary, given that the site's current setup is a traditional fully grid-dependent system. The grid-connected configurations, designated as GC1 and GC2, are associated with a fixed annual cash flow, corresponding to the difference between grid sales and purchases. The annual cash flow for GC1 and GC2 is -2,956.3 and -123,2 €, respectively. These values are contingent upon the assigned grid tariffs, simplified for this case study. It is important to note that the import of grid energy entails the consideration of taxes associated with carbon dioxide emissions. The CO_2 costs for GC1 and GC2 are 1,012.6 and 367.2 €, respectively. Each solution's final net present value is presented in Table 6.3, alongside the levelized cost of energy (LCOE).

Table 6.3: Small energy community: economic results

Configuration	Initial Investment [€]	O&M [€/year]	NPV [€]	LCOE [€/kWh]
SA1 - PV+Wind+PHS	259,177.0	3,151.8	-287,785.7	0.039
SA2 - PV+Wind+PHS+BESS	273,861.0	3,718.6	-307,615.0	0.044
GC1 - PV+PHS+Grid	205,914.0	2,259.1	-262,446.0	0.069
GC2 - Wind+PHS+Grid	157,000.0	1,965.0	-179,287.0	0.054

The grid-connected solution of wind and PHS (GC2) presents the lowest net present value (NPV) and required power installed, 125 kW, wherein 105 kW corresponds to energy generation sources, such as wind and hydropower. Concerning the selected site for the examination of a small energy community, the aforementioned grid-connected solution, designated as GC2, remains a viable option and the most economical. Since the site is not located on an island or in an extremely remote area and it benefits from existing electric grid infrastructure, this solution is particularly well suited to the configuration of a small energy system. In scenarios where integration with the general grid is not possible, alternative stand-alone configurations must be considered. If that restriction was imposed, then the first stand-alone solution (SA1) would be the most appropriate. The stand-alone solution with the battery auxiliary (SA2) possesses the highest NPV, whilst the integration of a BESS does not have a significant impact on the performance and flexibility of the system. It still requires a superior overall installed power, increasing initial investment and O&M costs as it can be seen in Table 6.3. The integration of pumped hydropower storage in this study proved advantageous in reducing grid dependency and the required installed power of primary energy sources, contributing to an energy storage capacity of 2.17 MWh. This storage potential can ensure hourly maximum loads for two days.

Chapter 7

Conclusions and Recommendations

7.1 Main conclusions

This thesis achieved the objective of developing advanced simulation and optimization models in the hybridization of the water sector, by the definition and design of mathematical algorithmic models within the water-energy nexus, designated as HY4RES models. The model was developed with the objective of facilitating the integration of renewable energies with pumped hydropower storage (PHS) creating hybrid energy systems, for a variety of applications. Thereby enhancing the PHS contribution and symbiosis with other energy sources, towards net-zero carbon emissions. Although this research examines scenarios incorporating a PHS system, which fulfills both water allocation needs and energy consumption requirements, the model is highly customizable and flexible to different applications, under the water-energy nexus. The development model was presented with two auxiliary alternatives (electric grid or battery energy storage system (BESS)), but these can be adapted to use other energy sources, such as hydrogen storage systems, which function similarly to a BESS.

The analysis conducted in the IST-Hydraulic laboratory (CERIS) and the software simulation of the pumped-storage performance were instrumental in comprehending the behavior and performance of the storage mechanism on PHS systems. From both the experimental and the simulation results, the storage efficiency could be characterized in environments with significant flow and gross head oscillations. The impact of diverse flows and subsequent head losses on the efficiency of the storage process was validated. The methodology employed for the computation of the PHS parameters in the developed HY4RES model was based on the results and behavior observed in the pumped-storage Lab. analysis. Since the model serves hybrid renewable systems, characterized by high fluctuation in power generation, the performance of the pumped-storage unit is similarly vulnerable to these same oscillations. Consequently, the fluctuating power supply to the pumps may result in the generation of diverse flows over a specific duration. This requires the utilization of variable-speed drive pumps to optimize efficiency and circumvent superfluous energy consumption, while simultaneously ensuring a minimal pumped volume. Ultimately, based on the behaviors learned by experimentation and simulation in Chapter 4, the average pump head and efficiency, computed for both case studies and inputted in the model, takes into account the variation of the gross head and associated head loss, as a function of the flow rate and pipeline characteristics. This approach is distinguished from the literature, which is used as a guideline on the mathematical expressions for the PHS systems, which typically assume that the average pump and turbine head are

both equal to the static gross head, i.e. without accounting for the reservoir level fluctuations nor the head losses. This simplified approach may result in inaccuracies, regarding flow rates and exacerbate discrepancies with real-world scenarios.

Regarding the irrigation system, large-scale case study, both optimization methods were capable of identifying an appropriate range of solutions for different scenarios. However, the multi-objective and multi-variable character of the non-dominated sorting genetic algorithm (NSGA-II) exhibited a higher level of complexity, which presented challenges in precisely tuning the problem to align with the modeled system. When an initial solution was obtained beforehand through trial and error in the Solver tool, using GRG nonlinear/evolutionary methods yielded a local solution that satisfied the defined reliability constraints. This proved more challenging in Python using the non-dominated sorting genetic algorithm (NSGA-II), as the system is quite complex with a multitude of iterations and correlations. The optimization problem encountered difficulties in yielding solutions that adhered to the reliability constraints, particularly for a huge water allocation value (e.g., 6000 m^3/ha). This is also attributable to the system's flexibility, as a higher water consumption significantly decreases the range of feasible solutions. Hence, the results demonstrate that as water consumption increases, the system's flexibility is diminished, thereby increasing the risk of failing to meet the full water allocation and energy needs.

Furthermore, in scenario 1 (PV+PHS+Grid), the dependence on the grid energy for higher water allocations is easily observed, in which solar energy is not enough to ensure sufficient water in the reservoir; therefore, the grid starts to power the pump station during night time, when the solar generation is null. For water needs of 800 and 1000 m^3/ha, the grid did not have to power the pumps to ensure a sufficient volume for water needs; on the contrary, for 3000 and 6000 m^3/ha, the grid energy significantly increased to power the pump station, 5 and 14 GWh annually, respectively.

This behavior is mitigated in scenario 2 (PV+Wind+PHS+Grid), wherein wind energy can be leveraged to power the pumps during nocturnal hours and mitigate the electric grid consumption. The primary distinction between the second and first scenarios is the autonomy of the renewable sources of the system from the grid. For instance, with 3000 m^3/ha of water allocation, the grid consumption to power the pumps drops 60% annually. This reinforces the sustainability and renewable solution for the application under study. Furthermore, with the same water allocation, scenario 2 can reproduce a positive lifetime cash flow, of 284,781.0 €, whereas scenario 1 was distinctively negative. In scenario 3 (PV+Wind+PHS+BESS), the system becomes more vulnerable, due to the absence of a robust and permanent backup energy source, such as the grid. If the water and energy needs are high, it becomes very challenging to ensure them, despite the BESS installed capacity, consequent to the tendency for the hourly energy discharge to exceed the energy charge. During the optimization phase, the Solver tool was not able to yield any solution that could satisfy energy needs to its extent. By restricting the BESS capacity to a maximum of the total solar and wind combined installed power, the system would never fully satisfy energy require-

ments. Therefore, a BESS with 8 MWh was obtained, presenting an energy reliability of 97.4% and water reliability of 100%.

From an economic standpoint, scenario 2 is the most attractive, with an NPV of −12 M€ for 3000 m^3/ha, as it maximizes the reduction in auxiliary dependence. Scenario 3 may prove an appropriate solution, particularly for off-grid locations. However, its vulnerability to higher consumption and additional investment costs highly compromises its viability. Ultimately, the two developed algorithms (in Solver and Python) were successfully designed and implemented, demonstrating the capability to produce reliable results for a techno-economic analysis. The irrigation system case study was an ideal application to test different optimization configurations since its large-scale nature produces a wide range of operation strategies and distinct solutions. The carbon emissions assessment made under the economic evaluation evidences the positive environmental impact of hybrid renewable solutions that significantly reduce the carbon footprint of highly polluting sectors, such as the agriculture sector, by reducing grid consumption through the integration of renewable sources. For 1000 m^3/ha, the scenario 1 solution reduced CO_2 emissions, associated with grid usage, by 88%; while scenario 2 can eliminate grid consumption and thus not contribute to carbon emissions. For 3000 m^3/ha, scenario 1 reduced CO_2 emissions by 45%, while scenario 2 reduced by 80%, equivalent to 4.4 10^6 kg of carbon dioxide. Regarding Scenario 3, since it replaces the electric grid with a BESS, it succeeds in completely reducing the carbon emissions associated with energy demand.

To further test and compare the developed HY4RES model, the methodology employs the HOMER commercial software as an optimization tool developed to study hybrid energy solutions. Both models show their flexibility in optimizing hybrid renewable solutions, presenting similar pattern results and enhancing the advantages and limitations of each model. The selected application's intrinsic nature as a water-energy nexus makes it an ideal subject for comparison between models. The comparison with the model developed in HOMER underlines the advantages and success of the HY4RES for applications within the water-energy nexus. HOMER is less restrictive concerning water needs, which results in a lower energy consumption by the system than that presented by the HY4RES. Therefore, in instances where there is a high demand for water and energy, and the HY4RES requires substantial grid support due to the limited availability of renewable resources, the HOMER model requires significantly less power from the grid. This phenomenon is also evident in the economic assessment, where the lower grid consumption by HOMER, results in superior net present values with significantly lower costs. While there is not a precise alignment between the values in the two models, the system behavior and results under various water-energy allocations demonstrate a similar pattern. The results discrepancies can be attributed to the inability of the HOMER model to guarantee 100% satisfaction of the irrigation water requirements, which produces a more straightforward and adaptable system, without the ability to rigorously assess water needs.

With the small-scale energy community case study, it was possible to assess the model's performance and versatility. In this case, the pumped hydro storage unit only serves the energy demand. The load consumption profile is less consistent than in the previous study, enhancing the model's flexibility to different consumption patterns and setups. Since the small energy community is located in a remote continental region, it is possible to evaluate both a stand-alone scenario and a grid-connected scenario. The designed PHS is capable of 2.2 MWh of potential energy storage and has autonomy for two days under a constant peak load of 44 kW.

The stand-alone scenarios, SA1 (PV+Wind+PHS) and SA2 (PV+Wind+PHS+BESS) succeeded in achieving grid independence, avoiding approximately 32 tons of CO_2 emissions. Nevertheless, they require a power installation of 220 and 270 kW, respectively. The integration of a battery storage system in GC2 made no significant advantages in comparison to GC1. Both scenarios require the over-dimension of the primary renewable power installation, i.e. solar and wind, to ensure that the system is capable of satisfying the energy needs during winter months, wherein the load profile is substantially higher. Therefore, the grid-connected scenarios, GC1 (PV+PHS+Grid) and GC2 (Wind+PHS+Grid) stand as suitable alternatives. With the optimization model, requiring minimum grid independence of 80% and positive grid balance, it is possible to maximize the advantages of a remote small energy community, while maintaining the synchronization with the nearby electric grid. This approach enables a more compact overall power installment. The solar configuration, GC1, yielded a total power installation of 200 kW with an 80.1% grid independence. However, the wind configuration, GC2, yielded 125 kW of power installment with 91.7% of grid independence. The superiority of the wind configuration can be attributed to the selected location, which exhibits optimal wind speeds, whereas solar irradiance is suboptimal. Furthermore, the peak load months occur during the winter, when solar energy is minimal, thereby enhancing the superiority of wind over solar energy. Ultimately, the grid-connected configuration with wind energy, GC2, presents the best NPV, -179,287 €, with the lowest initial investment and power installation required.

7.2 Recommendations for future work

Further generalization of the model could be undertaken to integrate hydropneumatic systems and simulate compressed-air energy storage systems. The models´ generalization and simplicity approach presents a limitation regarding the optimization of control systems. Further work could be conducted with regard to power systems control and grid stability analysis, utilizing toolboxes such as Simscape and PSAT on Simulink. Moreover, the HY4RES model could be enhanced with forecasting tools, to predict input data, such as renewable energy generation or consumption profiles, instead of using historical data. Machine learning could be adopted to enhance and train the model, to maximize the precision of the forecasts.

Bibliography

[1] E. Hallgrimsdottir, S. Pinnington, and K. Rai, "Hydropower : Unveiling the socioeconomic benefits," *Washington, D.C.: World Bank Group*, 2024.

[2] T. Keitel, "Powering the future: hydropower provides stable energy for fluctuating needs," *Waterpower Magazine*, 2024. [Online]. Available: https://www.waterpowermagazine.com/analysis/powering-the-future-hydropower-provides-stable-energy-for-fluctuating-needs/?cf-view

[3] IHA, "2024 world hydropower outlook: Opportunities to advance net zero," 2024, consulted in August 2024. [Online]. Available: https://www.hydropower.org/publications/2024-world-hydropower-outlook

[4] I. Muhammad and T. Baladraf, "Potential Design of Photovoltaics-Pumped Hydro Storage System at Ex-Paser Mine Holes in East Kalimantan," in *Proceedings of the 1st International Seminar on Teacher Training and Education, ISTED 2021, 17-18 July 2021, Purwokerto, Indonesia*. Purwokerto, Indonesia: EAI, 2021. [Online]. Available: http://eudl.eu/doi/10.4108/eai.17-7-2021.2312026

[5] B. Hammad, S. Al-Dahidi, Y. Aldahouk, D. Majrouh, and S. Al-Remawi, "Technical, Economic, and Environmental Investigation of Pumped Hydroelectric Energy Storage Integrated with Photovoltaic Systems in Jordan," *Sustainability*, vol. 16, no. 4, p. 1357, Feb. 2024. [Online]. Available: https://www.mdpi.com/2071-1050/16/4/1357

[6] IHA, "Pump it up with pumped storage hydropower," consulted in September 2024. [Online]. Available: https://www.hydropower.org/iha/pump-it-up

[7] L. Malka, A. Daci, A. Kuriqi, P. Bartocci, and E. Rrapaj, "Energy storage benefits assessment using multiple-choice criteria: The case of drini river cascade, albania," *Energies*, vol. 15, no. 11, 2022. [Online]. Available: https://www.mdpi.com/1996-1073/15/11/4032

[8] M. S. Javed, T. Ma, J. Jurasz, and M. Y. Amin, "Solar and wind power generation systems with pumped hydro storage: Review and future perspectives," *Renewable Energy*, vol. 148, pp. 176–192, 2020. [Online]. Available: https://www.sciencedirect.com/science/article/pii/S0960148119318592

[9] J. Fan, H. Xie, J. Chen, D. Jiang, C. Li, W. Ngaha Tiedeu, and J. Ambre, “Preliminary feasibility analysis of a hybrid pumped-hydro energy storage system using abandoned coal mine goafs,” *Applied Energy*, vol. 258, p. 114007, Jan. 2020. [Online]. Available: https://linkinghub.elsevier.com/retrieve/pii/S0306261919316940

[10] I. Amoussou, E. Tanyi, A. Ali, T. F. Agajie, B. Khan, J. B. Ballester, and W. B. Nsanyuy, “Optimal modeling and feasibility analysis of grid-interfaced solar pv/wind/pumped hydro energy storage based hybrid system,” *Sustainability*, vol. 15, no. 2, 2023. [Online]. Available: https://www.mdpi.com/2071-1050/15/2/1222

[11] D. Manolakos, G. Papadakis, D. Papantonis, and S. Kyritsis, “A stand-alone photovoltaic power system for remote villages using pumped water energy storage,” *Energy*, vol. 29, no. 1, pp. 57–69, 2004. [Online]. Available: https://www.sciencedirect.com/science/article/pii/S0360544203002196

[12] X. Zhang, G. Ma, W. Huang, S. Chen, and S. Zhang, “Short-term optimal operation of a wind-pv-hydro complementary installation: Yalong river, sichuan province, china,” *Energies*, vol. 11, no. 4, 2018. [Online]. Available: https://www.mdpi.com/1996-1073/11/4/868

[13] Y. He, S. Guo, J. Zhou, J. Ye, J. Huang, K. Zheng, and X. Du, “Multi-objective planning-operation co-optimization of renewable energy system with hybrid energy storages,” *Renewable Energy*, vol. 184, pp. 776–790, 2022. [Online]. Available: https://www.sciencedirect.com/science/article/pii/S0960148121017079

[14] T. Luz and P. Moura, “100% renewable energy planning with complementarity and flexibility based on a multi-objective assessment,” *Applied Energy*, vol. 255, p. 113819, 2019. [Online]. Available: https://www.sciencedirect.com/science/article/pii/S0306261919315065

[15] T. Ma, H. Yang, L. Lu, and J. Peng, “Optimal design of an autonomous solar–wind-pumped storage power supply system,” *Applied Energy*, vol. 160, pp. 728–736, 2015. [Online]. Available: https://www.sciencedirect.com/science/article/pii/S0306261914011751

[16] A. Panda, U. Mishra, M.-L. Tseng, and M. H. Ali, “Hybrid power systems with emission minimization: Multi-objective optimal operation,” *Journal of Cleaner Production*, vol. 268, p. 121418, 2020. [Online]. Available: https://www.sciencedirect.com/science/article/pii/S0959652620314657

[17] J. Jurasz, J. Mikulik, M. Krzywda, B. Ciapała, and M. Janowski, “Integrating a wind- and solar-powered hybrid to the power system by coupling it with a hydroelectric power station with pumping installation,” *Energy*, vol. 144, pp. 549–563, 2018. [Online]. Available: https://www.sciencedirect.com/science/article/pii/S0360544217320303

[18] M. Simão and H. M. Ramos, “Hybrid pumped hydro storage energy solutions towards wind and pv integration: Improvement on flexibility, reliability and energy costs,” *Water*, vol. 12, no. 9, 2020. [Online]. Available: https://www.mdpi.com/2073-4441/12/9/2457

[19] L. Stoyanov, I. Bachev, Z. Zarkov, V. Lazarov, and G. Notton, “Multivariate analysis of a wind–pv-based water pumping hybrid system for irrigation purposes,” *Energies*, vol. 14, no. 11, 2021. [Online]. Available: https://www.mdpi.com/1996-1073/14/11/3231

[20] D. Mazzeo, N. Matera, P. Luca, C. Baglivo, P. Congedo, and G. Oliveti, “A literature review and statistical analysis of photovoltaic-wind hybrid renewable system research by considering the most relevant 550 articles: An upgradable matrix literature database,” *Journal of Cleaner Production*, vol. 295, 05 2021.

[21] A. Mahesh and K. S. Sandhu, “Hybrid wind/photovoltaic energy system developments: Critical review and findings,” *Renewable and Sustainable Energy Reviews*, vol. 52, no. C, pp. 1135–1147, 2015. [Online]. Available: https://ideas.repec.org/a/eee/rensus/v52y2015icp1135-1147.html

[22] J. Margeta and Z. Glasnovic, “Theoretical settings of photovoltaic-hydro energy system for sustainable energy production,” *Solar Energy*, vol. 86, p. 972–982, 03 2012.

[23] Z. G. Jure Margeta, “Role of water-energy storage in pv-psh power plant development,” *Journal of Energy Engineering*, vol. 137, pp. 187–197, 12 2011.

[24] T. Ma, H. Yang, and L. Lu, “Technical feasibility study on a standalone hybrid solar-wind system with pumped hydro storage for a remote island in hong kong,” *Renewable Energy*, vol. 69, p. 7–15, 09 2014.

[25] J. Zhao, K. Graves, C. Wang, Y. G. Liao, and C.-P. Yeh, “A hybrid electric/hydro storage solution for standalone photovoltaic applications in remote areas,” 07 2012, pp. 1–6.

[26] J. Margeta and Z. Glasnovic, “Feasibility of the green energy production by hybrid solarÂ +Â hydro power system in europe and similar climate areas,” *Renewable and Sustainable Energy Reviews*, vol. 14, pp. 1580–1590, 08 2010.

[27] R. Li, B. Wu, X. Li, F. Zhou, and Y. Li, “Design of wind-solar and pumped-storage hybrid power supply system,” vol. 5, 07 2010, pp. 402–405.

[28] D. Manolakos, G. Papadakis, D. Papantonis, and S. Kyritsis, “A simulation-optimisation programme for designing hybrid energy systems for supplying electricity and fresh water through desalination to remote areas: Case study: the merssini village, donoussa island, aegean sea, greece,” *Energy*, vol. 26, no. 7, pp. 679–704, 2001. [Online]. Available: https://www.sciencedirect.com/science/article/pii/S0360544201000263

[29] T. Ma, H. Yang, L. Lu, and J. Peng, "Technical feasibility study on a standalone hybrid solar-wind system with pumped hydro storage for a remote island in hong kong," *Renewable Energy*, vol. 69, pp. 7–15, 2014. [Online]. Available: https://www.sciencedirect.com/science/article/pii/S0960148114001736

[30] Y. Ren, Y. Zheng, Y. P. Li, J. J. Huang, and D. Zhang, "Modeling and optimization of hybrid wind/pv pumped-storage power system," in *Measuring Technology and Mechatronics Automation*, ser. Applied Mechanics and Materials, vol. 48. Trans Tech Publications Ltd, 3 2011, pp. 693–696.

[31] R. J. Mahfoud, N. F. Alkayem, Y. Zhang, Y. Zheng, Y. Sun, and H. H. Alhelou, "Optimal operation of pumped hydro storage-based energy systems: A compendium of current challenges and future perspectives," *Renewable and Sustainable Energy Reviews*, vol. 178, p. 113267, 2023. [Online]. Available: https://www.sciencedirect.com/science/article/pii/S1364032123001235

[32] Q. Chen, M. Lv, Y. Gu, X. Yang, Z. Tang, Y. Sun, and M. Jiang, "Hybrid energy system for a coal-based chemical industry," *Joule*, vol. 2, no. 4, p. 607–620, Apr. 2018. [Online]. Available: https://doi.org/10.1016/j.joule.2018.02.015

[33] H. M. Ramos, M. Amaral, and D. Covas, "Pumped-storage solution towards energy efficiency and sustainability: Portugal contribution and real case studies," *Journal of Water Resource and Protection*, vol. 6, no. 12, 2014. [Online]. Available: https://www.scirp.org/journal/PaperInformation?PaperID=49847&#abstract

[34] EDP, "Inauguration of the floating solar power plant in alqueva," consulted in August 2024. [Online]. Available: https://www.edp.com/en/floating-solar-panels

[35] M. Bertsiou and E. Baltas, "Energy, economic and environmental analysis of a hybrid power plant for electrification, and drinking and irrigation water supply," *Environmental Processes*, vol. 9, 06 2022.

[36] M. Jiménez-Bello, A. Royuela, J. Manzano, A. G. Prats, and F. Martínez-Alzamora, "Methodology to improve water and energy use by proper irrigation scheduling in pressurised networks," *Agricultural Water Management*, vol. 149, no. C, pp. 91–101, 2015. [Online]. Available: https://ideas.repec.org/a/eee/agiwat/v149y2015icp91-101.html

[37] Y. Zhang, J. Lian, C. Ma, Y. Yang, X. Pang, and L. Wang, "Optimal sizing of the grid-connected hybrid system integrating hydropower, photovoltaic, and wind considering cascade reservoir connection and photovoltaic-wind complementarity," *Journal of Cleaner Production*, vol. 274, p. 123100, 07 2020.

[38] M. Abdelgaied, A. E. Kabeel, M. Zeleňáková, and H. F. Abd-Elhamid, "Floating photovoltaic plants as an effective option to reduce water evaporation in water-stressed regions and produce

electricity: A case study of lake nasser, egypt," *Water*, vol. 15, no. 4, 2023. [Online]. Available: https://www.mdpi.com/2073-4441/15/4/635

[39] J. Velasco Muñoz, J. A. Aznar-Sánchez, L. Belmonte, and I. Román-Sánchez, "Sustainable water use in agriculture: A review of worldwide research," *Sustainability*, vol. 10, 04 2018.

[40] M. Santafé, J. B. Soler, F.-J. Sanchez-Romero, P. Ferrer-Gisbert, J. Gozálvez, and F. Gisbert, "Theoretical and experimental analysis of a floating photovoltaic cover for water irrigation reservoirs," *Energy*, vol. 67, 04 2014.

[41] J. Haas, J. Khalighi, A. de la Fuente, S. Gerbersdorf, W. Nowak, and P.-J. Chen, "Floating photovoltaic plants: Ecological impacts versus hydropower operation flexibility," *Energy Conversion and Management*, vol. 206, p. 112414, 2020. [Online]. Available: https://www.sciencedirect.com/science/article/pii/S0196890419314219

[42] J. Monís, R. López-Luque, J. Reca, and J. Martinez, "Multistage bounded evolutionary algorithm to optimize the design of sustainable photovoltaic (pv) pumping irrigation systems with storage," *Sustainability*, vol. 12, p. 1026, 01 2020.

[43] E. Nyeche and E. Diemuodeke, "Modelling and optimisation of a hybrid pv-wind turbine-pumped hydro storage energy system for mini-grid application in coastline communities," *Journal of Cleaner Production*, vol. 250, p. 119578, 2020. [Online]. Available: https://www.sciencedirect.com/science/article/pii/S0959652619344488

[44] Y. Li, Z. Tong, J. Zhang, D. Liu, X. Yue, and M. A. Mahmud, "Operational characteristics assessment of a wind–solar–hydro hybrid power system with regulating hydropower," *Water*, vol. 15, no. 23, 2023. [Online]. Available: https://www.mdpi.com/2073-4441/15/23/4051

[45] J. M. García-Ruiz, J. I. López-Moreno, S. M. Vicente-Serrano, T. Lasanta–Martínez, and S. Beguería, "Mediterranean water resources in a global change scenario," *Earth-Science Reviews*, vol. 105, no. 3, pp. 121–139, 2011. [Online]. Available: https://www.sciencedirect.com/science/article/pii/S0012825211000134

[46] T. Falope, L. Lao, D. Hanak, and D. Huo, "Hybrid energy system integration and management for solar energy: A review," *Energy Conversion and Management: X*, vol. 21, p. 100527, 2024. [Online]. Available: https://www.sciencedirect.com/science/article/pii/S2590174524000059

[47] J. Li, L. Shi, and H. Fu, "Multi-objective short-term optimal dispatching of cascade hydro–wind–solar–thermal hybrid generation system with pumped storage hydropower," *Energies*, vol. 17, no. 1, 2024. [Online]. Available: https://www.mdpi.com/1996-1073/17/1/98

[48] N. Vakilifard, M. Anda, P. A. Bahri, and G. Ho, "The role of water-energy nexus in optimising water supply systems – review of techniques and approaches," *Renewable and Sustainable Energy Reviews*, vol. 82, pp. 1424–1432, 2018. [Online]. Available: https://www.sciencedirect.com/science/article/pii/S1364032117307621

[49] S. Padrón, J. Medina, and A. Rodríguez, "Analysis of a pumped storage system to increase the penetration level of renewable energy in isolated power systems. gran canaria: A case study," *Energy*, vol. 36, no. 12, pp. 6753–6762, 2011. [Online]. Available: https://www.sciencedirect.com/science/article/pii/S0360544211006888

[50] M. Moran, H. Shapiro, D. Boettner, and M. Bailey, *Fundamentals of Engineering Thermodynamics*. Wiley, 8th edition, 2014.

[51] T. Ma, H. Yang, and L. Lu, "Pumped storage-based standalone photovoltaic power generation system: Modeling and techno-economic optimization," *Applied Energy*, vol. 137, pp. 649–659, 01 2015.

[52] I. D. Spyrou and J. S. Anagnostopoulos, "Design study of a stand-alone desalination system powered by renewable energy sources and a pumped storage unit," *Desalination*, vol. 257, no. 1, pp. 137–149, 2010. [Online]. Available: https://www.sciencedirect.com/science/article/pii/S0011916410001104

[53] H. M. Ramos, J. Sintong, and A. Kuriqi, "Optimal integration of hybrid pumped storage hydropower toward energy transition," *Renewable Energy*, vol. 221, p. 119732, 12 2023.

[54] A. Garcia, F.-J. Sanchez-Romero, P. López-Jiménez, and M. Pérez-Sánchez, "A new optimization approach for the use of hybrid renewable systems in the search of the zero net energy consumption in water irrigation systems," *Renewable Energy*, vol. 195, pp. 853–871, 08 2022.

[55] H. Rauf, M. Gull, and N. Arshad, "Complementing hydroelectric power with floating solar pv for daytime peak electricity demand," *Renewable Energy*, vol. 162, 08 2020.

[56] IREA, "Battery storage and renewables: costs and markets to 2030," *Abu Dhabi*, 2017. [Online]. Available: https://www.irena.org/publications/2017/Oct/Electricity-storage-and-renewables-costs-and-markets

[57] PVGIS, consulted in March 2024. [Online]. Available: https://re.jrc.ec.europa.eu/pvg_tools/en/

[58] Renewables.ninja, consulted in June 2024. [Online]. Available: https://www.renewables.ninja/

[59] H. Ramos, *Guidelines for design of small hydropower plants*. Western Reg. Energy Agency & Network, 1999.

[60] J. Coelho, A. Alves, J. Morillo, O. Coronado-Hernández, M. Perez-Sanchez, and H. M. Ramos, "Hybrid energy solution to improve irrigation systems: Hy4res vs. homer optimization models," *Energies*, vol. 17, no. 16, 2024. [Online]. Available: https://www.mdpi.com/1996-1073/17/16/4037

[61] X. Yin, L. Cheng, X. Wang, J. Lu, and H. Qin, "Optimization for hydro-photovoltaic-wind power generation system based on modified version of multi-objective whale optimization algorithm," *Energy Procedia*, vol. 158, pp. 6208–6216, 2019, innovative Solutions for Energy Transitions. [Online]. Available: https://www.sciencedirect.com/science/article/pii/S187661021930503X

Appendix A. Extended Results and Algorithms

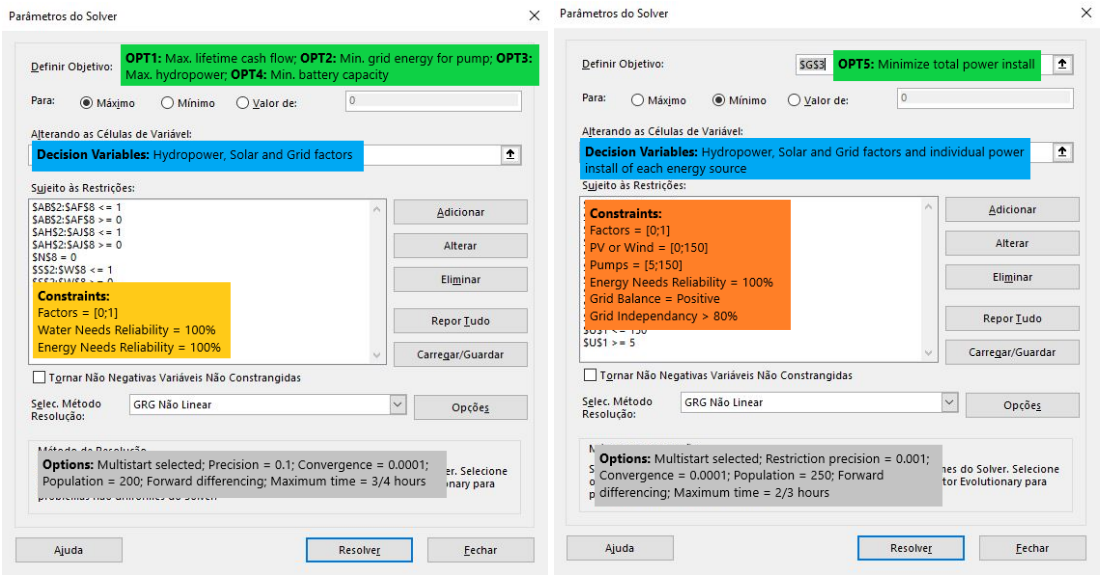

A.1(a) Irrigation System - large-scale case study

A.1(b) Energy Community - small-scale case study

Figure A.1: Excel-Solver optimization setup

Developed Excel-Solver GRG NonLinear Model - HY4RES-1

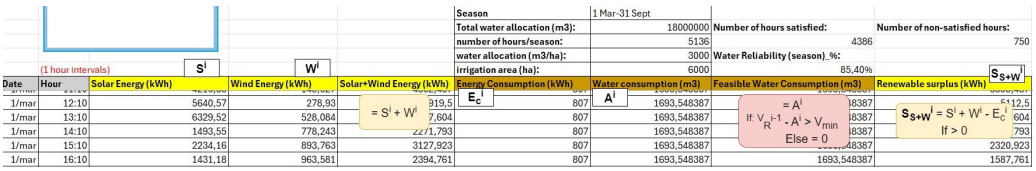

Figure A.2: Primary energy sources and Needs - Excel-Solver model

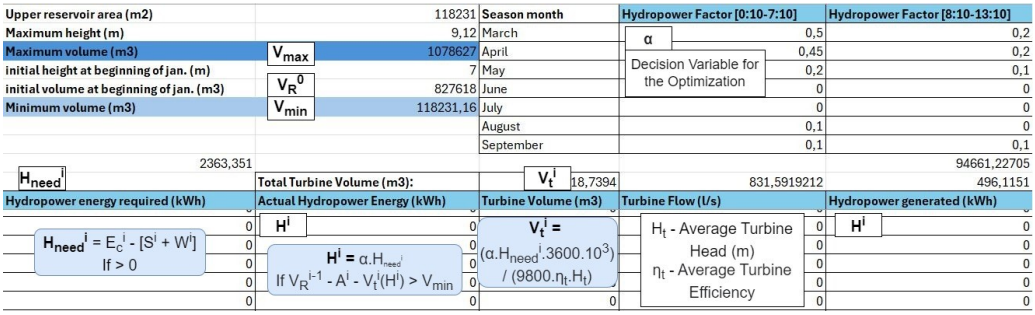

A.3(a) Hydropower

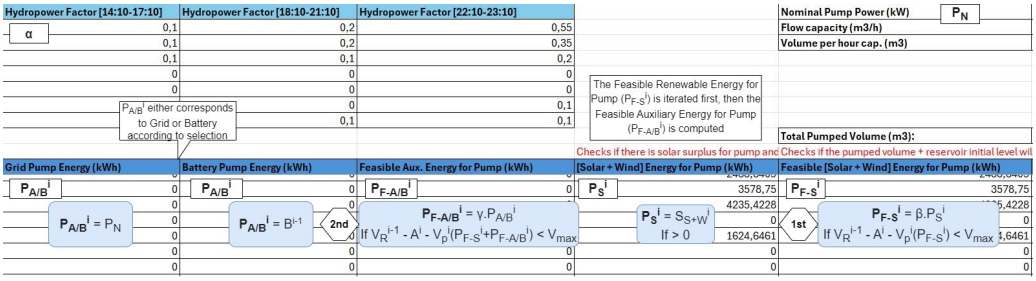

A.3(b) Pumped-storage

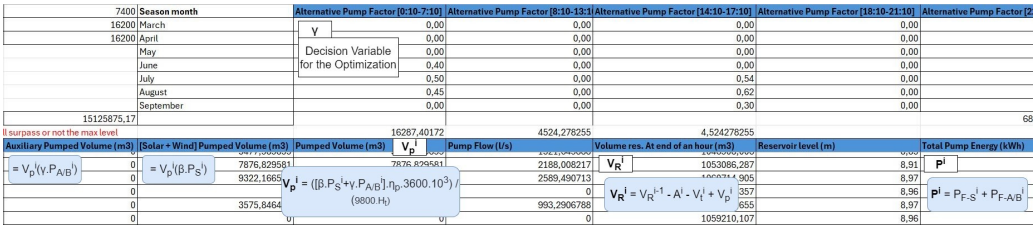

A.3(c) Pumped-storage cont.

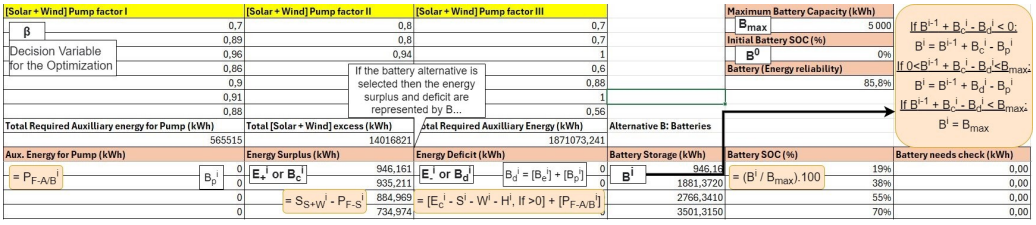

A.3(d) Solar factor + Excess/Deficit energy + Battery alternative

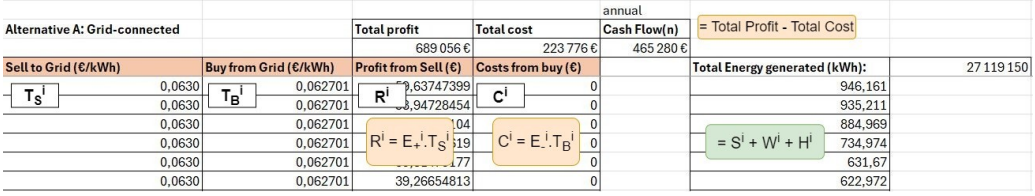

A.3(e) Grid alternative

Figure A.3: Excel-Solver model continuation

Listing 1: Python Model (Simulation) - HY4RES-2

```python
#Import libraries, packages, modules...
import pandas as pd
import numpy as np
import matplotlib.pyplot as plt
import seaborn as sb
import matplotlib.dates as mdates
from pymoo.core.problem import Problem
from pymoo.algorithms.moo.nsga2 import NSGA2
from pymoo.operators.sampling.rnd import FloatRandomSampling
from pymoo.operators.crossover.sbx import SBX
from pymoo.operators.mutation.pm import PM
from pymoo.optimize import minimize

decimal_places = 0 #to round desired values

### Solar,Wind and Consumption computation ###

# Load the predefined input data file: Energy generation sources, consumption, tariffs -(Please check columns name references in line 35)
print("Paste the input file directory (fully if not in the same origin) below.")
df_input_raw = pd.read_csv(input("Input File directory:"))
df_input_raw['time'] = pd.to_datetime(df_input_raw['time'], format='%Y%m%d:%H%M') #enter/update with the used date format
df_input_raw = df_input_raw.set_index(['time'], drop=True)
df_input_raw.rename(columns = {'solar_energy_kwh':'Solar Energy (kWh)', 'wind_energy_kwh':'Wind Energy (kWh)', 'sell_grid_eur/kwh':'Sell to Grid (Eur/kWh)', 'buy_grid_eur/kwh':'Buy from Grid (Eur/kWh)', 'energy_needs_kwh': 'Energy consumption (kWh)', 'water_needs_m3': 'Water consumption (m3)'}, inplace = True) # enter the used energy reference
df_input_raw = df_input_raw.rename_axis('Date')
df_renew_raw = df_input_raw.copy()

# Add Month, Day, and Hour columns
df_renew_raw['Month'] = pd.to_datetime(df_renew_raw.index, format='%Y-%m-%d %H:%M').month
df_renew_raw['Day'] = pd.to_datetime(df_renew_raw.index, format='%Y-%m-%d %H:%M').day
df_renew_raw['Hour'] = pd.to_datetime(df_renew_raw.index, format='%Y-%m-%d %H:%M').hour

# Add total solar+wind energy and ensure columns are in the correct order
#If the input wind data is the total energy generation of all the turbines then set the 'number_turbines' variable to 1
number_turbines = float(input("Number of Wind turbines (multiplicator):"))
df_renew_raw['Wind Energy (kWh)'] = df_renew_raw['Wind Energy (kWh)'] * number_turbines
df_renew_raw['Solar+Wind Energy (kWh)'] = df_renew_raw['Solar Energy (kWh)'] + df_renew_raw['Wind Energy (kWh)']
df_renew_raw = df_renew_raw[['Month', 'Day', 'Hour', 'Solar Energy (kWh)', 'Wind Energy (kWh)', 'Solar+Wind Energy (kWh)', 'Energy consumption (kWh)', 'Water consumption (m3)', 'Sell to Grid (Eur/kWh)', 'Buy from Grid (Eur/kWh)']]

#selection of period to simulate
start_date = '2020-01-01 00:10'
end_date = '2020-12-31 23:10'
df_renew_raw = df_renew_raw.loc[start_date:end_date]

#Solar+Wind Surplus and used for energy consumption#

df_renew_raw['Solar+Wind Surplus (kWh)'] = df_renew_raw['Solar+Wind Energy (kWh)'] - df_renew_raw['Energy consumption (kWh)']
df_renew_raw['Solar+Wind Surplus (kWh)'] = df_renew_raw['Solar+Wind Surplus (kWh)'].clip(lower=0)  # Ensure surplus is non-negative
df_renew_raw['Solar+Wind used for Consumption (kWh)'] = df_renew_raw['Solar+Wind Energy (kWh)'] - df_renew_raw['Solar+Wind Surplus (kWh)']

### PHS computation ###

##PHS parameters## Update with desired parameters
print("Enter the following parameters for PHS system.")
res_area = float(input("Reservoir Area (m2):")) #m2
max_height = float(input("Maximum Height (m):")) #m
max_volume = float(input("Maximum Volume (m3):")) #m3
min_height = float(input("Minimum Height (m):")) #m
min_volume = float(input("Minimum Volume (m3):")) #m3
initial_volume_jan = float(input("Initial Volume in 1st of January (m3):")) #m3
pump_head = float(input("General Pump Head (m):")) #m
pump_eff = float(input("General Pump Efficiency:"))
turb_head = float(input("General Turbine Head (m):")) #m
turb_eff = float(input("General Turbine Efficiency:"))
pump_power = float(input("Pump Nominal Power:")) #kW

#Hydropower energy required#

df_renewables = df_renew_raw.copy()
df_renewables['Hydropower energy required (kWh)'] = df_renewables['Energy consumption (kWh)'] - df_renewables['Solar+Wind Energy (kWh)'] #hydropower energy required to satisfy demand
df_renewables['Hydropower energy required (kWh)'] = df_renewables['Hydropower energy required (kWh)'].clip(lower=0)  # Ensure non-negative values

#Actual Hydropower Energy, Feasible Energy for Pump and Reservoir Volume variation Sim#

#Define Hydropower factor variables for Simulation
predefined_hydropower_factor_matrix = [
    [1, 1, 1, 1, 1],  # January
    [1, 1, 1, 1, 1],  # February
    [1, 1, 1, 1, 1],  # March
    [1, 1, 1, 1, 1],  # April
    [1, 1, 1, 1, 1],  # May
    [0.1, 0.1, 0.1, 0.1, 0.1],  # June
    [0.1, 0.1, 0.1, 0.1, 0.1],  # July
    [0.2, 0.2, 0.2, 0.2, 0.2],  # August
    [1, 1, 1, 1, 1],  # September
    [1, 1, 1, 1, 1],  # October
    [1, 1, 1, 1, 1],  # November
    [1, 1, 1, 1, 1],  # December
]

for idx, row in df_renewables.iterrows():
    month = int(row['Month'])
    hour = int(row['Hour'])

    if not (1 <= month <= 12) or not (0 <= hour < 24):
        df_renewables.at[idx, 'Hydropower factor'] = None  # Or any other default value
    else:
        if hour < 8:
            period = 0
        elif hour < 14:
            period = 1
        elif hour < 18:
            period = 2
        elif hour < 22:
            period = 3
        else:
            period = 4
```

```

        df_renewables.at[idx, 'Hydropower factor'] =
              predefined_hydropower_factor_matrix[month - 1][period]

#Define Grid factor variables for Simulation
predefined_alternative_factor_matrix = [
    [0, 0, 0, 0, 0],  # January
    [0, 0, 0, 0, 0],  # February
    [0, 0, 0, 0, 0],  # March
    [0, 0, 0, 0, 0],  # April
    [0, 0, 0, 0, 0],  # May
    [0, 0, 0, 0, 0],  # June
    [0, 0, 0, 0, 0],  # July
    [0, 0, 0, 0, 0],  # August
    [0, 0, 0, 0, 0],  # September
    [0, 0, 0, 0, 0],  # October
    [0, 0, 0, 0, 0],  # November
    [0, 0, 0, 0, 0],  # December
]

for idx, row in df_renewables.iterrows():
    month = int(row['Month'])
    hour = int(row['Hour'])

    if not (1 <= month <= 12) or not (0 <= hour < 24):
        df_renewables.at[idx, 'Alternative factor'] = None  # Or any
              other default value
    else:
        if hour < 8:
            period = 0
        elif hour < 14:
            period = 1
        elif hour < 18:
            period = 2
        elif hour < 22:
            period = 3
        else:
            period = 4

        df_renewables.at[idx, 'Alternative factor'] =
              predefined_alternative_factor_matrix[month - 1][period]

#Define Renewable factor for Simulation
predefined_renewable_factor_matrix = [
    [1, 1, 1],  # January
    [1, 1, 1],  # February
    [0.6, 0.6, 0.6],  # March
    [0.6, 0.6, 0.6],  # April
    [0.6, 0.6, 0.6],  # May
    [0.9, 0.95, 0.96],  # June
    [1, 1, 1],  # July
    [0.97, 0.95, 0.97],  # August
    [0.9, 0.8, 0.6],  # September
    [1, 1, 1],  # October
    [1, 1, 1],  # November
    [1, 1, 1],  # December
]

for idx, row in df_renewables.iterrows():
    month = int(row['Month'])
    day = int(row['Day'])

    if month == 2:
        max_days_in_month = 29
    elif month in [4, 6, 9, 11]:
        max_days_in_month = 30
    else:
        max_days_in_month = 31

    day = min(day, max_days_in_month)

    if day < 1 or day > max_days_in_month:
        df_renewables.at[idx, 'Renewable factor'] = None
    else:
        if day >= 21:
            period = 2
        elif day >= 11:
            period = 1
        else:
            period = 0

        df_renewables.at[idx, 'Renewable factor'] =
              predefined_renewable_factor_matrix[month - 1][period]

#repeat the minimum pump power restraint (0.2*nominal power)
#apply solar factors
df_renewables['Solar+Wind Energy for Pump (kWh)'] = df_renewables['
      Solar+Wind Surplus (kWh)'] * df_renewables['Renewable factor']
for i in range(len(df_renewables)):
    if df_renewables.iloc[i]['Solar+Wind Energy for Pump (kWh)'] >= 0.
          2*pump_power:
        if df_renewables.iloc[i]['Solar+Wind Energy for Pump (kWh)']
              <= pump_power:
            df_renewables.at[df_renewables.index[i], 'Solar+Wind
                  Energy for Pump (kWh)'] = df_renewables.iloc[i]['
                  Solar+Wind Energy for Pump (kWh)']
        else:
           df_renewables.at[df_renewables.index[i], 'Solar+Wind Energy
                  for Pump (kWh)'] = pump_power
    else:
        df_renewables.at[df_renewables.index[i], 'Solar+Wind Energy
              for Pump (kWh)'] = 0

# Initialize columns to be filled iteratively
df_renewables['Alternative Energy for Pump (kWh)'] = 0
df_renewables['Feasible Water Consumption (m3)'] = 0
df_renewables['Actual Hydropower Energy (kWh)'] = 0
df_renewables['Feasible Solar+Wind Energy for Pump (kWh)'] = 0
df_renewables['Feasible Alternative Energy for Pump (kWh)'] = 0
df_renewables['Reservoir Volume (end) (m3)'] = 0
df_renewables['Turbine Volume (m3)'] = 0
df_renewables['Pumped Volume (m3)'] = 0

#selection of alternative: A-Grid or B-Batteries (1 ON, 0 OFF)
def get_user_choice():
    while True:
        try:
            choice = int(input("Enter 1 for Grid (alt_A) or 0 for
                  Batteries (alt_B): "))
            if choice not in [0, 1]:
                raise ValueError
            return choice
        except ValueError:
            print("Invalid input. Please enter 1 or 0.")

#user input for alt_A
alt_A = get_user_choice()
#alt_B based on alt_A
alt_B = 1 - alt_A

print(f"alt_A: {alt_A}, alt_B: {alt_B}")

# Iteratively compute PHS and Alternatives

if alt_A == 1:
    for i in range(len(df_renewables)):
        if i == 0:
            prev_volume = initial_volume_jan
        else:
```

```
            prev_volume = df_renewables.iloc[i - 1]['Reservoir Volume (end) (m3)']

        # Compute feasible water consumption
        if prev_volume - df_renewables.iloc[i]['Water consumption (m3)'] >= min_volume:
            df_renewables.at[df_renewables.index[i], 'Feasible Water Consumption (m3)'] = df_renewables.iloc[i]['Water consumption (m3)']

        # Compute actual hydropower energy
        if prev_volume - df_renewables.iloc[i]['Feasible Water Consumption (m3)'] - (df_renewables.iloc[i]['Hydropower energy required (kWh)'] * df_renewables.iloc[i]['Hydropower factor'] * 1000 * 3600) / (9800 * turb_head * turb_eff) >= min_volume:
            df_renewables.at[df_renewables.index[i], 'Actual Hydropower Energy (kWh)'] = df_renewables.iloc[i]['Hydropower energy required (kWh)'] * df_renewables.iloc[i]['Hydropower factor']

        # Compute feasible solar energy for pump
        if prev_volume - df_renewables.iloc[i]['Feasible Water Consumption (m3)'] + (df_renewables.iloc[i]['Solar+Wind Energy for Pump (kWh)'] *pump_eff*1000*3600) / (9800 * pump_head) <= max_volume:
            df_renewables.at[df_renewables.index[i], 'Feasible Solar+Wind Energy for Pump (kWh)'] = df_renewables.iloc[i]['Solar+Wind Energy for Pump (kWh)']

        # Compute grid energy for pump based on actual hydropower energy
        if df_renewables.iloc[i]['Actual Hydropower Energy (kWh)'] == 0:
            pump_power_times_grid_factor = pump_power * df_renewables.iloc[i]['Alternative factor']
            if pump_power_times_grid_factor + df_renewables.iloc[i]['Feasible Solar+Wind Energy for Pump (kWh)'] <= pump_power:
                df_renewables.at[df_renewables.index[i], 'Alternative Energy for Pump (kWh)'] = pump_power_times_grid_factor

        # Compute feasible grid energy for pump
        if prev_volume - df_renewables.iloc[i]['Feasible Water Consumption (m3)'] + (df_renewables.iloc[i]['Feasible Solar+Wind Energy for Pump (kWh)'] *pump_eff*1000*3600) / (9800 * pump_head) + (df_renewables.iloc[i]['Alternative Energy for Pump (kWh)'] *pump_eff*1000*3600) / (9800 * pump_head) <= max_volume:
            df_renewables.at[df_renewables.index[i], 'Feasible Alternative Energy for Pump (kWh)'] = df_renewables.iloc[i]['Alternative Energy for Pump (kWh)']

        # Compute turbine volume
        df_renewables.at[df_renewables.index[i], 'Turbine Volume (m3)'] = (df_renewables.iloc[i]['Actual Hydropower Energy (kWh)'] * 1000 * 3600) / (9800 * turb_head * turb_eff)

        # Compute pumped volume
        df_renewables.at[df_renewables.index[i], 'Pumped Volume (m3)'] = (df_renewables.iloc[i]['Feasible Solar+Wind Energy for Pump (kWh)'] * pump_eff * 1000 * 3600) / (9800 * pump_head) + (df_renewables.iloc[i]['Feasible Alternative Energy for Pump (kWh)'] * pump_eff * 1000 * 3600) / (9800 * pump_head)

        # Compute reservoir volume at end
        df_renewables.at[df_renewables.index[i], 'Reservoir Volume (end) (m3)'] = prev_volume - df_renewables.iloc[i]['Feasible Water Consumption (m3)'] - df_renewables.iloc[i]['Turbine Volume (m3)'] + df_renewables.iloc[i]['Pumped Volume (m3)']

df_renewables['Turbine Flow (l/s)'] = df_renewables['Turbine Volume (m3)'] * 1000 / 3600 #Turbine average flow (l/s)
df_renewables['Hydropower Generated (kWh)'] = (df_renewables['Turbine Volume (m3)'] * 9800 * turb_eff * turb_head)/(1000*3600) #Hydropower generated (kWh)
df_renewables['Hydropower Generated (kWh)'] = df_renewables['Hydropower Generated (kWh)'].round().astype(int) #to fix Energy Deficit not being zero when it should due to approx.
df_renewables['Pumped Flow (l/s)'] = df_renewables['Pumped Volume (m3)'] * 1000 / 3600 #Turbine average flow (l/s)
df_renewables['Reservoir level (m)'] = df_renewables['Reservoir Volume (end) (m3)']/res_area #computes reservoir height
df_renewables = df_renewables[['Month','Day', 'Hour', 'Solar Energy (kWh)', 'Wind Energy (kWh)', 'Solar+Wind Energy (kWh)',
                               'Energy consumption (kWh)', 'Water consumption (m3)', 'Solar+Wind used for Consumption (kWh)', 'Solar+Wind Surplus (kWh)', 'Feasible Water Consumption (m3)',
                               'Hydropower energy required (kWh)', 'Hydropower factor', 'Actual Hydropower Energy (kWh)', 'Turbine Volume (m3)', 'Turbine Flow (l/s)', 'Hydropower Generated (kWh)',
                               'Solar+Wind Energy for Pump (kWh)', 'Renewable factor', 'Feasible Solar+Wind Energy for Pump (kWh)',
                               'Alternative Energy for Pump (kWh)', 'Alternative factor', 'Feasible Alternative Energy for Pump (kWh)', 'Pumped Volume (m3)', 'Pumped Flow (l/s)',
                               'Reservoir Volume (end) (m3)', 'Reservoir level (m)',
                               'Sell to Grid (Eur/kWh)', 'Buy from Grid (Eur/kWh)']]

#Surplus and Deficit Energy, after solar+wind and PHS#
df_renewables['Energy Surplus (kWh)'] = df_renewables['Solar+Wind Surplus (kWh)'] - df_renewables['Feasible Solar+Wind Energy for Pump (kWh)']
df_renewables['Energy Deficit (kWh)'] = np.where(
    df_renewables['Energy consumption (kWh)'] - df_renewables['Solar+Wind Energy (kWh)'] - df_renewables['Hydropower Generated (kWh)'] > 0,
    df_renewables['Energy consumption (kWh)'] - df_renewables['Solar+Wind Energy (kWh)'] - df_renewables['Hydropower Generated (kWh)'] + df_renewables['Feasible Alternative Energy for Pump (kWh)'],
    df_renewables['Feasible Alternative Energy for Pump (kWh)']
)
df_renewables['Energy Deficit (kWh)'] = df_renewables['Energy Deficit (kWh)'].clip(lower=0)  # Ensure non-negative values
df_renewables['Energy Deficit (kWh)'] = df_renewables['Energy Deficit (kWh)'].round(decimal_places)
df_total = df_renewables.copy()
#Profit and Costs#
df_total['Profit from Sell (Eur)'] = df_total['Energy Surplus (kWh)'] * df_total['Sell to Grid (Eur/kWh)'] * alt_A
df_total['Profit from Sell (Eur)'] = df_total['Profit from Sell (Eur)'].round(decimal_places)
```

```
    df_total['Costs from buy (Eur)'] = df_total['Energy Deficit (kWh)'] * df_total['Buy from Grid (Eur/kWh)'] * alt_A
    df_total['Costs from buy (Eur)'] = df_total['Costs from buy (Eur)'].round(decimal_places)
    # Cash flow #
    profit_sum = df_total['Profit from Sell (Eur)'].sum()
    costs_sum = df_total['Costs from buy (Eur)'].sum()
    CF = profit_sum - costs_sum
    CF = CF.round(decimal_places)
    print("Total profits:", profit_sum,'Eur')
    print("Total Costs:", costs_sum,'Eur')
    print("Cash Flow (yearly):", CF,'Eur')

if alt_B == 1:
    print("Enter the parameters for the Battery plant")
    max_battery = int(input("Maximum Battery Capacity (kWh):")) # maximum battery capacity in kWh
    initial_battery = int(input("Initial Battery Capacity (kWh):")) # initial capacity in kWh

    df_renewables.drop(columns=['Sell to Grid (Eur/kWh)', 'Buy from Grid (Eur/kWh)'], inplace=True)
    df_renewables['Battery Storage (kWh)'] = 0
    df_renewables['Battery SOC (%)'] = 0
    df_renewables['Energy Needs check'] = 0

    for i in range(len(df_renewables)):
        if i == 0:
            prev_volume = initial_volume_jan
            prev_battery = initial_battery
        else:
            prev_volume = df_renewables.iloc[i - 1]['Reservoir Volume (end) (m3)']
            prev_battery = df_renewables.iloc[i - 1]['Battery Storage (kWh)']

        # Compute feasible water consumption
        if prev_volume - df_renewables.iloc[i]['Water consumption (m3)'] >= min_volume:
            df_renewables.at[df_renewables.index[i], 'Feasible Water Consumption (m3)'] = df_renewables.iloc[i]['Water consumption (m3)']

        # Compute actual hydropower energy
        if prev_volume - df_renewables.iloc[i]['Feasible Water Consumption (m3)'] - (df_renewables.iloc[i]['Hydropower energy required (kWh)'] * df_renewables.iloc[i]['Hydropower factor'] * 1000 * 3600) / (9800 * turb_head * turb_eff) >= min_volume:
            df_renewables.at[df_renewables.index[i], 'Actual Hydropower Energy (kWh)'] = df_renewables.iloc[i]['Hydropower energy required (kWh)'] * df_renewables.iloc[i]['Hydropower factor']

        # Compute feasible solar energy for pump
        if prev_volume - df_renewables.iloc[i]['Feasible Water Consumption (m3)'] + (df_renewables.iloc[i]['Solar+Wind Energy for Pump (kWh)'] *pump_eff*1000*3600) / (9800 * pump_head) <= max_volume:
            df_renewables.at[df_renewables.index[i], 'Feasible Solar+Wind Energy for Pump (kWh)'] = df_renewables.iloc[i]['Solar+Wind Energy for Pump (kWh)']

        # Compute battery energy for pump based on actual hydropower energy
        if df_renewables.iloc[i]['Actual Hydropower Energy (kWh)'] == 0:
            pump_power_times_bat_factor = prev_battery * df_renewables.iloc[i]['Alternative factor']
            if pump_power_times_bat_factor + df_renewables.iloc[i]['Feasible Solar+Wind Energy for Pump (kWh)'] <= pump_power:
                df_renewables.at[df_renewables.index[i], 'Alternative Energy for Pump (kWh)'] = pump_power_times_bat_factor

        # Compute feasible batteries energy for pump
        if prev_volume - df_renewables.iloc[i]['Feasible Water Consumption (m3)'] + (df_renewables.iloc[i]['Feasible Solar+Wind Energy for Pump (kWh)'] *pump_eff*1000*3600) / (9800 * pump_head) + (df_renewables.iloc[i]['Alternative Energy for Pump (kWh)'] *pump_eff*1000*3600) / (9800 * pump_head) <= max_volume:
            df_renewables.at[df_renewables.index[i], 'Feasible Alternative Energy for Pump (kWh)'] = df_renewables.iloc[i]['Alternative Energy for Pump (kWh)']

        # Compute turbine volume
        df_renewables.at[df_renewables.index[i], 'Turbine Volume (m3)'] = (df_renewables.iloc[i]['Actual Hydropower Energy (kWh)'] * 1000 * 3600) / (9800 * turb_head * turb_eff)

        # Compute pumped volume
        df_renewables.at[df_renewables.index[i], 'Pumped Volume (m3)'] = (df_renewables.iloc[i]['Feasible Solar+Wind Energy for Pump (kWh)'] * pump_eff * 1000 * 3600) / (9800 * pump_head) + (df_renewables.iloc[i]['Feasible Alternative Energy for Pump (kWh)'] * pump_eff * 1000 * 3600) / (9800 * pump_head)

        # Compute reservoir volume at end
        df_renewables.at[df_renewables.index[i], 'Reservoir Volume (end) (m3)'] = prev_volume - df_renewables.iloc[i]['Feasible Water Consumption (m3)'] - df_renewables.iloc[i]['Turbine Volume (m3)'] + df_renewables.iloc[i]['Pumped Volume (m3)']

        #Hydropower Generated
        df_renewables['Hydropower Generated (kWh)'] = (df_renewables['Turbine Volume (m3)'] * 9800 * turb_eff * turb_head)/(1000*3600) #Hydropower generated (kWh)
        df_renewables['Hydropower Generated (kWh)'] = df_renewables['Hydropower Generated (kWh)'].round().astype(int)

        #compute charge and discharge energy
        df_renewables.at[df_renewables.index[i], 'Energy Surplus (kWh)'] = df_renewables.iloc[i]['Solar+Wind Surplus (kWh)'] - df_renewables.iloc[i]['Feasible Solar+Wind Energy for Pump (kWh)']
        if df_renewables.iloc[i]['Energy consumption (kWh)'] - df_renewables.iloc[i]['Solar+Wind Energy (kWh)'] - df_renewables.iloc[i]['Hydropower Generated (kWh)'] > 0:
            df_renewables.at[df_renewables.index[i], 'Energy Deficit (kWh)'] = df_renewables.iloc[i]['Energy consumption (kWh)'] - df_renewables.iloc[i]['Solar+Wind Energy (kWh)'] - df_renewables.iloc[i]['Hydropower Generated (kWh)'] + df_renewables.iloc[i]['Feasible Alternative Energy for Pump (kWh)']
        else:
            df_renewables.at[df_renewables.index[i], 'Energy Deficit (kWh)'] = df_renewables.iloc[i]['Feasible Alternative Energy for Pump (kWh)']

        # Compute Batteries storage
        if prev_battery + (df_renewables.iloc[i]['Energy Surplus (kWh)']) - df_renewables.iloc[i]['Energy Deficit (kWh)'] < 0:
            df_renewables.at[df_renewables.index[i], 'Battery Storage (kWh)'] = prev_battery + df_renewables.iloc[i]['Energy Surplus (kWh)'] - df_renewables.iloc[i]['
```

```
                    Feasible Alternative Energy for Pump (kWh)']
367
368         if prev_battery + df_renewables.iloc[i]['Energy Surplus (kWh)'
                ] - df_renewables.iloc[i]['Energy Deficit (kWh)'] >= 0:
369             if prev_battery + df_renewables.iloc[i]['Energy Surplus (
                    kWh)'] - df_renewables.iloc[i]['Energy Deficit (kWh)
                    '] >= max_battery:
370                 df_renewables.at[df_renewables.index[i], 'Battery
                        Storage (kWh)'] = max_battery
371             else:
372                 df_renewables.at[df_renewables.index[i], 'Battery
                        Storage (kWh)'] = prev_battery + df_renewables.
                        iloc[i]['Energy Surplus (kWh)'] - df_renewables.
                        iloc[i]['Energy Deficit (kWh)']
373
374         #SOC
375         df_renewables.at[df_renewables.index[i], 'Battery SOC (%)'] =
                df_renewables.iloc[i]['Battery Storage (kWh)'] /
                max_battery * 100
376
377         #Consumption Needs check#
378         if i == 0:
379             df_renewables.at[df_renewables.index[i], 'Energy Needs
                    check'] = 0
380         elif df_renewables.iloc[i]['Energy Deficit (kWh)'] -
                df_renewables.iloc[i]['Feasible Alternative Energy for
                Pump (kWh)'] > prev_battery:
381             df_renewables.at[df_renewables.index[i], 'Energy Needs
                    check'] = df_renewables.iloc[i]['Energy Deficit (kWh
                    )'] - df_renewables.iloc[i]['Feasible Alternative
                    Energy for Pump (kWh)']
382         else:
383             df_renewables.at[df_renewables.index[i], 'Energy Needs
                    check'] = 0
384
385     df_renewables['Turbine Flow (l/s)'] = df_renewables['Turbine
            Volume (m3)'] * 1000 / 3600 #Turbine average flow (l/s)
386     df_renewables['Pumped Flow (l/s)'] = df_renewables['Pumped Volume
            (m3)'] * 1000 / 3600 #Turbine average flow (l/s)
387     df_renewables['Reservoir level (m)'] = df_renewables['Reservoir
            Volume (end) (m3)']/res_area
388     df_renewables = df_renewables[['Month','Day', 'Hour', 'Solar
            Energy (kWh)', 'Wind Energy (kWh)', 'Solar+Wind Energy (kWh)
            ',
389                                    'Energy consumption (kWh)', 'Water
                                           consumption (m3)', 'Solar+
                                           Wind used for Consumption (
                                           kWh)', 'Solar+Wind Surplus (
                                           kWh)', 'Feasible Water
                                           Consumption (m3)',
390                                    'Hydropower energy required (kWh)',
                                           'Hydropower factor', 'Actual
                                           Hydropower Energy (kWh)', '
                                           Turbine Volume (m3)', '
                                           Turbine Flow (l/s)', '
                                           Hydropower Generated (kWh)',
391                                    'Solar+Wind Energy for Pump (kWh)',
                                           'Renewable factor', '
                                           Feasible Solar+Wind Energy
                                           for Pump (kWh)',
392                                    'Alternative Energy for Pump (kWh)'
                                           , 'Alternative factor', '
                                           Feasible Alternative Energy
                                           for Pump (kWh)', 'Pumped
                                           Volume (m3)', 'Pumped Flow (l
                                           /s)',
393                                  'Reservoir Volume (end) (m3)', '
                                           Reservoir level (m)', 'Energy
                                            Surplus (kWh)', 'Energy
                                           Deficit (kWh)',
394                                  'Battery Storage (kWh)', 'Battery
                                           SOC (%)', 'Energy Needs check
                                           ']]
395
396     #Energy Needs Reliability if Batteries are used
397     start_date_Erel = '2020-03-01 00:10' #define start date with
                energy consumption
398     end_date_Erel = '2020-09-30 23:10' #define end date with energy
                consumption
399     energy_period = df_renewables.loc[start_date_Erel:end_date_Erel]
400     non_zero_count_Erel = (energy_period['Energy Needs check'] != 0).
                sum()
401     total_count_Erel = len(energy_period)
402     E_rel = (1-(non_zero_count_Erel / total_count_Erel)) * 100
403     print("Energy Needs Reliability (%)", E_rel)
404     df_total = df_renewables.copy()
405
406 # Compute Water Reliability #
407 start_date_Wrel = '2020-03-01 00:10' #Define start date with water
            consumption
408 end_date_Wrel = '2020-09-30 23:10' #Define end date with water
            consumption
409 irrigation_period = df_total.loc[start_date_Wrel:end_date_Wrel]
410 non_zero_count = (irrigation_period['Feasible Water Consumption (m3)']
            != 0).sum()
411 total_count = len(irrigation_period)
412 W_rel = non_zero_count / total_count * 100
413 print("Water Needs Reliability (%)", W_rel)
414
415 total_pumped_volume = df_total['Pumped Volume (m3)'].sum()
416 total_turbine_volume = df_total['Turbine Volume (m3)'].sum()
417 print("Total Pumped Volume (m3):", total_pumped_volume)
418 print("Total Turbine Volume (m3):", total_turbine_volume)
419 total_hydropower_generated = (total_turbine_volume * 9800 * turb_eff *
            turb_head)/(1000*3600)
420 print("Total Hydropower Generated (kWh):", total_hydropower_generated)
421 Total_excess_solarwind = df_total['Energy Surplus (kWh)'].sum()
422 print("Total Solar+Wind Excess (kWh):", Total_excess_solarwind)
423
424 ## Total Alternative Energy for Pump ##
425 if alt_A == 1:
426     Total_Alternative_Energy_for_Pump = df_total['Feasible Alternative
            Energy for Pump (kWh)'].sum()
427     print("Total Grid Energy for Pump (kWh):",
            Total_Alternative_Energy_for_Pump)
428     Total_Grid_Energy = df_total['Energy Deficit (kWh)'].sum()
429     print("Total Grid Energy:", Total_Grid_Energy)
430
431 #Reservoir percentage full#
432 df_total['Reservoir Fulness (%)'] = (df_total['Reservoir Volume (end)
            (m3)'] / max_volume) * 100
433 df_total['Reservoir Fulness (%)'] = df_total['Reservoir Fulness (%)'].
            round(decimal_places)
```

Listing 2: Python Model (NSGA-II Optimization) - HY4RES-2 - Scenario 1/2

```python
# Create a copy of df_total for optimization
df_optimization = df_total.copy()
#---------------------#
    ## NSGA-II ## W/ Pymoo
#---------------------#
# Maximize Hydropower Generated and Minimize Grid energy used for pumping (with W_rel = 100%)

#Biased Initialization
initial_hydropower_factors = np.array([
    [0.5, 0.2, 0.1, 0.2, 0.55], #1-10 March
    [0.5, 0.2, 0.1, 0.2, 0.55], #11-20 March
    [0.5, 0.2, 0.1, 0.2, 0.55], #21-31 March
    [0.45, 0.2, 0.1, 0.2, 0.35], #1-10 April
    [0.45, 0.2, 0.1, 0.2, 0.35], #11-20 April
    [0.45, 0.2, 0.1, 0.2, 0.35], #21-30 April
    [0.2, 0.1, 0.1, 0.1, 0.2], #1-10 May
    [0.2, 0.1, 0.1, 0.1, 0.2], #11-20 May
    [0.2, 0.1, 0.1, 0.1, 0.2], #21-31 May
    [0, 0, 0, 0, 0],  #1-10 June
    [0, 0, 0, 0, 0],  #11-20 June
    [0, 0, 0, 0, 0],  #21-30 June
    [0, 0, 0.01, 0, 0],  #1-10 July
    [0, 0, 0.01, 0, 0],  #11-20 July
    [0, 0, 0.01, 0, 0.05],  #21-31 July
    [0.1, 0, 0.01, 0, 0.1],  #1-10 August
    [0.1, 0, 0.01, 0, 0.1],  #11-20 August
    [0.1, 0, 0.01, 0, 0.1],  #21-31 August
    [0.1, 0.1, 0.15, 0.1, 0.1],  #1-10 September
    [0.1, 0.1, 0.15, 0.1, 0.1],  #11-20 September
    [0.1, 0.1, 0.15, 0.1, 0.1],  #21-30 September
])
initial_aux_factors = np.array([
    [0, 0, 0, 0, 0],  #1-10 March
    [0, 0, 0, 0, 0],  #11-20 March
    [0, 0, 0, 0, 0],  #21-31 March
    [0, 0, 0, 0, 0],  #1-10 April
    [0, 0, 0, 0, 0],  #11-20 April
    [0, 0, 0, 0, 0],  #21-30 April
    [0, 0, 0, 0, 0],  #1-10 May
    [0, 0, 0, 0, 0],  #11-20 May
    [0, 0, 0, 0, 0],  #21-31 May
    [0.2, 0, 0, 0, 0.38],  #1-10 June
    [0.2, 0, 0, 0, 0.38],  #11-20 June
    [0.2, 0, 0, 0, 0.38],  #21-30 June
    [0.44, 0, 0.3, 0, 0.45],  #1-10 July
    [0.44, 0, 0.3, 0, 0.45],  #11-20 July
    [0.44, 0, 0.3, 0, 0.45],  #21-31 July
    [0.4, 0, 0.34, 0, 0.42],  #1-10 August
    [0.4, 0, 0.34, 0, 0.42],  #11-20 August
    [0.4, 0, 0.34, 0, 0.42],  #21-31 August
    [0, 0, 0, 0, 0],  #1-10 September
    [0, 0, 0, 0, 0],  #11-20 September
    [0, 0, 0, 0, 0],  #21-30 September
])
initial_solar_factors = np.array([
    [0.9, 0.9, 0.9, 0.9, 0.9],  #1-10 March
    [0.9, 0.9, 0.9, 0.9, 0.9],  #11-20 March
    [0.9, 0.9, 0.9, 0.9, 0.9],  #21-31 March
    [0.9, 0.9, 0.9, 0.9, 0.9],  #1-10 April
    [0.9, 0.9, 0.9, 0.9, 0.9],  #11-20 April
    [0.9, 0.9, 0.9, 0.9, 0.9],  #21-30 April
    [0.9, 0.9, 0.9, 0.9, 0.9],  #1-10 May
    [0.9, 0.9, 0.9, 0.9, 0.9],  #11-20 May
    [0.9, 0.9, 0.9, 0.9, 0.9],  #21-31 May
    [0.9, 0.9, 0.9, 0.9, 0.9],  #1-10 June
    [0.9, 0.9, 0.9, 0.9, 0.9],  #11-20 June
    [0.9, 0.9, 0.9, 0.9, 0.9],  #21-30 June
    [0.9, 0.9, 0.9, 0.9, 0.9],  #1-10 July
    [0.9, 0.9, 0.9, 0.9, 0.9],  #11-20 July
    [0.9, 0.9, 0.9, 0.9, 0.9],  #21-31 July
    [0.9, 0.9, 0.9, 0.9, 0.9],  #1-10 August
    [0.9, 0.9, 0.9, 0.9, 0.9],  #11-20 August
    [0.9, 0.9, 0.9, 0.9, 0.9],  #21-31 August
    [0.9, 0.9, 0.9, 0.9, 0.9],  #1-10 September
    [0.9, 0.9, 0.9, 0.9, 0.9],  #11-20 September
    [0.9, 0.9, 0.9, 0.9, 0.9],  #21-30 September
])

#initial feasible solution
initial_solution = np.concatenate([
    initial_hydropower_factors.flatten(),
    initial_aux_factors.flatten(),
    initial_solar_factors.flatten()
])

# Custom sampling to include biased initialization
class BiasedSampling(Sampling):
    def __init__(self, biased_solution):
        self.biased_solution = biased_solution
        self.vtype = float
        self.repair = None

    def _do(self, problem, n_samples, **kwargs):
        # Number of random samples to generate
        n_random_samples = n_samples - 1

        # Generate random samples
        random_samples = FloatRandomSampling()._do(problem, n_random_samples, **kwargs)

        # Combine the biased solution with random samples
        samples = np.vstack([self.biased_solution, random_samples])

        return samples


def apply_factors(df_applyfactors, factors, column_name, periods):
    for idx, row in df_applyfactors.iterrows():
        month = int(row['Month'])
        day = int(row['Day'])
        hour = int(row['Hour'])

        if not (1 <= month <= 12) or day < 1 or day > 31 or not (0 <= hour < 24):
            df_applyfactors.at[idx, column_name] = None
        else:
            if day >= 21:
                period_day = 2
            elif day >= 11:
                period_day = 1
            else:
                period_day = 0

            if hour < 8:
                period_hour = 0
            elif hour < 14:
                period_hour = 1
            elif hour < 18:
                period_hour = 2
            elif hour < 22:
                period_hour = 3
            else:
                period_hour = 4

            if month in periods:
```

```
                df_applyfactors.at[idx, column_name] = factors[periods
                    .index(month) * 3 + period_day][period_hour]
            else:
                df_applyfactors.at[idx, column_name] = 1

class EnergyOptimizationProblem(Problem):
    def __init__(self):
        super().__init__(n_var=315, n_obj=2, n_constr=1, xl=0.0, xu=1.
            0)

    def _evaluate(self, x, out, *args, **kwargs):
        global df
        df = df_optimization.copy()

        # Debugging: Check the size of the individuals
        print(f"Evaluating batch of individuals, each of size {x.shape
            [1]}")

        F = []
        G = []

        for individual in x:
            hydropower_factors = np.array(individual[:105]).reshape(21
                , 5)
            aux_factors = np.array(individual[105:210]).reshape(21, 5)
            solar_factors = np.array(individual[210:315]).reshape(21,
                5)

            periods = [3, 4, 5, 6, 7, 8, 9]

            apply_factors(df, hydropower_factors, 'Hydropower factor',
                periods)
            apply_factors(df, aux_factors, 'Auxiliary factor', periods
                )
            apply_factors(df, solar_factors, 'Solar factor', periods)

            df['Solar Energy for Pump (kWh)'] = df['Solar+Wind Surplus
                (kWh)'] * df['Solar factor']
            for i in range(len(df)):
                if df.iloc[i]['Solar Energy for Pump (kWh)'] >= 0.2 *
                    pump_power:
                    df.at[df.index[i], 'Solar Energy for Pump (kWh)']
                        = df.iloc[i]['Solar Energy for Pump (kWh)']
                else:
                    df.at[df.index[i], 'Solar Energy for Pump (kWh)']
                        = 0

            # Initialize columns to be filled iteratively
            df['Auxiliary Energy for Pump (kWh)'] = 0
            df['Feasible Water Consumption (m3)'] = 0
            df['Actual Hydropower Energy (kWh)'] = 0
            df['Feasible Solar+Wind Energy for Pump (kWh)'] = 0
            df['Feasible Auxiliary Energy for Pump (kWh)'] = 0
            df['Reservoir Volume (end) (m3)'] = 0
            df['Turbine Volume (m3)'] = 0
            df['Pumped Volume (m3)'] = 0

            for i in range(len(df)):
                if i == 0:
                    prev_volume = initial_volume_jan
                else:
                    prev_volume = df.iloc[i - 1]['Reservoir Volume (
                        end) (m3)']

                if prev_volume - df.iloc[i]['Water consumption (m3)']
                    >= min_volume:
                    df.at[df.index[i], 'Feasible Water Consumption (m3
                        )'] = df.iloc[i]['Water consumption (m3)']

                if prev_volume - df.iloc[i]['Feasible Water
                    Consumption (m3)'] - (df.iloc[i]['Hydropower
                    energy required (kWh)'] * df.iloc[i]['Hydropower
                     factor'] * 1000 * 3600) / (9800 * turb_head *
                    turb_eff) >= min_volume:
                    df.at[df.index[i], 'Actual Hydropower Energy (kWh)
                        '] = df.iloc[i]['Hydropower energy required
                        (kWh)'] * df.iloc[i]['Hydropower factor']

                if prev_volume - df.iloc[i]['Feasible Water
                    Consumption (m3)'] + (df.iloc[i]['Solar Energy
                    for Pump (kWh)'] * pump_eff * 1000 * 3600) / (98
                    00 * pump_head) <= max_volume:
                    df.at[df.index[i], 'Feasible Solar+Wind Energy for
                         Pump (kWh)'] = df.iloc[i]['Solar Energy for
                         Pump (kWh)']

                if df.iloc[i]['Actual Hydropower Energy (kWh)'] == 0:
                    pump_power_times_grid_factor = pump_power * df.
                        iloc[i]['Auxiliary factor']
                    if pump_power_times_grid_factor + df.iloc[i]['
                        Feasible Solar+Wind Energy for Pump (kWh)']
                        <= pump_power:
                        df.at[df.index[i], 'Auxiliary Energy for Pump
                            (kWh)'] = pump_power_times_grid_factor

                if prev_volume - df.iloc[i]['Feasible Water
                    Consumption (m3)'] + (df.iloc[i]['Feasible Solar
                    +Wind Energy for Pump (kWh)'] * pump_eff * 1000
                    * 3600) / (9800 * pump_head) + (df.iloc[i]['
                    Auxiliary Energy for Pump (kWh)'] * pump_eff * 1
                    000 * 3600) / (9800 * pump_head) <= max_volume:
                    df.at[df.index[i], 'Feasible Auxiliary Energy for
                        Pump (kWh)'] = df.iloc[i]['Auxiliary Energy
                        for Pump (kWh)']

                df.at[df.index[i], 'Turbine Volume (m3)'] = (df.iloc[i
                    ]['Actual Hydropower Energy (kWh)'] * 1000 * 360
                    0) / (9800 * turb_head * turb_eff)
                df.at[df.index[i], 'Pumped Volume (m3)'] = (df.iloc[i
                    ]['Feasible Solar+Wind Energy for Pump (kWh)'] *
                     pump_eff * 1000 * 3600) / (9800 * pump_head) +
                    (df.iloc[i]['Feasible Auxiliary Energy for Pump
                    (kWh)'] * pump_eff * 1000 * 3600) / (9800 *
                    pump_head)
                df.at[df.index[i], 'Reservoir Volume (end) (m3)'] =
                    prev_volume - df.iloc[i]['Feasible Water
                    Consumption (m3)'] - df.iloc[i]['Turbine Volume
                    (m3)'] + df.iloc[i]['Pumped Volume (m3)']

            df['Turbine Flow (l/s)'] = df['Turbine Volume (m3)'] *
                1000 / 3600
            df['Hydropower Generated (kWh)'] = (df['Turbine Volume
                (m3)'] * 9800 * turb_eff * turb_head) / (1000 *
                3600)
            df['Hydropower Generated (kWh)'] = df['Hydropower
                Generated (kWh)'].round().astype(int)
            df['Pumped Flow (l/s)'] = df['Pumped Volume (m3)'] * 1
                000 / 3600
            df['Reservoir level (m)'] = df['Reservoir Volume (end)
                (m3)'] / res_area

            df['Energy Surplus (kWh)'] = df['Solar+Wind Surplus (
                kWh)'] - df['Feasible Solar+Wind Energy for Pump
                (kWh)']
            df['Energy Deficit (kWh)'] = np.where(
                df['Energy consumption (kWh)'] - df['Solar+Wind
                    Energy (kWh)'] - df['Hydropower Generated (
                    kWh)'] > 0,
```

```
                df['Energy consumption (kWh)'] - df['Solar+Wind
                    Energy (kWh)'] - df['Hydropower Generated (
                    kWh)'] + df['Feasible Auxiliary Energy for
                    Pump (kWh)'],
                df['Feasible Auxiliary Energy for Pump (kWh)']
            )
            df['Energy Deficit (kWh)'] = df['Energy Deficit (kWh)'
                ].clip(lower=0)

            df['Profit from Sell €()'] = df['Energy Surplus (kWh)'
                ] * df['Sell to Grid €(/kWh)']
            df['Profit from Sell €()'] = df['Profit from Sell €()'
                ].round(decimal_places)
            df['Costs from buy €()'] = df['Energy Deficit (kWh)']
                * df['Buy from Grid €(/kWh)']
            df['Profit from Sell €()'] = df['Profit from Sell €()'
                ].round(decimal_places)

        irrigation_period_opt = df.loc[start_date_Wrel:
            end_date_Wrel]
        non_zero_count_opt = (irrigation_period_opt['Feasible
            Water Consumption (m3)'] != 0).sum()
        total_count_opt = len(irrigation_period_opt)
        water_reliability_opt = non_zero_count_opt /
            total_count_opt * 100
        # Debugging print statements
        print("Water Reliability:", water_reliability_opt)

        total_hydropower_generated = df['Hydropower Generated (kWh
            )'].sum()
        total_grid_energy_for_pump = df['Feasible Auxiliary Energy
             for Pump (kWh)'].sum()
        """
        if water_reliability_opt < 100:
            total_hydropower_generated = -1e12
            total_grid_energy_for_pump = 1e12
            print("Applying extreme penalty due to water
                reliability constraint.")
        """
        penalty_multiplier = 1e10
        penalty = penalty_multiplier * max(0, 100 -
            water_reliability_opt)
        if penalty != 0:
            print("Applying penalty of:", penalty)

        #F.append([-total_hydropower_generated,
            total_grid_energy_for_pump])
            F.append([-total_hydropower_generated + penalty,
                total_grid_energy_for_pump + penalty])
            G.append([-water_reliability_opt + 100])

        out["F"] = np.array(F)
        out["G"] = np.array(G)

problem = EnergyOptimizationProblem()

biased_sampling = BiasedSampling(initial_solution)

algorithm = NSGA2(
    pop_size=250,
    sampling=biased_sampling,
    crossover=SBX(prob=0.9, eta=15),
    mutation=PM(prob=0.3, eta=20),
    eliminate_duplicates=True
)

res = minimize(
    problem,
    algorithm,
    ('n_gen', 10),
    verbose=True,
    return_least_infeasible=True
)

pareto_front = res.F

# Plot Pareto front
plt.scatter(-pareto_front[:, 0], pareto_front[:, 1])
plt.title('Pareto Front')
plt.xlabel('Total Hydropower Generated (kWh)')
plt.ylabel('Total Grid Energy for Pump (kWh)')
plt.grid(True)
plt.show()

# Extract all solutions from the final population
pop = res.pop
F = pop.get("F")
# Select the best solution based on the objective values
best_solution_idx = np.argmax(F[:, 0])  # Since we are maximizing
    hydropower
best_solution = pop[best_solution_idx].X
print("Best Solution:", best_solution)
```

Irrigation System - large-scale case study

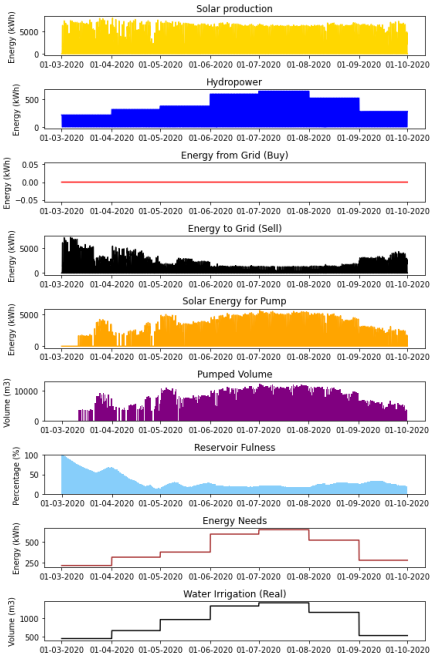

A.4(a) OPT1

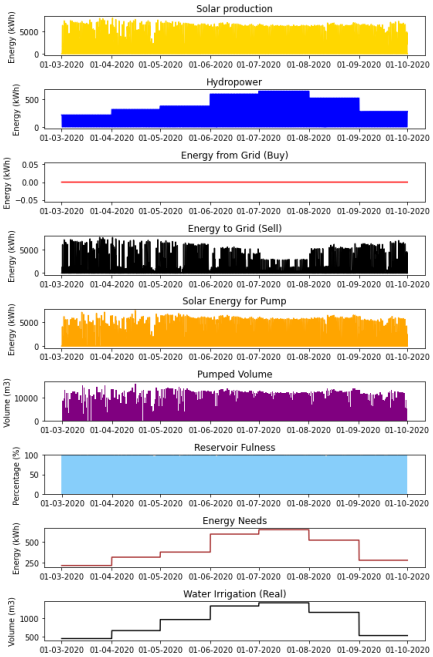

A.4(b) OPT2

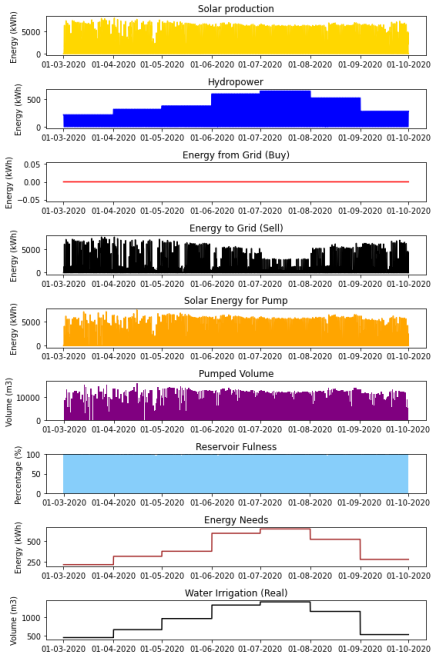

A.4(c) OPT3

Figure A.4: Scenario 1: Yearly energy and water volume balance, 800 m^3/ha

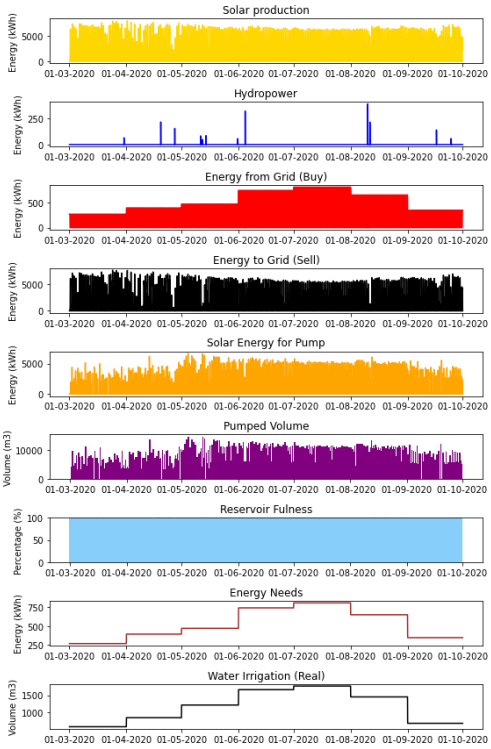

A.5(a) OPT1

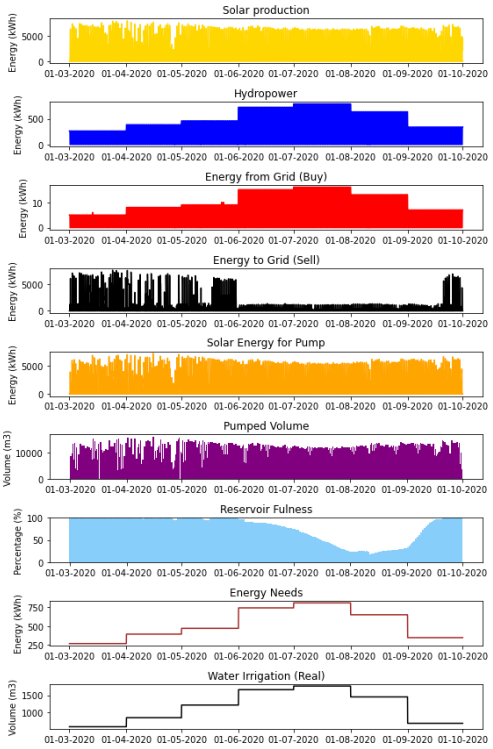

A.5(b) OPT2

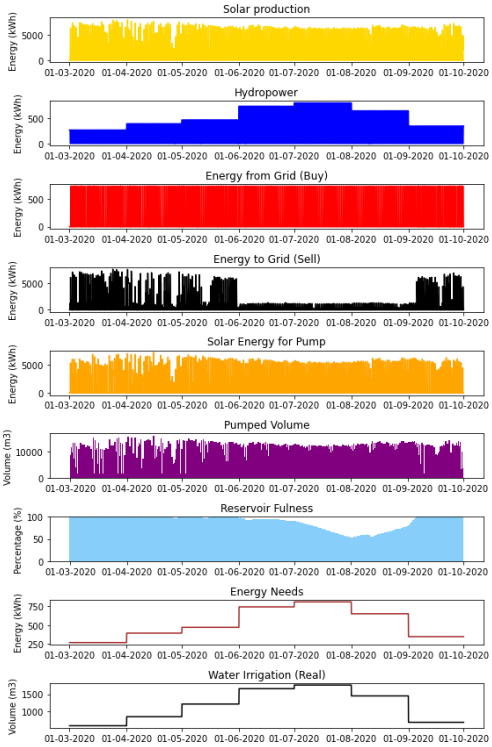

A.5(c) OPT3

Figure A.5: Scenario 1: Yearly energy and water volume balance, 1000 m^3/ha

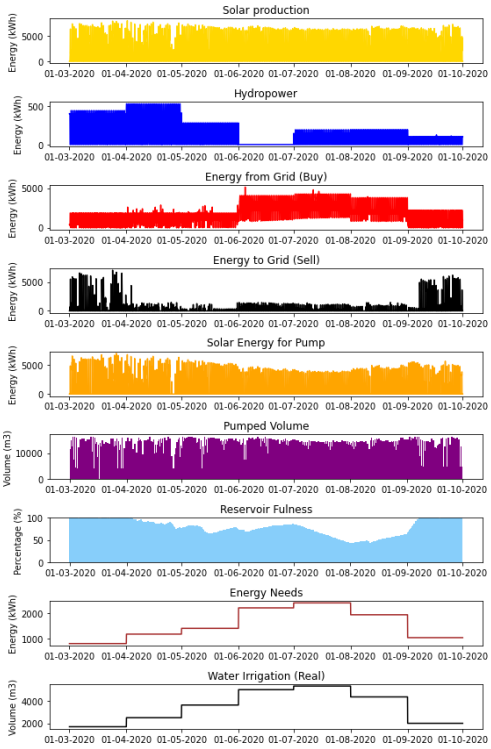

A.6(a) OPT2

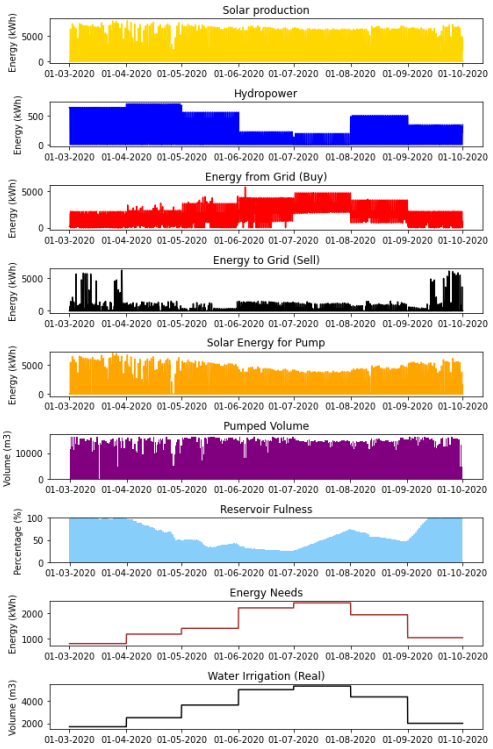

A.6(b) OPT3

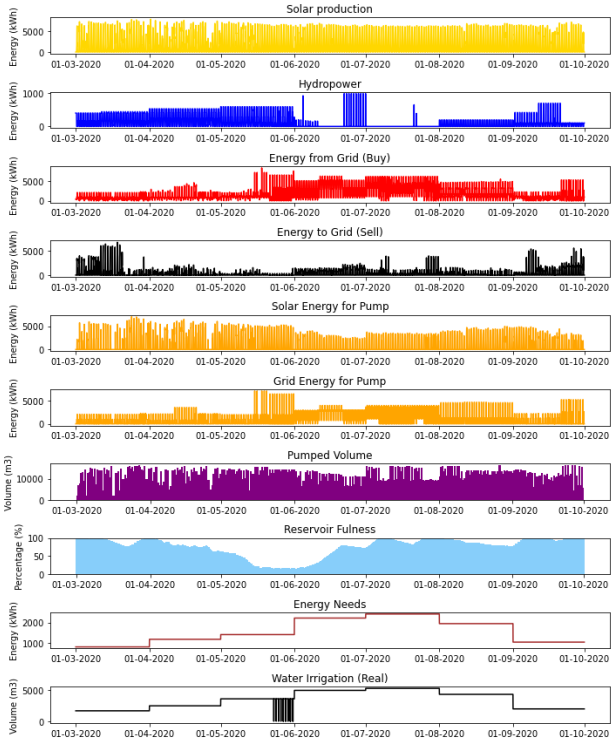

A.6(c) NSGA-II

Figure A.6: Scenario 1: Yearly energy and water volume balance, 3000 m^3/ha

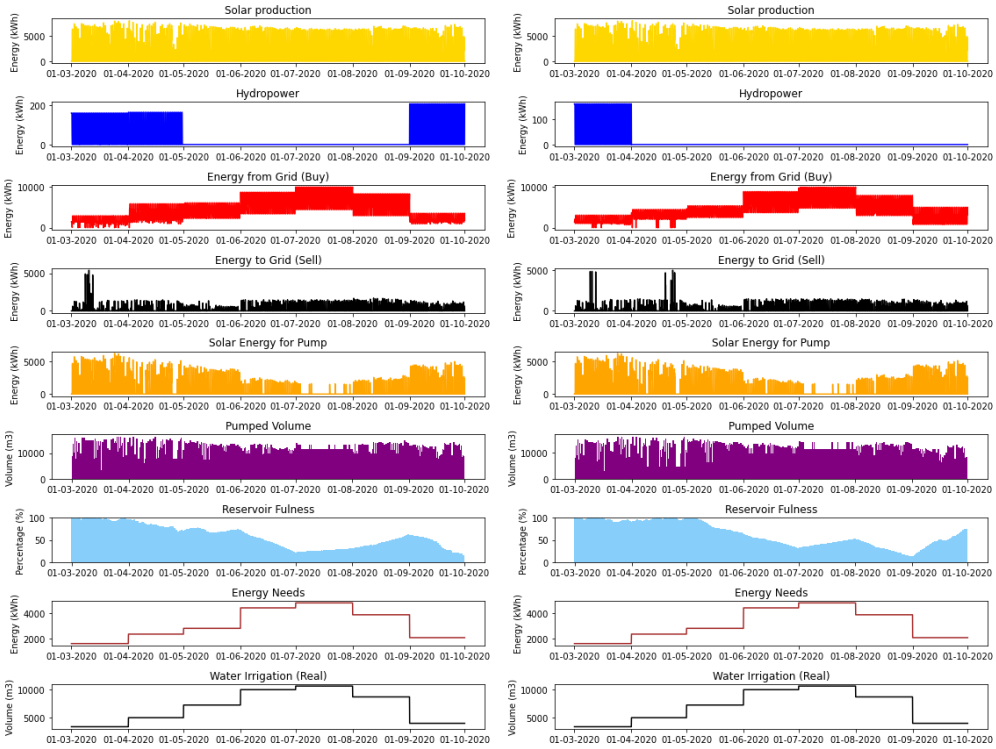

A.7(a) OPT1

A.7(b) OPT2

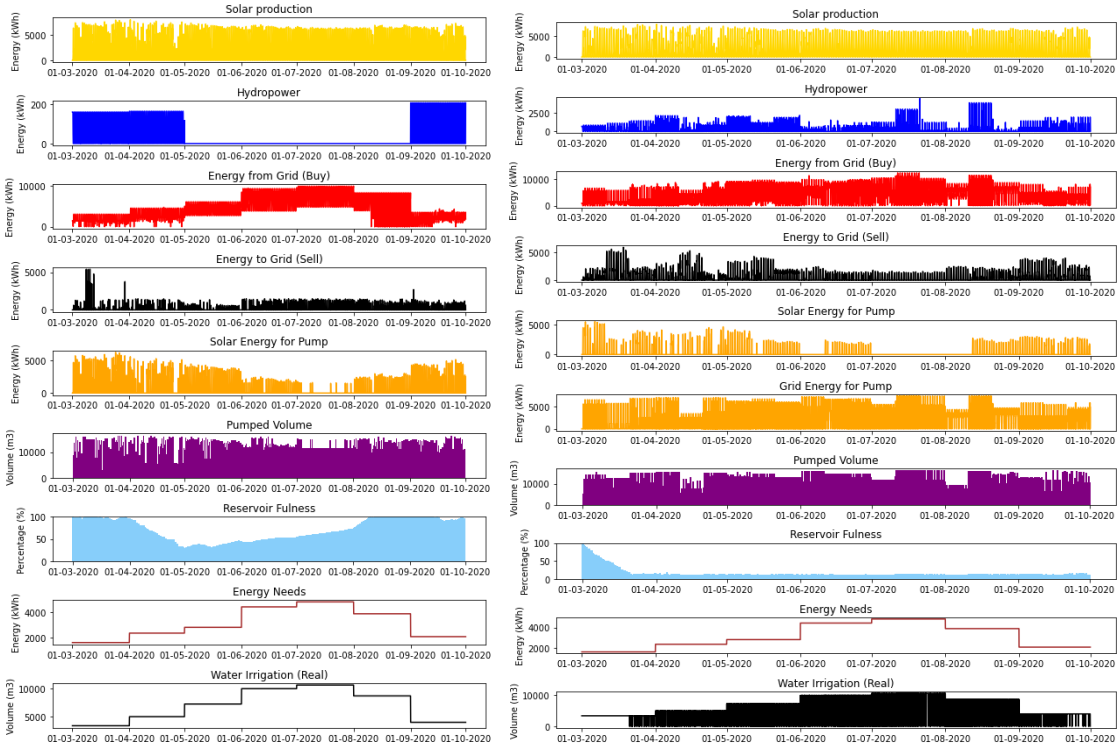

A.7(c) OPT3

A.7(d) NSGA-II

Figure A.7: Scenario 1: Yearly energy and water volume balance, 6000 m^3/ha

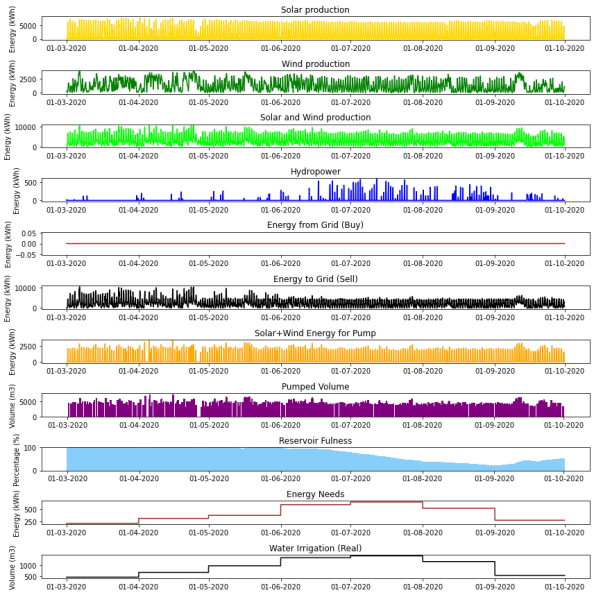

A.8(a) OPT1 - 800 m^3/ha

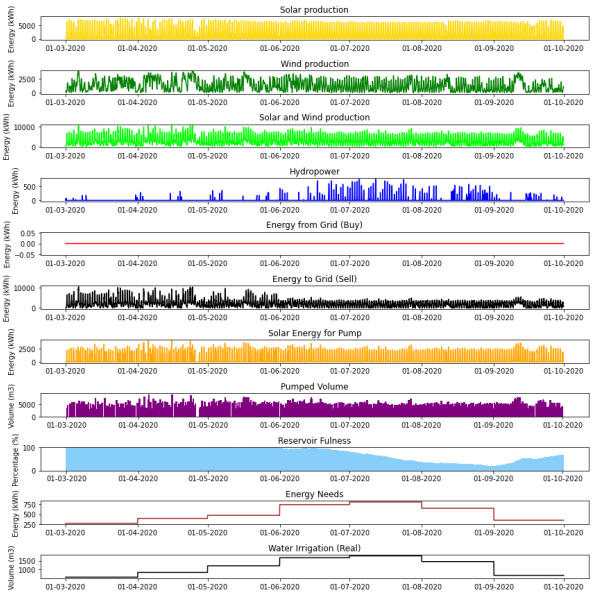

A.8(b) OPT1 - 1000 m^3/ha

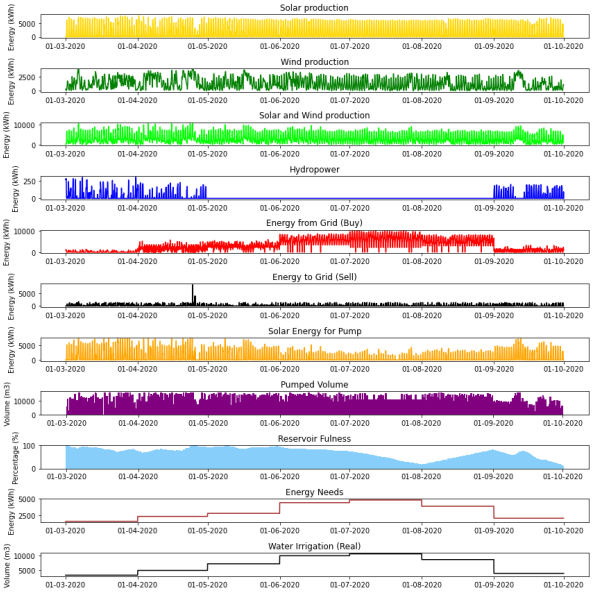

A.8(c) OPT1 - 6000 m^3/ha

Figure A.8: Scenario 2: Yearly energy and water volume balance, OPT1

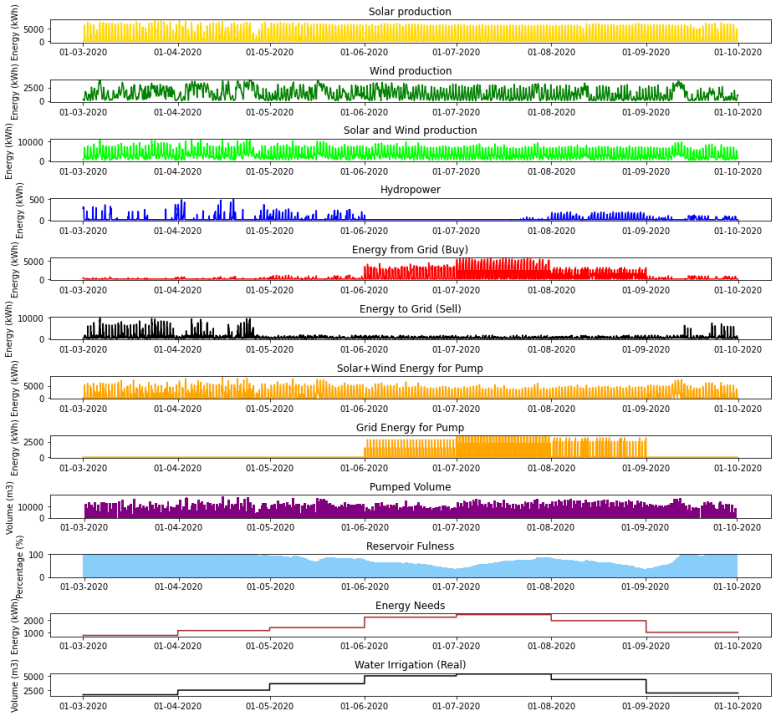

A.9(a) NSGA-II - 3000 m^3/ha

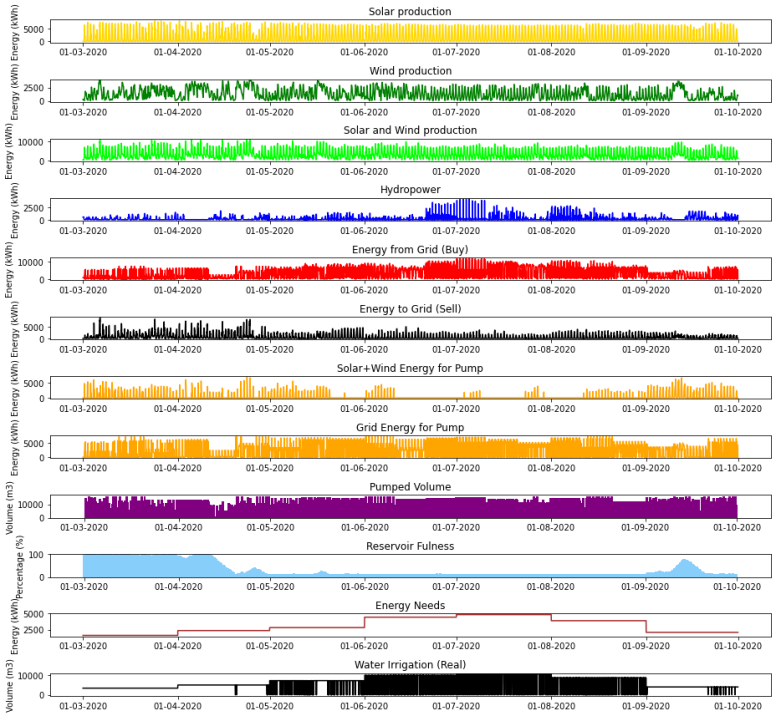

A.9(b) NSGA-II - 6000 m^3/ha

Figure A.9: Scenario 2: Yearly energy and water volume balance, NSGA-II

A.10(a) OPT4 - 1000 m^3/ha

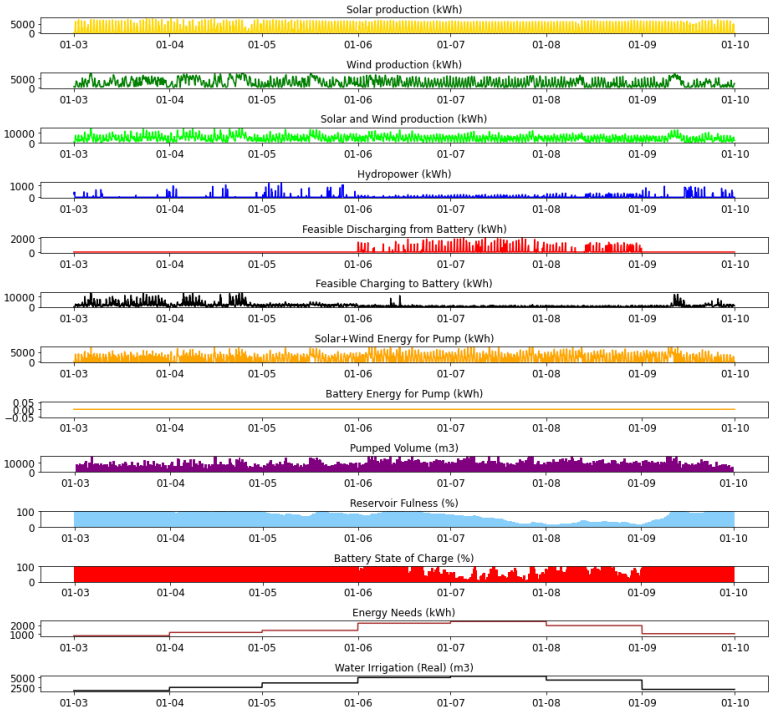

A.10(b) OPT4 - 3000 m^3/ha

Figure A.10: Scenario 3: Yearly energy and water volume balance, OPT4

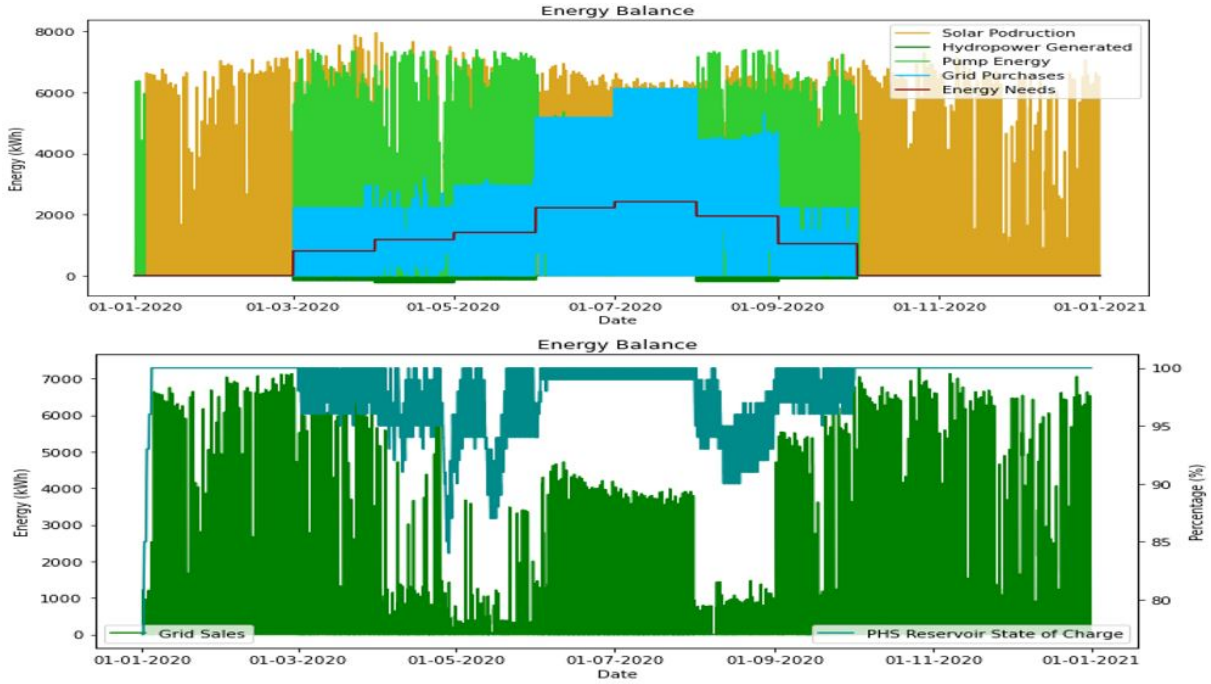

A.11(a) OPT1 - HY4RES Model

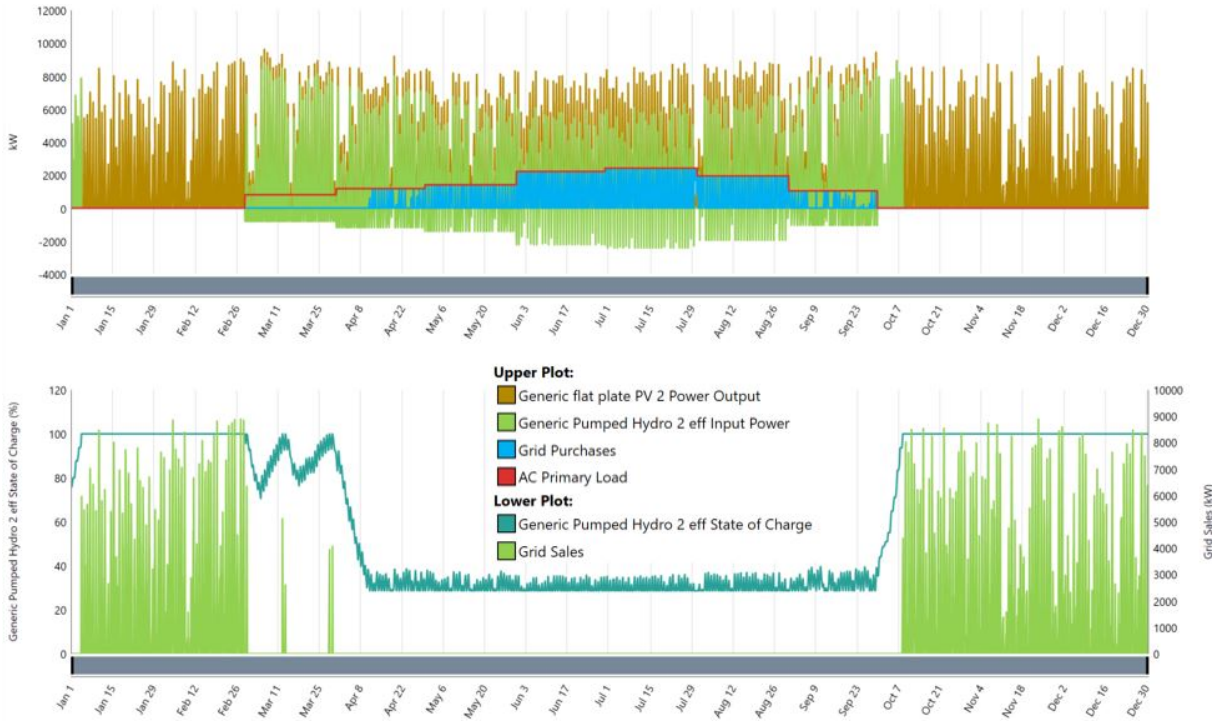

A.11(b) HOMER

Figure A.11: Model VS. HOMER, 3000 m^3/ha

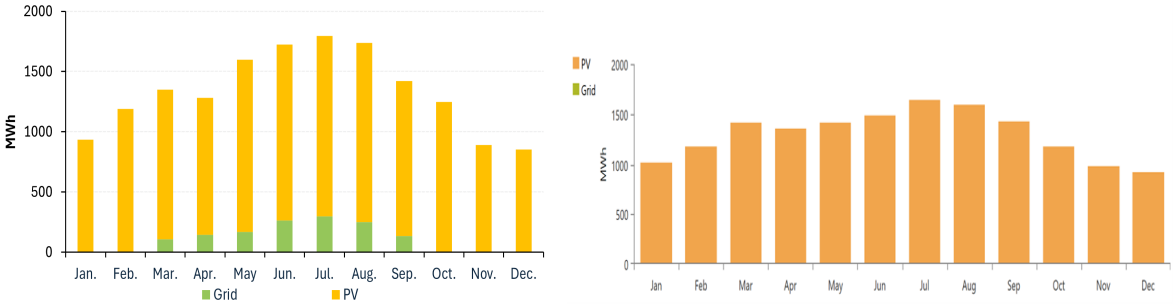

A.12(a) HY4RES Model

A.12(b) HOMER

Figure A.12: Monthly PV production and Grid purchases, 1000 m^3/ha

Energy Community - small-scale case study

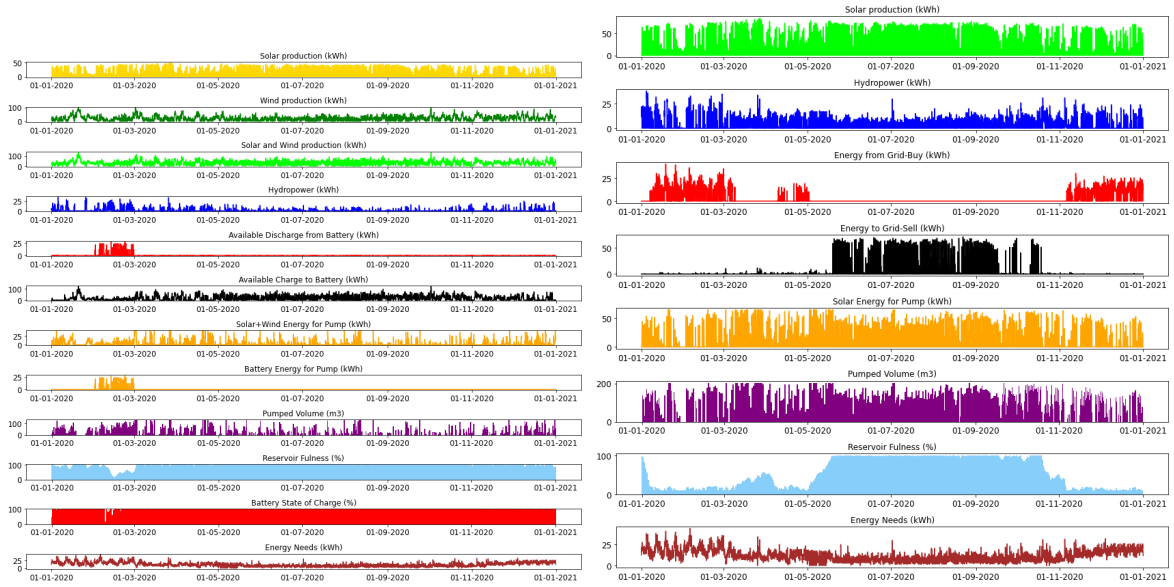

A.13(a) SA2 - PV+Wind+PHS+BESS

A.13(b) GC1 - PV+PHS+Grid

Figure A.13: Stand-alone versus grid-connected, extended solutions